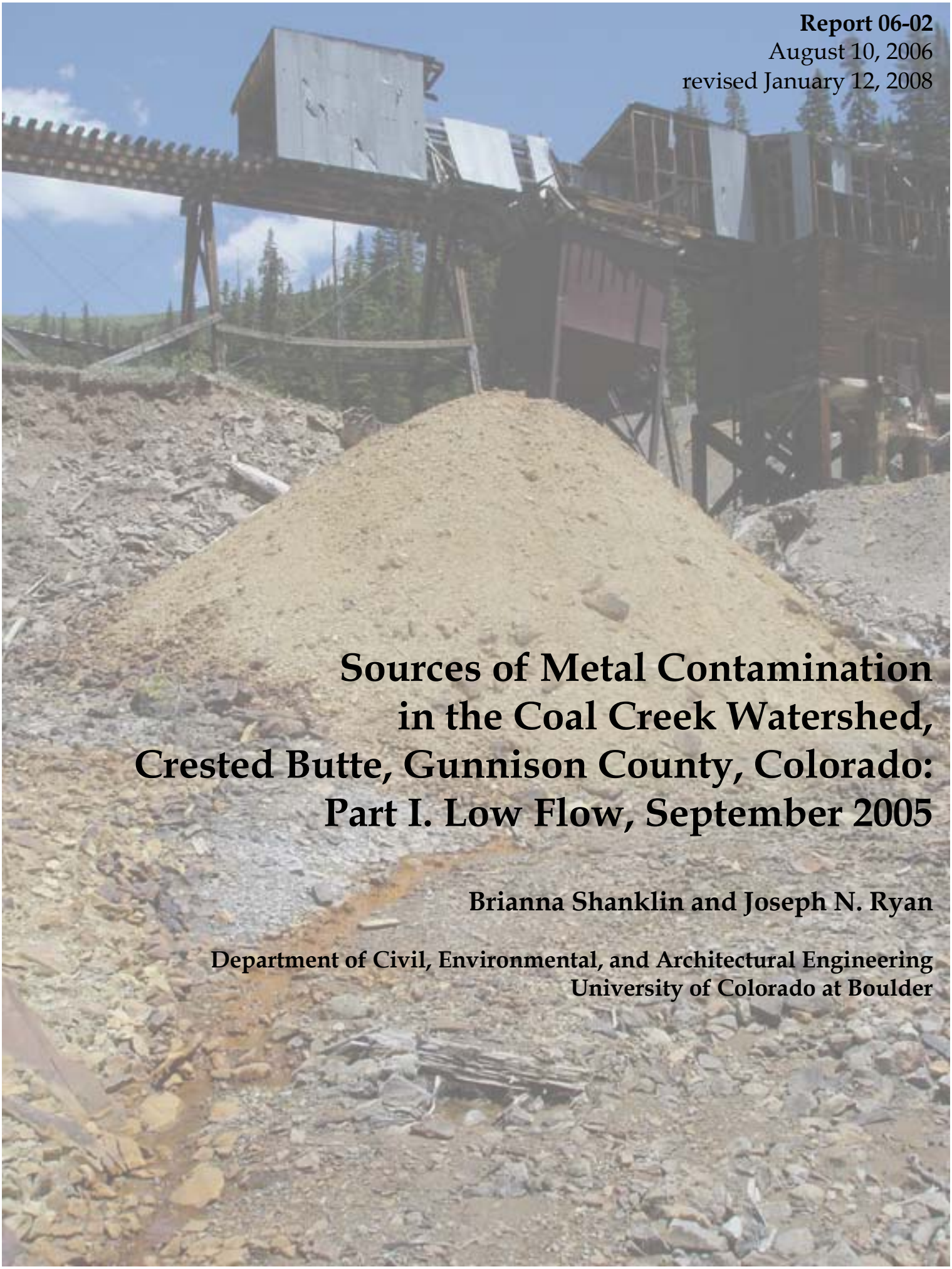

**Report 06-02**
August 10, 2006
revised January 12, 2008

# Sources of Metal Contamination in the Coal Creek Watershed, Crested Butte, Gunnison County, Colorado: Part I. Low Flow, September 2005

**Brianna Shanklin and Joseph N. Ryan**

**Department of Civil, Environmental, and Architectural Engineering**
**University of Colorado at Boulder**

**Report 06-02**

Department of Civil, Environmental, and Architectural Engineering
University of Colorado at Boulder

August 10, 2006
January 12, 2008, revised

# Sources of Metal Contamination in the Coal Creek Watershed, Crested Butte, Gunnison County, Colorado: Part I. Low Flow, September 2005

Brianna Shanklin and Joseph N. Ryan

Department of Civil, Environmental, and Architectural Engineering
University of Colorado at Boulder

**Contact Information:**

Prof. Joseph N. Ryan
University of Colorado
428 UCB
Boulder, CO 80309-0428

phone: 303 492 0772
fax: 303 492 7317
email: joseph.ryan@colorado.edu

## EXECUTIVE SUMMARY

This report details the results of a study conducted by University of Colorado researchers for the Coal Creek Watershed Coalition on the source of metals in the Coal Creek watershed during low flow. Coal Creek is the main water supply for the Town of Crested Butte in Gunnison County, Colorado. The study was funded by the University of Colorado's Outreach Committee.

Previous sampling has shown that Coal Creek is contaminated by metals and acidity from the Standard Mine on Elk Creek, a tributary of Coal Creek, and from a naturally occurring iron fen and gossan located just west of the Keystone Mine. Drainage from the Keystone Mine, which has been treated at the Mount Emmons treatment facility since 1981, also contributes metals to Coal Creek just downstream of Crested Butte's water supply intake. To confirm these results and to locate any other inputs of metals and acidity to Coal Creek, a spatially detailed investigation of contaminant sources was performed by University of Colorado researchers in September, 2005. The study was conducted at low flow because contaminant concentrations and toxicity to aquatic organisms are often highest during low flow. A companion study was completed in June, 2006, to locate metal sources at high flow; the results of the high flow investigation will be available as Part 2 of this report.

A lithium chloride tracer-dilution test and synoptic sampling of Coal Creek allowed for the quantification of both surface and hyporheic flow and provided spatially detailed concentration and metal loading profiles for aluminum, arsenic, barium, cadmium, chromium, copper, iron, lead, manganese, nickel, and zinc along a 9.4 km reach of Coal Creek. Water draining from the iron fen and gossan near Keystone Mine was identified as the largest metal contributor in the watershed. It was a major source of aluminum, cadmium, iron, manganese, and zinc to Coal Creek. Elk Creek, which contains the Standard Mine drainage, was identified as a major source of cadmium and zinc. An unnamed tributary draining Evans Basin and located 1.1 km downstream of Elk Creek was identified as a major source of chromium, iron, and nickel. Detailed results are presented in Table 14.

The Mt. Emmons Treatment Plant added calcium to Coal Creek at concentrations seven times greater than background. Large daily fluctuations in calcium concentration and hardness coinciding with times of discharge release and discontinuation are expected. These fluctuations result in daily changes in hardness-based aquatic life standards set by the Colorado Department of Public Health and Environment. Metal speciation is also affected by the hardness fluctuations. Partitioning between the dissolved and colloidal phases was investigated for aluminum, arsenic, lead, and zinc.

## ACKNOWLEDGMENTS

Funding for this project was provided by the University of Colorado Outreach Committee and facilitated by Wynn Martens of the University of Colorado. Christina Progess the U.S. Environmental Protection Agency project manager for the Superfund cleanup at the Standard Mine, arranged for analysis of the metal concentrations in the water samples.

Scientific and technical assistance and field and laboratory support were provided by the following people:

- Steve Glazer, Tyler Martineau, and Anthony Poponi of the Coal Creek Watershed Coalition,
- Larry Adams and John Hess of the Town of Crested Butte,
- Christina Progess, Carol Beard, and Jessica Brown of the U.S. Environmental Protection Agency,
- John Perusek and Adolph Ortiz of Phelps-Dodge, operators of the Mt. Emmons Treatment Plant,
- Susan Bautts, Christie Chatterley, Lynné Diaz, Tim Dittrich, Jeff Wong, Natalie Mladenov, and JoAnn Silverstein of the University of Colorado,
- Suzanne Anderson of the Institute for Arctic and Alpine Research at the University of Colorado, and
- John Drexler and Fred Luiszer of the Laboratory for Environmental and Geological Studies at the University of Colorado

## TABLE OF CONTENTS

## LIST OF TABLES

## LIST OF FIGURES

# INTRODUCTION

Over 600 km of stream reach are affected by metal-rich, acidic drainage from abandoned mining sites in Colorado (Wentz, 1974). Acid mine drainage occurs when pyrite ($FeS_2$) and other metal sulfide minerals are leached and then oxidized. Acidic water with high iron and sulfate concentrations is the product of pyrite oxidation.

Acid mine drainage from abandoned mines as well as metal-laden drainage from a natural iron deposit are suspected to degrade water quality in the Coal Creek watershed, due west of Crested Butte, Colorado (Figure 1). The watershed has a 100-year mining legacy, with excavation and milling operations beginning in 1874 and continuing until 1974 (EPA, 2005a). The major mines in the district were the Standard Mine, the Keystone Mine, and the Forest Queen Mine. The Standard Mine was added to the National Priority List ("Superfund") in September 2005. Until the beginning of site remediation during the summer of 2006, drainage emanating from the Standard Mine flowed into an unlined, non-engineered holding pond that overflowed into Elk Creek. Elk Creek flows into Coal Creek about 3 km downstream of the Standard Mine site. Coal Creek serves as the main drinking water supply for the Town of Crested Butte's 1,500 residents. Risk of catastrophic failure of this holding pond and influx of a large quantity of metal-laden water into Crested Butte's drinking water supply was the major threat posed by the Standard Mine site; ongoing contamination of Elk Creek and Coal Creek is caused by the continued drainage from the Standard Mine.

Drainage from the Keystone Mine is treated at the Mount Emmons Treatment Plant and then released into Coal Creek just downstream of Crested Butte's drinking water intake. Ownership and managerial responsibility of this treatment plant was re-acquired by U.S. Energy Corporation in February 2006. U.S. Energy has announced plans to resume mining operations on Mount Emmons to exploit a "world-class" molybdenum deposit underneath the mountain (U.S. Energy, 2006).

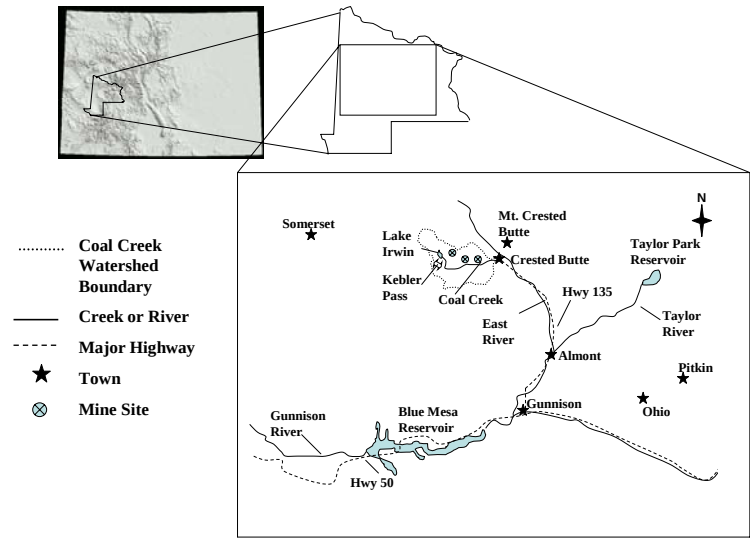


**Figure 1.** The Coal Creek watershed is located west of the Town of Crested Butte in northern Gunnison County, Colorado.

Water flowing from and over a gossan (a naturally-occurring surface deposit of iron-rich minerals oxidized by exposure to the atmosphere) also drains into Coal Creek. The gossan is located just west of the Keystone Mine. Much of the gossan drainage flows

into a wetland known locally as the "iron fen." Water flowing from the iron fen is acidic and contains high concentrations of aluminum, iron, manganese, and zinc.

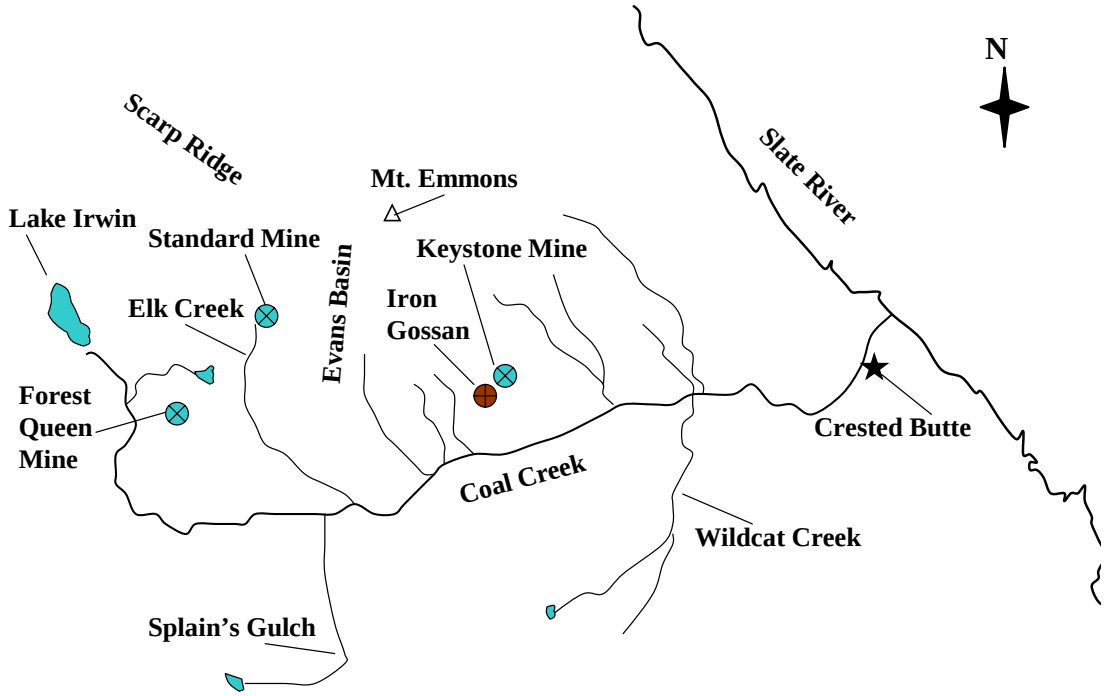


**Figure 2**. The Coal Creek watershed with Coal Creek, its major tributaries, mines, and other geographical features identified.

The Coal Creek Watershed Coalition (CCWC), a community group based in Crested Butte, is working to restore aquatic life habitat and protect other water uses in Coal Creek (CCWC, 2006). Recreation is the primary contributor to the local economy. The CCWC hopes that well-directed remedial action in the Coal Creek watershed will create a sustainable fish population and promote fishing in Coal Creek.

This report describes the results of a metal-loading tracer-dilution experiment (Kimball, 1997) that we performed at low flow in September, 2005, to assist the Coal Creek Watershed Coalition with identification of the significant sources of metal contamination in the watershed. The highest metal concentrations, which are most toxic to aquatic life, commonly occur during the low-flow season when only a small volume of water is available to dilute pollutants (Paschke et al., 2005). Additional experiments have been conducted at the onset of runoff in the watershed in April, 2007, and at high flow in June, 2006. The metal-loading tracer-dilution experiments allow calculation of metal loading rates (units of mass of metal per time) at a high spatial resolution in the Coal Creek watershed. Samples were taken at sites separated by 100-200 m in Coal Creek and from every flowing tributary. Spatially-detailed characterization of Coal Creek metal loads is required for proper remedial action. The objectives of this study were to (1) quantify and locate sources of metal input to Coal Creek, (2) investigate specific metal contributions to Coal Creek from the Standard Mine (Elk Creek) and the iron gossan, and (3) assess relationships and interactions between metal partitioning between the dissolved and colloidal phases.

# BACKGROUND

## *Field site*

The Coal Creek watershed (Figures 1 and 2) drains an area of approximately 65 $km^2$ in the Ruby-Anthracite Range of northern Gunnison County, Colorado. Coal Creek originates near Lake Irwin in the northwestern portion of the watershed. The downstream reach of Coal Creek flows through the Crested Butte on the eastern edge of the watershed before ultimately entering the Slate River, which flows south into the East River, and then into the Gunnison River. County Highway 12, the Kebler Pass Road, parallels Coal Creek along most of the length of Coal Creek.

Elevations in the watershed range from about 2,900 m in Crested Butte to about 4,300 m at the peaks of the Ruby Range. Glacial erosion during the Pleistocene epoch shaped the Coal Creek valley. Laccoliths, or dome-shaped igneous intrusions, other resistant sedimentary rock, or crystalline or volcanic rocks characterize the higher mountains. The valley bottom is underlain by sand and gravel deposited by glacial ice or melt water (Streufert, 1999). Vegetation includes aspen, fir, and spruce forests along with treeless alpine tundra vegetation at higher elevations. Slope and aspect greatly influence microclimates. North-facing slopes receive more snowfall and have higher soil moisture contents. This greater moisture content supports more dense vegetation, especially coniferous forests (Soule, 1976). South-facing slopes are drier and are vegetated by sagebrush and grasses. Mean annual rainfall for the watershed is 60 cm (WRCC, 2006). The majority of precipitation falls as snow with average annual snowfall of 500 cm in Crested Butte and 1,270 cm at Kebler Pass, which is located on the western edge of the watershed.

Snowmelt dominates stream flow in Coal Creek. The mean annual flow rate of Coal Creek measured just downstream of the confluence with Elk Creek is $1.46 \times 10^7$ $m^3$ $y^{-1}$. The average flow rate is 0.46 $m^3$ $s^{-1}$; during September, the average flow rate is only 0.058 $m^3$ $s^{-1}$ (USGS, 2006).

The watershed is now used primarily for residential development, recreation, and water supply. Coal Creek serves as the drinking water supply for the Crested Butte. The drinking water intake diverts water from Coal Creek at a rate of 0.079 $m^3$ $s^{-1}$ (Larry Adams, personal communication, 2006). Two irrigation diversions take flow from Coal Creek to Smith Ranch (the Spann-Nettick ditch) and Town Ranch (the Halazon ditch). Overflow from the drinking water supply reservoir is returned to Coal Creek 60 m downstream of the Spann-Nettick diversion and 15 m upstream of the Halazon diversion.

## *Abandoned mines and natural metal deposits in the Coal Creek watershed*

The Coal Creek watershed is rich in mineral resources. Hard rock mining began in this area, which is also known as the Ruby Mining District, in 1874 when the watershed belonged to the Ute Indian Reservation (EPA, 2005a). Active mining ceased in 1974.

Vein deposits are contained in north-northeast-trending faults, dikes, and small stocks on the eastern faces of the Ruby Range. These veins are rich in copper, gold, lead, molybdenum, ruby silver, and zinc (Streufert, 1999). The three largest mines were the Standard Mine, the Keystone Mine, and the Forest Queen Mine, all of which lie on the southern face of Scarp Ridge (EPA, 2005b).

The Standard Mine was added to the U.S. Environmental Protection Agency (EPA) National Priority List in September 2005. The mine sits on 4 ha of land located approximately 16 km northwest of Crested Butte. The defunct Standard Metals Corporation owns the patented mining claims. The U.S. Forest Service owns the surrounding land. Popular hiking trails parallel the site and no access restrictions were in place. Before the start of the EPA remediation during the summer of 2006, the mine site contained

- numerous open adits and shafts, one of which was draining contaminated water from the mine,
- a dilapidated mill and other mine buildings,
- a 5-m high railroad trestle bridge in poor condition,
- a non-engineered, unlined surface impoundment, or tailings pond (90 m diameter, 4.5 m depth), and
- 63,000 $m^3$ of waste rock and mill tailings.

Acid mine drainage from the adit and the waste rock and tailings piles flowed into Elk Creek, which flows through the site. At high flow, some of the contaminated water flowed into the tailings pond, which overflowed back into Elk Creek. The rate of acid mine drainage from the Standard Mine ranges from 0.064 to 13 L $s^{-1}$. Contaminants in the acid mine drainage include arsenic, barium, cadmium, chromium, copper, lead, and zinc (EPA, 2005a). During the summer of 2006, the EPA removed the railroad trestle bridge and buildings, drained the tailings pond, and diverted the acid mine drainage and Elk Creek flow around the tailings pond. Downstream of the Standard Mine, aquatic life if nearly absent from Elk Creek (CDPHE, 2006). Elk Creek flows into Coal Creek at a distance of 3.2 km from the Standard Mine. The drinking water intake for the Crested Butte is in Coal Creek at a distance of 3.4 km downstream of the confluence of Elk Creek with Coal Creek.

The Keystone Mine is located approximately 5.0 km northwest of Crested Butte under the south slope of Mt. Emmons (Streufert, 1999). Lead, zinc, and silver were extracted from the Keystone Mine until the mid-1970s (U.S. Energy, 2006). Acid mine drainage from the abandoned Keystone Mine contains high concentrations of lead, zinc, and cadmium. The drainage is treated at the Mt. Emmons Treatment Plant, which was built in 1981 (CCWC, 2006). The Mt. Emmons Plant also treats flow emitted from exploratory cores. These cores were drilled by the Amax Corporation as part of a feasibility study investigating the extent of molybdenum and diamond deposits. The plant cost $14 million to build and the yearly operational costs are about $1 million (U.S. Energy, 2006). On February 28, 2006, U.S. Energy Corporation and Crested Corporation re-acquired the Mt. Emmons property from the Phelps-Dodge Corporation. With the acquisition also came the responsibility of running the Mt. Emmons Treatment Plant.

This 2,185 ha property contains a "world-class" molybdenum deposit. Reserves are estimated at 140 million tonnes of 0.44 percent molybdenum disulfide ($MoS_2$) (Streufert, 1999). The owners are actively pursuing development and mining given the favorable pricing environment for molybdic oxide. They are also considering the use of the Mt. Emmons Treatment Plant in future milling operations (U.S. Energy, 2006).

Silver was the main metal extracted at the Forest Queen Mine. A mill was located on-site (Hornbaker, 1984). One adit at this inactive mine drains into Coal Creek just below the old Irwin town site southeast of Lake Irwin. The flow appears to be quite low. Ongoing studies aim to determine the effect of this drainage on Coal Creek (CCWC, 2006).

An iron gossan is located just west of the Keystone Mine (Figure 3). Its surface area is approximately 1.2 ha. A gossan is formed when a series of springs flow through mineralized and fractured bedrock rich in pyrite ($FeS_2$) (CCCOSC, 2006). This process forms peat terraces composed of limonite, which is natural aggregates of hydrous ferric oxide lacking crystallization. The oxidation of pyrite produces acidic byproducts that lower the pH of water in contact with the gossan. A gossan is characterized by dark reddish-brown or moderate brown color (Kelly, 1958). Some of the water flowing over and from the gossan drains into a wetland located southwest of the gossan. The wetland, which contains acidic, metal-rich water, is known locally as "the iron fen." Recent sampling of the water flowing from the iron fen revealed high concentrations of aluminum, iron, manganese, and zinc and a pH of 3.4 (EPA, 2005a). At low flow (September 2005), drainage from the gossan and iron fen entered Coal Creek approximately 1.9 km upstream of Crested Butte's drinking water intake from two distinct surface tributaries. Observations also indicate that some of the gossan and iron fen drainage enters Coal Creek as dispersed subsurface flow. The iron fen supports a unique vegetative community that includes the round-leaved sundew (*Drosera rotundifolia*), a small, carnivorous plant that has not been found anywhere else in the central or southern Rocky Mountains. The U.S. Forest Service has expressed concerned that molybdenum mining on Mt. Emmons may alter or exterminate the sundew population. Another concern is the alteration of groundwater flow by mining operations, which may remove water from springs that feed the fen (USFS, 1981).

### *Metal-loading tracer-dilution method*

A metal-loading tracer-dilution experiment provides data for the calculation of metal loading rates (in units of mass of metal per time). The metal loading rate is calculated as the product of the metal concentration (mass of metal per volume of water) and the stream flow rate (volume of water per time). Metal loading rates of streams and tributaries are used to account for flow rate in comparisons of sources of metals to a watershed (Kimball, 1997). The stream flow rate is quantified using the tracer-dilution method. Metal concentrations are determined by synoptic sampling during a tracer-dilution experiment. Tracer dilution and synoptic sampling are described in the following paragraphs.

The tracer-dilution method allows quantification of stream flow rate by monitoring the dilution of a tracer as it is transported downstream. The tracer of known and constant concentration is injected at a constant rate until the tracer reaches a steady concentration over the reach of the stream being investigated. Flow rate is determined by a mass balance for the tracer which includes the flow rate and tracer concentration of the stream above the injection, the flow rate and tracer concentration of the injection, and the downstream tracer concentration. With these parameters, the downstream flow rate can be calculated (Kimball, 1997).

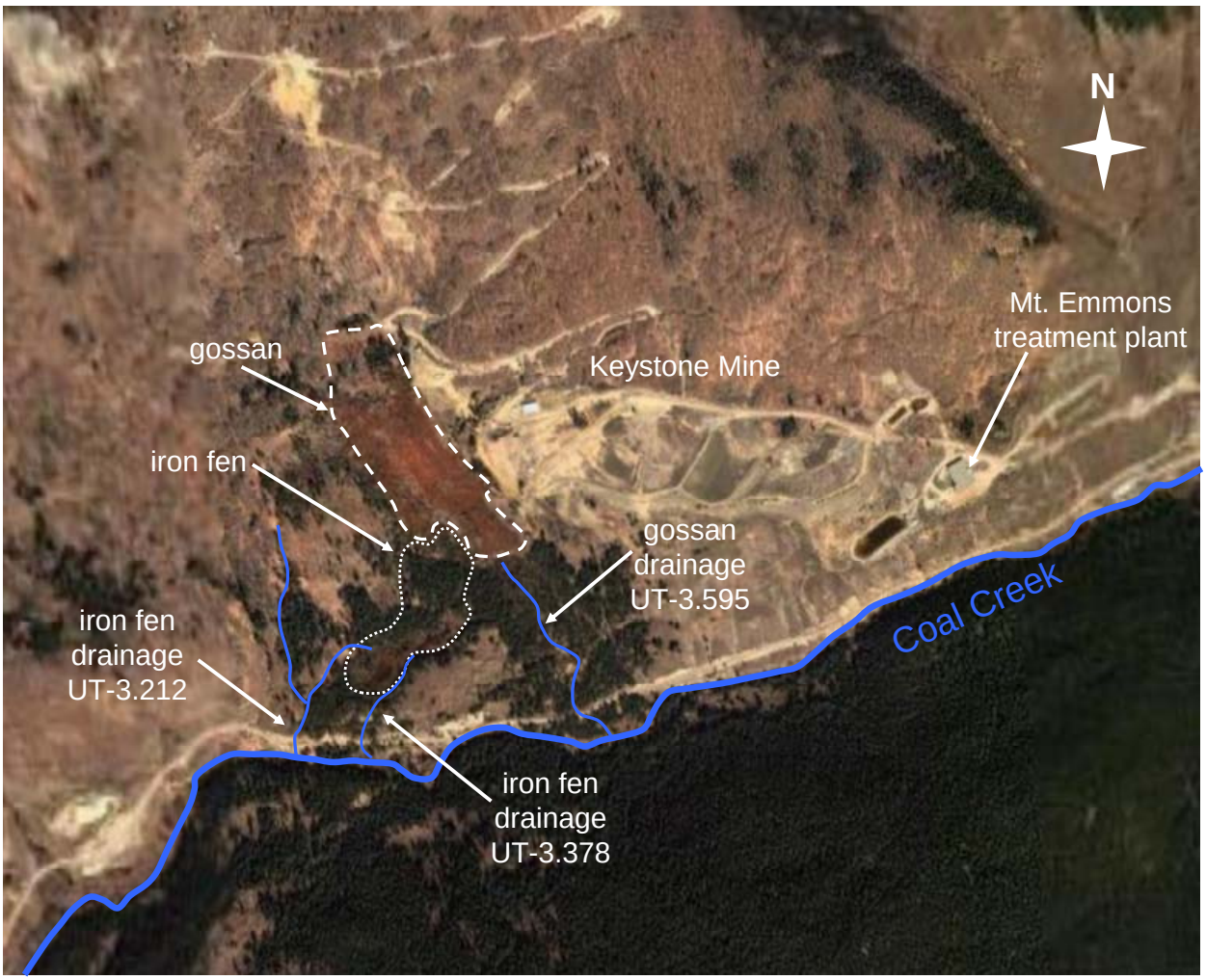


**Figure 3**. Aerial view of Coal Creek near the Keystone Mine at the base of Mt. Emmons, including the gossan located just west of the Keystone Mine, the iron fen, unnamed tributaries at stream distances of 3.212, 3.378, 3.595 km downstream of the injection site used for this study, and the Mt. Emmons treatment plant. Coal Creek flows to the northeast. The aerial photo was retrieved using Google Earth™ (http://earth.google.com).

The tracer-dilution method accounts for flow in the stream channel and flow through the hyporheic zone (the layer of streambed sediment that exchanges water with the stream). Flow through the hyporheic zone is normally substantial for high-gradient, shallow mountain streams such as Coal Creek (Bencala et al., 1990). Traditional current meter flow measurements typically underestimate the flow of mountain streams because water flowing in the hyporheic zone is not measured. The tracer-dilution method also accounts for dispersed groundwater inputs as well as seeps or springs discharging over a large area. These non-point sources affect quantification of flow because they contribute to the dilution of the tracer; however, the portion of flow attributable to surface tributaries versus dispersed groundwater sources cannot be distinguished.

The typical application of the tracer-dilution method does not account for losses of flow from a stream (e.g., flow from the stream to groundwater over a "losing reach," withdrawal water to an irrigation ditch or water supply) because losses of flow do not change the concentration of the injected tracer. Flow in losing reaches of streams can be measured by extensive sampling at multiple locations to account for mass balance of the tracer.

The tracer-dilution method requires that the tracer to be (1) transported conservatively through the stream, (2) present in concentrations well above the background concentration of the tracer, and (3) injected until the entire stream reach, including the hyporheic zone, are saturated with the tracer. Conservative transport of the tracer requires that the tracer not react with solids in the stream or hyporheic zone (e.g., stream sediments, suspended sediment). Tracers must not degrade during the tracer-dilution experiment by chemical or biological reactions (e.g., hydrolysis, photolysis). If the tracer transport is conservative, then it can be assumed that all downstream decreases in the tracer concentration are caused by dilution of the tracer by addition of tributary and groundwater inflows of low tracer concentration (Kimball et al., 2002). The concentration of the tracer must be adequately high to clearly distinguish the added tracer from background concentrations. The background tracer concentration of all downstream tributaries must also be exceeded. For the tracer concentration to accurately provide flow rates, the injection must continue until all parts of the stream, including the hyporheic zone and all surface storage zones, become saturated with tracer. Under these steady-state conditions, the tracer reaches a "plateau concentration" (Bencala et al., 1990).

Synoptic sampling is the spatially detailed sampling of stream sites and all tributary inflows that provides a one-time description of stream and tributary chemistry. It gives a "snapshot" of stream chemistry and flow that allows quantification of in-stream loads (Kimball, 1997). The "snapshot" is not instantaneous, but represents the sampling period of several hours. A sample site spacing of hundreds of meters is recommended for practical analysis of stream chemistry (Bencala et al., 1990).

# MATERIALS AND METHODS

### *Low-flow tracer-dilution experiment*

The September 2005, low-flow tracer-dilution experiment was performed along a 9.4 km reach of Coal Creek from about 1 km above Splain's Gulch to the northern edge of the Town of Crested Butte. Low flow tracer-dilution studies aid in identifying sources contributing to these toxic metal concentrations.

Lithium chloride (LiCl) was used as the tracer for this study. Lithium is reported to act conservatively in streams with low pH (Paschke et al., 2005). The background lithium concentration of natural waters is typically low. Chloride is commonly known as the "universal tracer" and is expected to behave conservatively in most aquatic environments (Bencala et al., 1987), but background chloride concentrations may be high.

### *Preliminary tracer injection*

Prior to injection of the lithium chloride tracer, a sodium chloride (NaCl) pulse tracer test was conducted to determine stream velocity. The purpose of the test was to estimate the time required for the tracer to reach the downstream end of the study reach.

The NaCl solution was made by mixing 22.7 kg of NaCl and 151 L of stream water in a 210 L polyethylene barrel. At 12:28 on September 3, 2005, the entire barrel containing the NaCl solution instantaneously added to Coal Creek at the injection site. Downstream transport of the tracer was documented using conductivity meters (Orion, models 105 and 122) at five sample sites located within the first 1.3 km of the study reach. The background conductivity was measured at each of these sites. The conductivity was then monitored until it peaked and began to decline. Stream velocity was calculated by dividing the distance traveled by the time required for the conductivity to peak at each monitoring site. The stream velocity was estimated at 0.061 m $s^{-1}$.

Using the conductivity data collected during this preliminary tracer injection (not included in this report), we determined that a 43 h injection would be required for the LiCl tracer to reach the downstream end of the study reach, the north side of the Crested Butte, at a distance of 9.387 km.

### *Tracer Injection procedure*

The initial batch of the lithium choride tracer solution was prepared by pumping stream water into a 405 L polyethylene tank and adding approximately 34 kg of lithium chloride (LiCl anhydrous technical grade; FMC Industrial Chemicals, CAS no. 7447-41-8). The stream water was pumped into the tank using a pump driven by a gasoline engine (Honda WX-10). The concentration of lithium chloride in the injection

solution was selected to produce a lithium concentration 100 times greater than the upstream (background) lithium concentration at the downstream end of the stream reach. The solution was mixed with a paddle and recirculated with a pump (Fluid Metering Instruments PM6014 pump, Q410-2 pump head) for 90 min until the lithium chloride was completely dissolved (Figure 4).

**Figure 4.** Lithium chloride was added to the injection solution and stirred with a paddle for 90 min until the salt was completely dissolved.

The stock tracer solution was replenished twice during the injection period (Table 1). On the September 4 at 09:10, 150 L of the original tracer solution remained. A new batch was prepared by pumping 208 L of stream water into a 210 L polyethylene barrel. A second barrel was used for mixing the new solution to avoid interrupting the injection process. Lithium chloride was added to the 210 L polyethylene barrel until the conductivity of the second stock tracer solution matched the conductivity of the original tracer solution. The conductivity of the original solution was measured as 107.0 mS $cm^{-1}$ with a conductivity meter (Orion, model 105) calibrated with a 1413 μS $cm^{-1}$ standard. A total of 16 kg of lithium chloride was added to the second stock tracer solution. The final conductivity of the second stock tracer solution was 109.5 mS $cm^{-1}$. The newly mixed tracer solution was pumped into the original 405 L tank at 09:40 on September 4. The conductivity of the replenished tank was 107.5 mS $cm^{-1}$.

On September 4 at 17:45, 220 L of tracer solution remained in the injection tank and the conductivity was measured at 110.5 mS $cm^{-1}$. A third stock tracer solution was prepared by pumping 208 L of stream water into the 210 L polyethylene barrel and adding 17 kg of LiCl so that the conductivity reached 109.7 mS $cm^{-1}$. This third batch of tracer solution was pumped into the 405 L tank and lasted for the remaining duration of the injection.

The tracer solution was injected into Coal Creek using a pump (Fluid Metering Intstuments PM6014 pump, Q410-2 pump head, V200 stroke rate controller). Tubing (Fisherbrand silicon tubing, 9.5 mm diameter, 3.0 mm wall) was used to transfer the tracer solution from the 405 L mixing tank through the metering pump and into the creek at the injection site. The lithium chloride tracer was injected over a period of 50.5 h. A constant injection rate of 250 mL $min^{-1}$ was desired to ensure steady-state conditions. The actual measured injection rate varied from 185-280 mL $min^{-1}$ (Table 1).

For this study, 47 in-stream sites and 13 tributary sites were selected (Figure 5). The in-stream sample sites were intended to bracket all surface tributary inflows. A global positioning receiver (Garmin GPS 12) global positioning receiver was used to space the in-stream sites at intervals of about 200 m and to record all sampling locations. The sample site spacing provided spatially detailed concentration profiles to examine metal inputs. This sampling regime is more intensive and expensive than simply measuring water-quality parameters at an outlet downstream of acid mine drainage. However, it quantifies impacts from individual sources to provide information necessary for restoration decisions (Kimball et al., 2001).

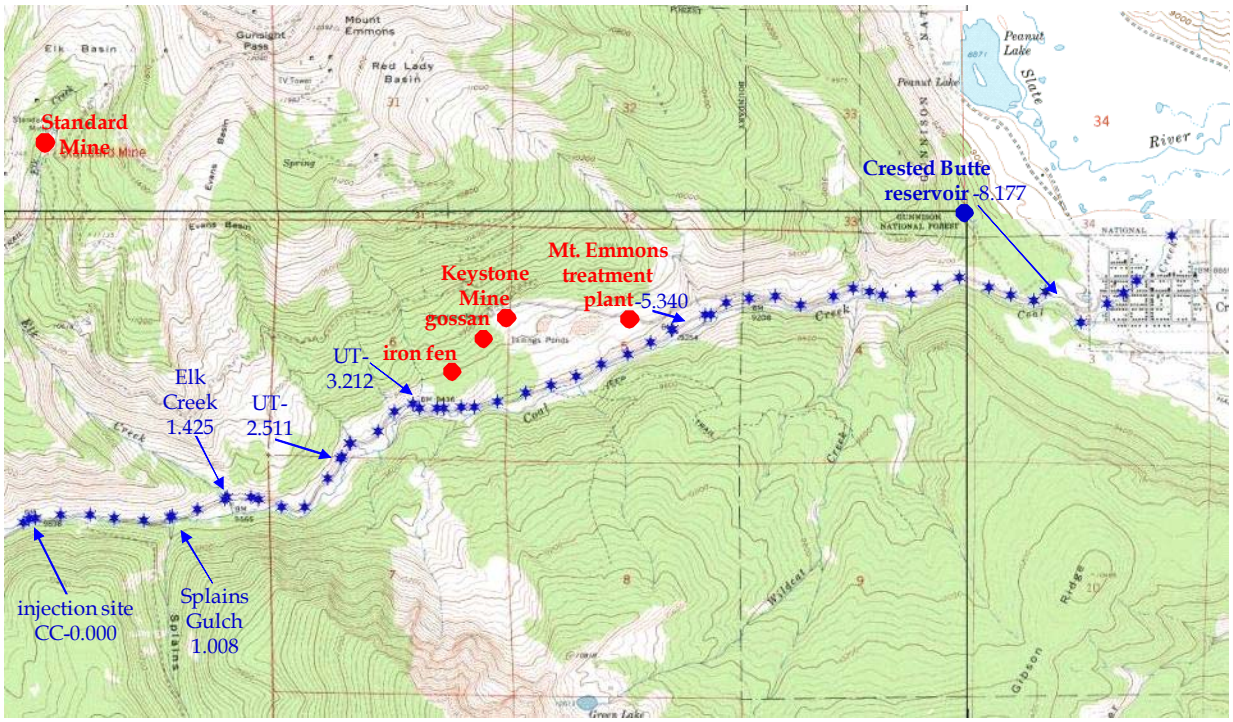


**Figure 5.** Coal Creek synoptic sample sites including in-stream sites (blue). Tributary sampling sites are not shown. Distances from the tracer injection site (distance 0.000 km at the upstream end of the study reach) are given in kilometers. The Standard Mine, Keystone Mine, iron gossan, and Town of Crested Butte drinking water reservoir are also shown.

In-stream sample sites were designated with the letters "CC-" followed by a number representing the distance in kilometers from the injection site. An upstream site located 51 m upstream of the injection site (designated "CC-(-0.051)") was sampled every 4 h for the duration of the injection to provide background lithium and chloride concentrations. The upstream site was designated "CC-0.000". The most downstream site ("CC-9.387") was located on the northern edge of the Town of Crested Butte at a distance of 9.387 km downstream of the injection site. At the downstream site, samples were collected every 45 min on the day of synoptic sampling to identify the leading edge of the tracer plume.

Surface tributary sample sites were designed either as the name of the tributary (e.g., Splain's Gulch, Elk Creek, the Mt. Emmons Treatment Plant effluent channel, the drinking water return reservoir) or as "UT-" for unnamed or unidentified tributaries.

The distances are presented with a precision of 1 m, or 0.001 km, to clearly establish the downstream order. The downstream order of the sites is accurate, but the precision of the downstream distances is not 0.001 km. We estimate that the precision of the downstream distances is about 10 m, or 0.010 km, because the locations were determined by global positioning system.

***Sampling procedures***

Synoptic sampling began 50 h after the start of the injection. The sampling event lasted approximately 5.5 h. The sampling was conducted by a six-member team. One individual remained at the injection site taking upstream and injection samples at regular time intervals and monitoring the injection pump to maintain a steady injection rate. A second individual stayed at the downstream end of the study reach, CC-9.387, taking samples every 45 min from 11:00 to 19:50 on the day of synoptic sampling. The downstream site was monitored for the entire day to allow for development of a breakthrough curve. Ideally, a rising tracer concentration followed by a plateau of the tracer concentration over time would indicate the time of tracer arrival at CC-9.387. The four remaining team members conducted synoptic sampling of Coal Creek from 15:00 to 19:50. Sampling began on the upstream section of the study reach. Team members successively proceeded, or "leap-frogged", towards the downstream end of the study reach until samples were obtained at each synoptic site.

For tributaries entering Coal Creek from culverts on the north side of the creek, synoptic samples were taken from the culverts immediately south of County Highway 12 (Figure 6). Drainage entering Coal Creek from the north is typically routed along the highway, through a pipe underneath the highway, and then down-slope into Coal Creek. Field reconnaissance in June 2006, during high flow conditions, indicated that the majority of the flow from the iron fen and gossan tributaries is absorbed into the ground before entering Coal Creek. Approximately 50% of the flow from UT-3.212 and 100% of the flow from UT-3.455 and UT-3.595 re-entered the groundwater system before entering Coal Creek (Figure 6). During low flow, it is likely that even a larger percentage of the flow would be absorbed before entering Coal Creek.

At each sample site, stream water samples were collected in a 1 L bottle (Nalgene 1 L high density polyethylene wide mouth) and a 60 mL amber glass bottle. Samples were kept on ice in coolers for field preservation. Duplicate samples were collected at nine sites for quality assurance.

**Table 1.** Sequence of events for the September 2005 Coal Creek metal-loading tracer-dilution study.

| Date | Clock Time | Experiment Time (h) | Activity |
|---|---|---|---|
| 9/3/2005 | 900 | | Synoptic sample sites marked with GPS |
| | 1130 | | First stock tracer solution prepared, 34 kg LiCl and stream water added to 405 L tank |
| | 1300 | 0.0 | Start of injection period, pump rate set to 250 mL $min^{-1}$ |
| | 1300 | 0.0 | Upstream site sampling begins |
| 9/4/2005 | 730 | 18.5 | Pump rate decreased to 185 mL $min^{-1}$ overnight, reset pump rate to 250 mL $min^{-1}$ |
| | 940 | 20.7 | 150 L of original injection solution remaining, conductivity of solution = 107.0 mS $cm^{-1}$ |
| | 940 | 20.7 | Begin mixing second batch of stock tracer solution, 16 kg LiCl added to 210 L barrel, conductivity = 109.5 mS $cm^{-1}$ |
| | 1000 | 21.0 | Stock tracer solution replenished with second batch, new conductivity = 107.5 mS $cm^{-1}$ |
| | 1110 | 22.2 | Injection flow rate measured at 280 mL $min^{-1}$ then reset to 255 mL $min^{-1}$ |
| | 1600 | 27.0 | Flow rate measured at 250 mL $min^{-1}$ |
| | 1745 | 28.8 | 220 L of tracer solution remaining in 405 L tank, conductivity = 110.5 mS $cm^{-1}$ |
| | 1745 | 28.8 | Third stock tracer solution prepared by mixing 17 kg LiCl and stream water in 210 L barrel, conductivity = 109.7 mS $cm^{-1}$ |
| | 1750 | 29.3 | Third stock tracer solution added to 405 L tank, new conductivity = 110 mS $cm^{-1}$ |
| | 1830 | 29.5 | Flow rate measured at 280 mL $min^{-1}$ then reset to 250 mL $min^{-1}$ |
| | 0600 - 2000 | 17.0 - 31.0 | Injection monitored |
| 9/5/2006 | 0 | 35.0 | Flow rate measured at 250 mL $min^{-1}$ |
| | 620 | 41.3 | Flow rate measured at 230 mL $min^{-1}$ then reset to 250 mL $min^{-1}$ |
| | 1110 | 46.2 | Downstream site sampling begins, continues at 45 min intervals throughout day |
| | 1110 | 46.2 | Flow rate measured at 260 mL $min^{-1}$ then reset to 250 mL $min^{-1}$ |
| | 1300 | 48.0 | Flow rate measured at 260 mL $min^{-1}$ then reset to 250 mL $min^{-1}$ |
| | 1500 | 50.0 | Synoptic sampling began |
| | 1530 | 50.5 | Tracer injection discontinued |
| | 1530 | 50.5 | Upstream site sampling discontinued |
| | 2030 | 55.5 | Synoptic sampling finished |

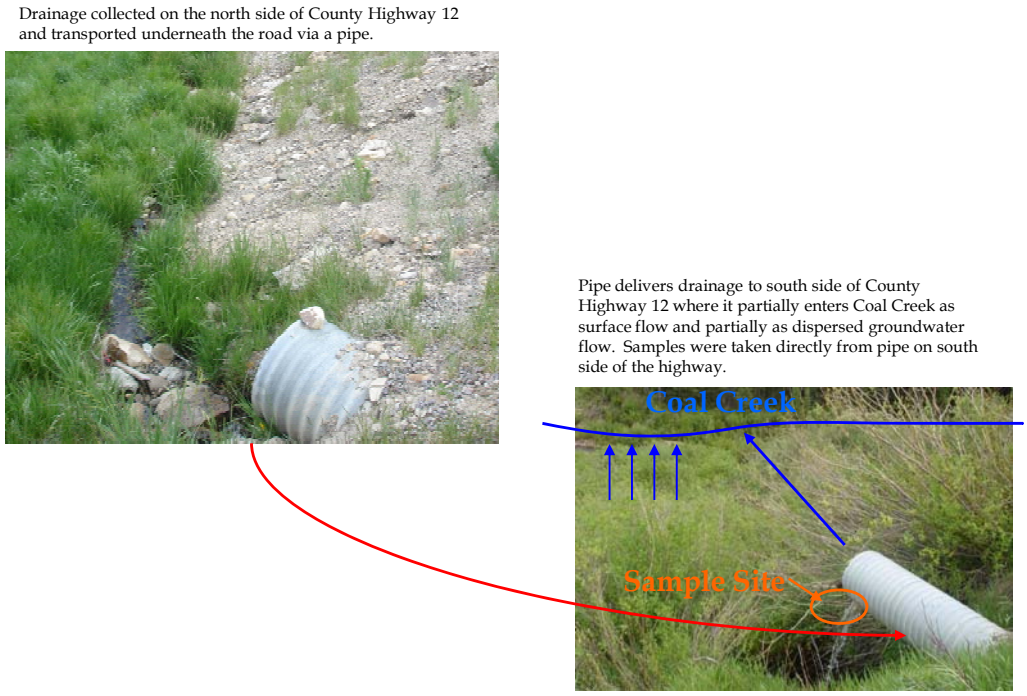


**Figure 6.** Illustration of tributary drainage transported down culvert paralleling County Highway 12, through pipe underneath the road, and into Coal Creek. A portion of the flow enters Coal Creek as a surface point source while a portion enters Coal Creek as dispersed subsurface flow.

### *Sample processing and preservation*

A portion (300 mL) of each 1 L sample was filtered through nylon membranes (Fisherbrand, 0.45 µm pore size, 47 mm diameter) using filtration vessels (Nalgene 500 mL filter holder with receiver) upon arrival at the field laboratory. We used 0.45 µm because the lithium and metal analyses were to be performed by the EPA. The EPA and others have historically used 0.45 µm filters because of their ready availability and greater capacity for filtration before clogging (Morrison and Benoit, 2001; EPA, 2006). The historical use of the 0.45 µm filters also allows for comparison to previous studies. One disadvantage of this size filter is that the pore size is operationally defined and causes ambiguous separation of particle size classes. Many colloids in natural waters pass through 0.45 µm filters (Pham and Garnier, 1998; Morrison and Benoit, 2001). On the opposite end of the spectrum, membrane clogging can occur during filtration, reducing the effective pore size and causing the retention of an increasing mass of colloids.

Filtration vessels were rinsed three times with high-purity water (Millipore Milli-Q, greater than 18 Mohm resistivity) following each filtration. The membrane filters were handled with tweezers. Lab personnel wore gloves at all times during the filtration. A vacuum pump (Gast 0523-101Q-G582DX) with attached tubing (Fisherbrand peristaltic

tubing, 6.4 mm diameter, 2.4 mm wall) was used to apply suction to the filtration vessels and increase the filtration rate. Another 300 mL of the 1 L sample was not filtered. The filtered sample composed the dissolved portion and provided dissolved constituent concentrations. The unfiltered sample provided total concentrations. The colloidal concentration was indirectly determined as the difference between the total and dissolved concentrations.

Both the total and dissolved samples were acidified to a pH of less than 2 with trace metal-grade nitric acid (Fisher Chemical). One mL of nitric acid was added to each 250 mL filtered and unfiltered sample using a pipette (Fisherbrand 100-1000 µL Finnpipette, U16138, and Fisherbrand Redi-Tip General Purpose 101-1000 µL pipette tips, 21-197-8F). Each 300 mL sample was further divided into a 250 mL sample and a 30 mL sample (Nalgene 250 mL and 30 mL high density polyethylene wide mouth sample bottles). The 250 mL samples were sent to the EPA laboratory for inorganic constituent analysis. The 30 mL sample along with any additional remaining sample was kept as backup at the University of Colorado at Boulder. The 60 mL samples in glass amber bottles remained unfiltered to provide total organic carbon (TOC) concentrations. TOC samples were preserved by reducing pH to less than 2 by pipetting 0.5 mL of phosphoric acid (Fisher Chemical) into the glass amber bottle.

The 250 mL total and dissolved samples were prepared, labeled, and documented in accordance with the EPA Superfund Analytical Services/Contract Laboratory Program for multi-media, multi-concentration inorganic analysis, ILMO5.3 (EPA, 2006). These total and dissolved samples were shipped overnight on ice to an EPA contract laboratory for analysis.

### *Analytical Methods*

Sample pH was measured in the field lab within 24 h of collection (Thermo Orion 250A+ meter, 9157BN electrode). The pH meter was calibrated using pH 4 and 7 standards at room temperature. Samples were stored at room temperature before pH measurement.

Total organic carbon (TOC) concentrations were measured using a TOC analyzer (Sievers, 800 Series) about 30 d after sample collection. The instrument converts organic carbon in the sample to carbon dioxide ($CO_2$) by oxidizing organic carbon. A gas-permeable membrane selectively allows only the $CO_2$ to pass through for measurement. The quantity of $CO_2$ produced through oxidation is directly proportional to the amount of carbonaceous material in the sample. The analyzer uses a conductometric TOC measurement technique. This technique uses conductivity meters that are not susceptible to drift or fluctuation. Calibration is only required once annually so no calibration was performed prior to these runs. Vials (Fisherbrand 15 mL glass amber vials) were labeled, filled with sample, and then loaded into the TOC autosampler. Two sample vials of high-purity water were run first to flush the system of any trace organic carbon. A vial of high-purity water was also run as the last sample to wash the analyzer tubing of any residual organic carbon.

Total and dissolved concentrations of the following twenty-three elements were measured by inductively coupled plasma-atomic emission spectrometry (ICP-AES) and inductively coupled plasma-mass spectrometry (ICP-MS): aluminum, antimony, arsenic, barium, beryllium, cadmium, calcium, chromium, cobalt, copper, iron, lead, lithium, magnesium, manganese, nickel, potassium, selenium, silver, sodium, thallium, vanadium, and zinc. ICP-MS analysis was performed for constituents measured below ICP-AES detection limits. The ICP-AES and ICP-MS analyses were carried out by an EPA contract laboratory, Liberty Analytical Corporation (Cary, NC). Additional ICP-AES (ARL 3410+ and AIM 1250 sampler) analyses were performed to measure the lithium concentrations of the injectate samples at the Laboratory for Environmental and Geological Studies (LEGS), Department of Geological Sciences, University of Colorado at Boulder. These additional analyses were performed to ensure the accuracy of the measured injectate lithium concentrations. Detection limits for ICP-AES and ICP-MS analyses are listed in Table 2.

EPA contract labs must use a computer-controlled ICP-AES with background correction, a radio frequency generator, and a supply of argon gas of welding grade or better. The EPA performs a digestion on samples analyzed with ICP-AES. The digestion consists of adding 50-100 mL of well-mixed sample, 2 mL nitric acid, and 10 mL hydrochloric acid to a heating vessel. The vessel is heated at 92-95 $^{o}$C for 2 h or until sample volume is reduced by half. The sample is cooled and filtered to remove insoluble material. The sample volume is adjusted to back to pre-digestion volume with reagent water. Sample vessels are then filled and placed in the sampling carousel.

EPA contract labs must use an ICP-MS capable of scanning 5-250 atomic mass units (amu) with a minimum resolution of 1 amu peak width at 5% peak height, a conventional or extended range detector, high purity (99.99%) argon gas, a variable speed peristaltic pump, and a mass-flow controller on the nebulizer gas supply. The EPA also performs a digestion on samples analyzed with ICP-MS as described above for the ICP-AES. Following digestion, samples are ready for ICP-MS analysis.

Dissolved chloride ion concentrations were analyzed using an ion chromatograph (IC; Dionex model ICS-2000) at the Institute for Arctic and Alpine Research (INSTAAR) at the University of Colorado at Boulder. An additional filtration was performed (Onguard II Na Cartridges, Dionex PN062948) prior to IC runs to remove trace metals that might be harmful to the anion exchange column. Only dissolved chloride concentrations were measured because particulates present in unfiltered samples damage IC columns. Four standards were used for IC analysis:

1. 0.20 mg $L^{-1}$ $Cl^{-}$, 0.05 mg $L^{-1}$ $SO_4^{2-}$, 0.005 mg $L^{-1}$ $NO_3^{-}$
2. 2.00 mg $L^{-1}$ $Cl^{-}$, 0.50 mg $L^{-1}$ $SO_4^{2-}$, 0.050 mg $L^{-1}$ $NO_3^{-}$
3. 20.0 mg $L^{-1}$ $Cl^{-}$, 5.00 mg $L^{-1}$ $SO_4^{2-}$, 0.50 mg $L^{-1}$ $NO_3^{-}$
4. 200.0 mg $L^{-1}$ Cl, 50.0 mg $L^{-1}$ $SO_4^{2-}$, 5.00 mg $L^{-1}$ $NO_3^{-}$.

Results were corrected for machine drift using a linear regression technique based on calibration standards analyzed at the beginning and end of each run. Blanks composed of high-purity water were run intermittently throughout each run to flush the IC.

The IC detects different ions based on the different rates at which they migrate through the IC column. These rates depend on the extent of interaction with ion exchange sites on the column. Ions are identified based on their retention time in the column. They are quantified by integrating sample chromatograph peak areas and comparing them to peak areas produced by the standards. The nitric acid used to preserve the samples created large nitrate peaks on the chromatographs. The nitrate peak blocked detection of elements with similar retention times such as bromide. However, chloride detection was not impaired as chloride elutes considerably later than nitrate. Detection limits for IC analyses are listed in Table 2.

Six suspended sediment samples were analyzed for relative elemental composition using an electron microprobe (JEOL JXA-8600) at LEGS, Department of Geological Sciences, University of Colorado at Boulder. The microprobe is equipped with four wavelength-dispersive spectrometers and one energy-dispersive spectrometer. Analytical sensitivity ranges from 50-500 mg $kg^{-1}$. Samples were prepared as a flat mounts and secured with epoxy. They were then coated with a thin carbon layer using a carbon evaporator. Digital x-ray mapping images and elemental spectra (Geller dPic hardware) were obtained.

### *Flow rate calculations*

The tracer-dilution method assumes conservation of mass (Table 3, Equations 1 and 2) between upstream and downstream sample locations. Conservation of mass requires that flow or mass at a downstream sample location is equal to flow or mass at an upstream sample location plus the flow or mass entering the stream at the injection site (Kimball et al., 2002). Steady-state conditions dependent upon a constant injection tracer concentration and a constant tracer injection rate are assumed. Table 3 displays the equations used for flow rate determination.

All inflow between two sites bracketing a visible tributary was assumed to be due to tributary inflow. This might not be the case in reality, because the tracer-dilution method quantifies flow from point sources as well as flow from distributed groundwater input or springs or seeps discharging over a large area. However, the fraction of flow input attributable to dispersed sources cannot be quantified using tracer-dilution. Tributary flow rates were calculated as the difference between flow at the sample location upstream of the tributary and flow at the sample location downstream of the tributary.

The quantity $Q_{lest}$ in Equation 6 (Table 3) was estimated. Flow downstream of tributaries containing background tracer concentrations greater than in-stream concentrations had to be estimated because tracer-dilution equations break down under these conditions and no direct flow meter measurements were taken. $Q_{lest}$ was estimated by field personnel as a percentage of in-stream flow just upstream of the tributary confluence with Coal Creek.

**Table 2.** Minimum detection limits reported for target analytes measured using ICP-AES, ICP-MS, and IC analysis.

| **Analyte** | **ICP-AES CRQL[1], µg $L^{-1}$** | **ICP-MS CRQL, µg $L^{-1}$** | **IC DL[3], µg $L^{-1}$** |
|---|---|---|---|
| Aluminum | 200 | -- | |
| Antimony | 60 | 2 | |
| Arsenic | 10 | 1 | |
| Barium | 200 | 10 | |
| Beryllium | 5 | 1 | |
| Cadmium | 5 | 1 | |
| Calcium | 5000 | -- | |
| Chloride | | | 200 |
| Chromium | 10 | 2 | |
| Cobalt | 50 | 1 | |
| Copper | 25 | 2 | |
| Iron | 100 | -- | |
| Lead | 10 | 1 | |
| Lithium | 5, 2[2] | -- | |
| Magnesium | 5000 | -- | |
| Manganese | 15 | 1 | |
| Nickel | 40 | 1 | |
| Potassium | 5000 | -- | |
| Selenium | 35 | 5 | |
| Silver | 10 | 1 | |
| Sodium | 5000 | -- | |
| Thallium | 25 | 1 | |
| Vanadium | 50 | 1 | |
| Zinc | 60 | 2 | |

[1] CRQLs are contract required quantitation limits. These are minimum levels are quantitation acceptable under the contract Statement of Work (SOW; EPA, 2006).

[2] Detection limit reported by LEGS.

[3] Detection limit reported by INSTAAR.

**Table 3.** Equations used to calculate flow rates and mass loading rates (Kimball et al., 2002) for Coal Creek tracer-dilution study.

| Calculated Variable | Equation | Variable Definition |
|---|---|---|
| Mass balance downstream from injection site | $M_B = Q_B C_B$ (1)<br>$M_B = Q_A C_A + Q_{inj} C_{inj}$ (2)<br>$Q_B = Q_A + Q_{inj}$ (3) | $M_B$, mass loading rate downstream of injection site<br>$C_A$, tracer concentration upstream of injection site<br>$C_B$, tracer concentration downstream of injection site<br>$C_{inj}$, injectate tracer concentration<br>$Q_A$, flow rate upstream of injection site<br>$Q_B$, flow rate downstream of injection site<br>$Q_{inj}$, injection flow rate |
| Flow rate at first site downstream of injection site with uniform background concentration | $Q_B = Q_{inj} \frac{C_{inj} - C_A}{C_B - C_A}$ (4) | All variables defined above |
| Flow rate at subsequent downstream sites with uniform background concentration and upstream surface inflow contribution | $Q_C = Q_B \frac{C_B - C_I}{C_C - C_I}$ (5) | $C_C$, tracer concentration at downstream site<br>$C_I$, tracer concentration of inflow site<br>$Q_C$, flow rate at downstream site |
| Flow rate at sites downstream of inflow with tracer concentration above background tracer concentration | $Q_D = \frac{Q_C C_C + Q_{Iest} C_{IN}}{C_D}$ (6) | $C_{IN}$, tracer concentration of inflow with non-uniform background concentration<br>$C_D$, tracer concentration downstream of inflow of concentration $C_{IN}$<br>$Q_{Iest}$, visually estimated inflow rate |

### *Metal-loading calculations*

Stream flow and metal concentration at each synoptic sample site were multiplied to obtain a metal-loading rate (kg $d^{-1}$) for each site. These metal-loading rates produce a metal-loading profile for the length of the study reach. The load at the downstream end of a stream reach is equal to the load at the upstream end plus load contributions from all sources between the ends of the reach. The load is used to identify metal sources within the watershed. Increases in the metal load between sites indicate a metal source. Metal load decreases indicate a net loss of dissolved metal resulting from precipitation, sorption, or chemical reactions. The downstream load minus the upstream load between two sites is defined as the net load change. The cumulative load is the sum of the positive load changes for the entire study reach. The cumulative load is held constant for a negative load change between sites.

The cumulative load approximates the minimum possible metal load contributed to the stream (Kimball et al., 2002). The tributary load (%) is defined as

$$tributary\ load\,(\%) = \frac{load_i}{\sum_i load} \times 100 \qquad (7)$$

where $load_i$ (kg $d^{-1}$) is the loading rate at a specific tributary and the sum of the loads is the cumulative total of all tributary inputs (kg $d^{-1}$).

### *Water quality standards and hardness*

All surface waters in the State of Colorado must meet physical and chemical water quality requirements set by the Colorado Department of Public Health and Environment (CDPHE). Coal Creek is classified as a Class 1 – Cold Water Aquatic Life stream because the summer water temperature does not often exceed 20 $^{o}$C and as a Domestic Water Supply because Coal Creek supplies Crested Butte's drinking water (CDPHE, 2005). As such, Coal Creek must meet all requirements put forth by the CDPHE for these stream types. For protection of aquatic life, CDPHE gives chronic and acute toxicity limits for metals. The chronic standard is defined as the concentration limit that protects 95% of the genera from the chronic toxic effects of metals. Acute toxicity is defined as the concentration limit that protects 95% of the genera from the lethal affects of metals. Standard exceedances should not occur more than once every three years on average (CDPHE, 2005).

Many of the CDPHE metal standards are based on hardness measured as mg $L^{-1}$ $CaCO_3$. Hardness was calculated as the sum of the total calcium and magnesium ion concentrations:

$$Hardness = 50.05\,([Ca] + [Mg]) \qquad (8)$$

where [Ca] and [Mg] are the total concentrations of the calcium and magnesium ion in units of milliequivalents per liter (meq $L^{-1}$). Calcium and magnesium concentrations

were measured at each synoptic sample site and allowed for hardness calculations at each site. A hardness profile for the entire length of the stream was developed. The standard and acute toxicity limits calculated as a function of hardness were compared to measured metal concentrations along Coal Creek for cadmium, chromium(III), copper, lead, manganese, nickel, and zinc. Parameters that are not hardness-based including pH and acute and chronic toxicity standards for aluminum, arsenic, chromium(VI), and iron were also compared to measured values.

The Mt. Emmons Treatment Plant adds lime during the treatment process to raise the pH of Keystone Mine drainage to between 10 and 10.5 (John Perusek, personal communication, July 15, 2005). Cadmium and manganese require this pH increase for precipitation and removal. The addition of calcium results in a significant increase in the hardness of Coal Creek downstream of the treatment plant effluent. The increase in hardness increases the CDPHE hardness-based aquatic life standards. Competition between calcium and metals for binding sites on colloids is expected to reduce the toxicity of metals to aquatic life.

# RESULTS

## *Overview*

The following chapter presents pH, total organic carbon (TOC), calcium and magnesium concentrations, hardness, metal concentrations, metal loading, and mineralogical data resulting from multiple laboratory analyses of samples collected during synoptic sampling of Coal Creek on September 5, 2005. The results represent stream chemistry at the time of the synoptic sampling. The flow in Coal Creek was low. Weather conditions were mostly sunny with a temperature of approximately 21°C. A light rain fell for approximately 30 min during synoptic sampling. This rain event was not heavy enough to significantly influence flow or to create any runoff.

## *Surface Tributaries and Wetlands*

Two of the main natural tributaries to Coal Creek, Splain's Gulch and Elk Creek, are located at 1.008 km and 1.425 km, respectively. Two unnamed tributaries, UT-3.212 and UT-3.455, drain the iron fen. UT-3.595 contains drainage directly from the gossan (Figure 3). Crested Butte's drinking water intake at 5.296 km is followed immediately by the Mt. Emmons Treatment Plant effluent release channel at 5.340 km. The Spann Nettick ditch located at 8.047 km diverts flow out of Coal Creek between CC-7.844 and CC-8.085. Overflow from the drinking water reservoir is returned to Coal Creek through at 8.097 km. The Halazon diversion is located immediately downstream of the drinking water return flow at 8.177 km.

A large wetland exists between CC-2.021 and CC-2.580. Smaller wetlands occurred between CC-3.165 and CC-3.455 near the two iron fen drainages. Site CC-2.467 is located in the wetland reach of Coal Creek and the sample was mistakenly taken from an apparently stagnant side channel that did not exchange with the creek flow; therefore, a tracer concentration for CC-2.467 was not available. This absent data produces a discontinuity in flow and metal loading graphs at CC-2.467.

## *Coal Creek pH*

The pH in Coal Creek varied from a minimum of 6.97 at CC-2.580 to a maximum of 7.69 at CC-9.387 (Figure 7), a range of only 0.72 pH units. The pH of Coal Creek at the Crested Butte drinking water intake (D.W. Intake) is 7.24. The Colorado Department of Public Health and Environment (CDPHE) set a pH window of 6.5-9.0 as the standard for cold water aquatic life. The acceptable pH range for a domestic drinking water supply is 5.0-9.0 (CDPHE, 2005). Cold water aquatic life and domestic drinking water supply criteria for stream pH were met at all sample locations in Coal Creek. The pH of unnamed tributaries UT-3.212, UT-3.455, and UT-3.595 fell below the minimum pH standard. Unnamed tributaries UT-5.517 and UT-6.692 came within 0.1 pH units of the minimum aquatic life standard.

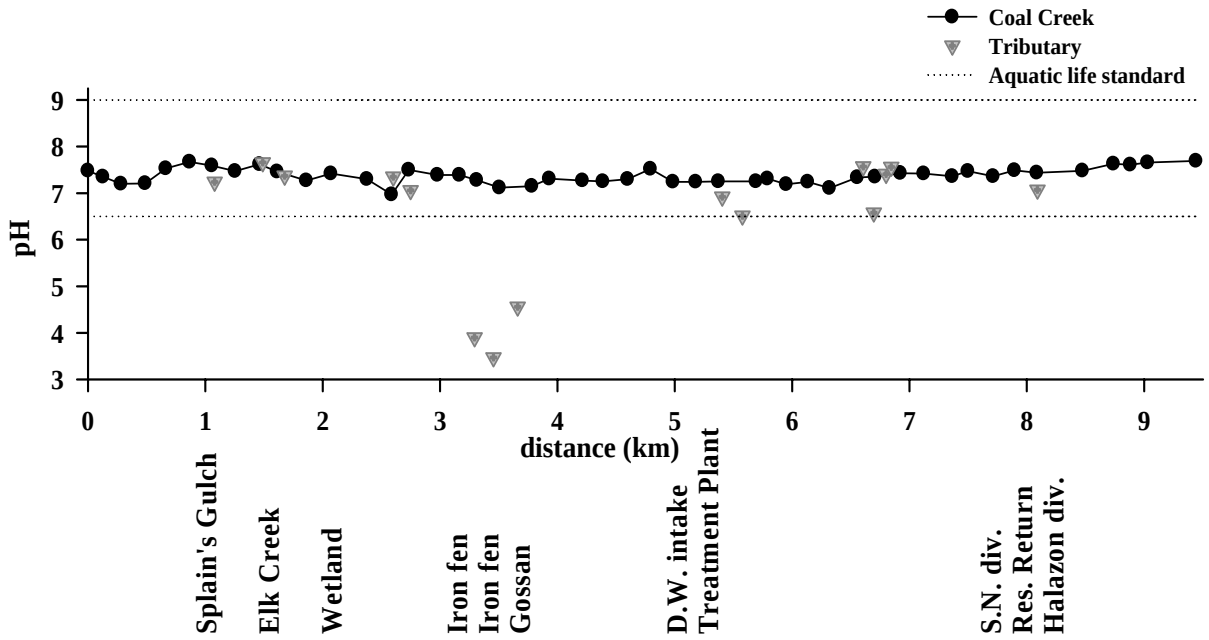


**Figure 7.** Coal Creek and surface tributary pH measured in the field lab within 24 h of collection. Stream and tributary pH is compared to the aquatic life standards for pH recommended by the CDPHE (CDPHE, 2005). The Crested Butte drinking water intake is designated "D.W. intake" and the reservoir return is designated as "Res. Return"; the Mount Emmons treatment plant effluent as "Treatment Plant"; the Spann Nettick diversion as "S.N. div."; and the Halazon diversion as "Halazon div.".

### *Coal Creek total organic carbon*

Total organic carbon (TOC) concentrations were measured because TOC can influence metal transport. Coal Creek total organic carbon concentrations ranged from a minimum of 1.5 mg $L^{-1}$ at CC-6.872 to a maximum of 4.7 mg $L^{-1}$ at CC-0.613 (Figure 8). TOC concentrations show a general decrease within this range from the upstream end of the study reach to CC-6.872. Higher TOC concentrations in the upstream reach may be attributable to lower flow and carbon inputs from the wetland. UT-3.212 contains 1.3 mg $L^{-1}$ TOC and was the tributary with the lowest TOC concentration. UT-6.573 contains the highest tributary TOC concentration with 3.4 mg $L^{-1}$.

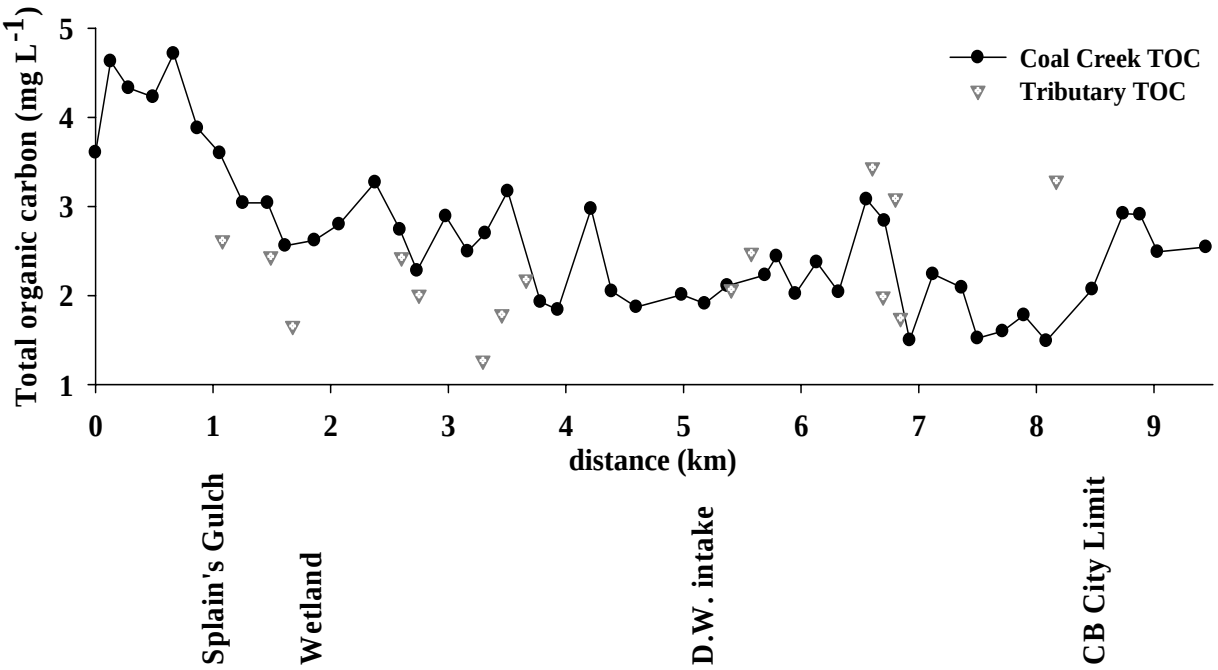


**Figure 8.** Coal Creek and tributary total organic carbon concentration. The Crested Butte drinking water intake is designated "D.W. intake"; the Town of Crested Butte's city limits as "CB City Limit".

### *Calcium and magnesium concentration and hardness*

Total calcium and magnesium concentrations were used to calculate hardness in mg $L^{-1}$ as $CaCO_3$ (Figure 9). Approximately 93% of the calcium and 94% of the magnesium was available in the dissolved form. Magnesium concentration remained nearly constant along the entire study reach. The only tributary contributing a magnesium concentration greater than the in-stream maximum was UT-3.595 with a magnesium concentration of 14.0 mg $L^{-1}$.

Calcium concentrations varied significantly from a minimum of 12.5 mg $L^{-1}$ at CC-1.412 to a maximum of 154 mg $L^{-1}$ at CC-6.505 (Figure 9). Calcium concentrations remained steady near an average of 17.8 mg $L^{-1}$ from the upstream site to CC-5.312. Downstream of CC-5.312 and the Mt. Emmons Treatment Plant effluent, calcium concentrations increase until the maximum occurs at CC-6.505. A gradual decline in calcium concentration was observed following the peak at CC-6.505. Steeper concentration decreases were detected between CC-6.605 and CC-6.872 as calcium concentration drops from 148 to 120 mg $L^{-1}$ and between CC-8.085 and CC-8.352 as concentration drops from 104 to 52.2 mg $L^{-1}$. The treatment plant effluent had a calcium concentration of 167 mg $L^{-1}$.

Hardness ranges from a minimum of 43.2 mg $L^{-1}$ as $CaCO_3$ at CC-1.412 to a maximum of 400 mg $L^{-1}$ as $CaCO_3$ at CC-6.505 (Figure 9). Like calcium, hardness remained stable near an average of 57.1 mg $L^{-1}$ as $CaCO_3$ between the upstream site and

CC-5.312. Downstream of CC-5.312 and the Mt. Emmons Treatment Plant effluent release, hardness steadily increases until the in-stream maximum occurs at CC-6.505. Hardness gradually decreases downstream of CC-6.505. The Mt. Emmons Treatment Plant effluent had a hardness of 521 mg $L^{-1}$ as $CaCO_3$.

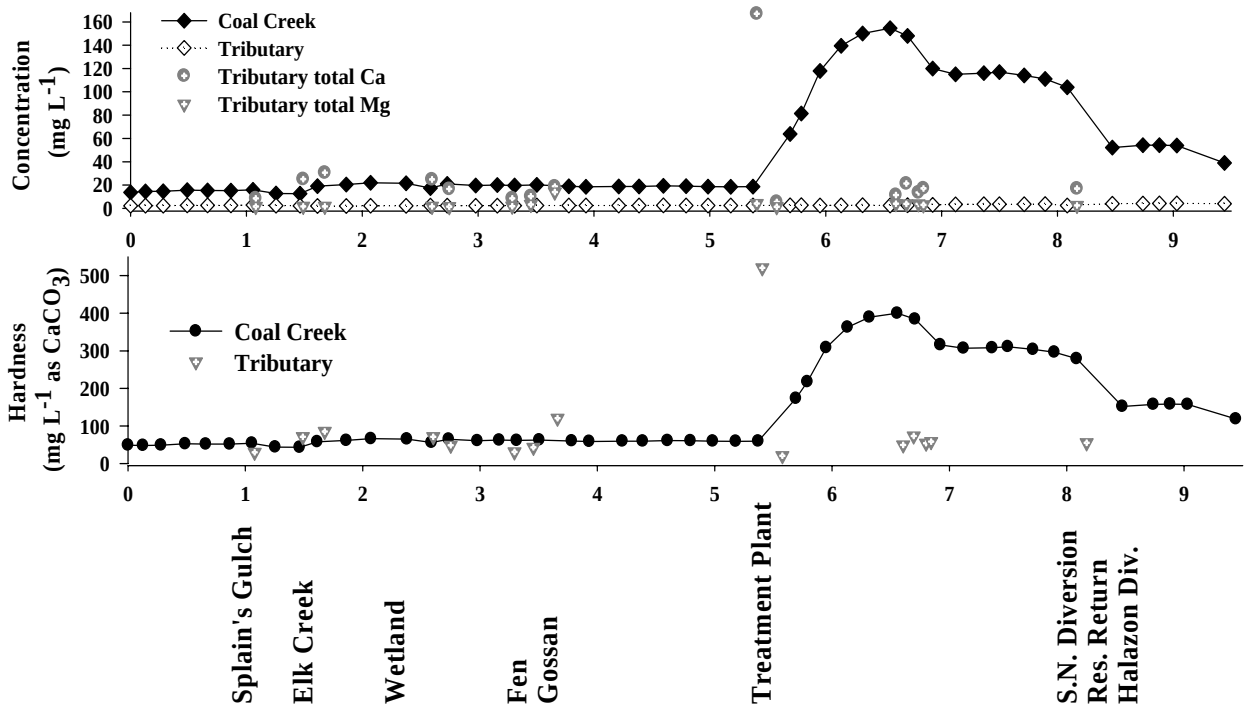


**Figure 9.** Coal Creek and tributary total calcium and magnesium concentration and hardness as mg $L^{-1}$ $CaCO_3$. The Crested Butte drinking water intake is designated "D.W. intake" and the reservoir return is designated as "Res. Return"; the Mount Emmons treatment plant effluent as "Treatment Plant"; the Spann Nettick diversion as "S.N. div."; and the Halazon diversion as "Halazon div.".

### *Sodium chloride pulse tracer test*

Arrival of the sodium chloride tracer at five sample sites was documented using a conductivity meter. The stream velocity was calculated as the distance traveled by the tracer from the injection point to the monitor site divided by the time between the pulse injection (12:28) and the time that conductivity peaked at the monitor site (Table 4). The

**Table 4.** The time of the conductivity peak in response to the pulse NaCl tracer at five sample sites. The stream velocity was calculated at each site as described above and used to estimate the time required for the LiCl tracer to reach the most downstream sample site.

| Site | Conductivity Peak Time | Velocity (km $h^{-1}$) |
|---|---|---|
| CC-0.077 | 12:43 | 0.308 |
| CC-0.438 | 14:03 | 0.289 |
| CC-0.613 | 16:01 | 0.173 |
| CC-0.816 | 17:15 | 0.171 |
| CC-1.006 | 18:37 | 0.166 |

calculated velocities showed a decreasing trend with downstream distance. The average velocity was 0.22 km $h^{-1}$. Based on this average velocity in this upstream reach of the study reach, an injection time of 43 h was required for the LiCl tracer to reach the most downstream sample site at 9.387 km. Background conductivity was approximately 100 µS $cm^{-1}$ at all monitor sites.

### *Injection tracer concentration*

Thirteen injection tank samples were taken over the course of the injection period and analyzed for lithium and chloride concentration (Table 5). These samples were taken directly from the injection tubing that transported the injection solution from the tank into Coal Creek. Lithium concentration was measured by both the Environmental Protection Agency (EPA) and the Laboratory for Environmental and Geological Sciences (LEGS) using ICP-AES.

The EPA lithium concentrations for the injection tank varied from $1.78 \times 10^4$ to $3.68 \times 10^4$ mg $L^{-1}$ ($\sigma = 6.06 \times 10^3$ mg $L^{-1}$). The LEGS lithium concentrations for the injection tank varied only from $1.13 \times 10^4$ to $1.24 \times 10^4$ mg $L^{-1}$ ($\sigma = 4.31 \times 10^2$ mg $L^{-1}$). Furthermore, the lithium chloride (34 kg) was added to the 405 L injection tank to produce a desired lithium concentration of 2 M, or $1.39 \times 10^4$ mg $L^{-1}$, and the lithium concentrations measured by LEGS was much closer to this expected lithium concentration than the EPA data. Therefore, the LEGS lithium concentrations were used for all flow calculations. The average lithium concentration of the injection solution was determined by dropping the highest and lowest lithium concentration and averaging the remaining concentrations. The average chloride concentration of the injection solution was determined in the same manner.

The injection solution was replenished twice. The lithium concentration in the LEGS data

**Table 5**. Injection solution lithium and chloride concentrations over the injection period. Lithium concentrations were measured using ICP-AES analysis at the Laboratory for Environmental and Geological Studies (LEGS) and by the Environmental Protection Agency (EPA). Chloride concentrations were measured using IC analysis at the Institute for Arctic and Alpine Research (INSTAAR).

| Sample Name | LEGS Li (mg $L^{-1}$) | EPA Li (mg $L^{-1}$) | INSTAAR Cl (mg $L^{-1}$) |
|---|---|---|---|
| CC-Inj 9/3 13:07 | 11,300 | 25,300 | 67,000 |
| CC-Inj 9/3 15:07 | 11,500 | 19,400 | 74,900 |
| CC-Inj 9/3 17:14 | 11,400 | 27,100 | 73,200 |
| CC-Inj 9/3 17:14 | | 36,800 | |
| CC-Inj 9/3 17:14 | | 13,500 | |
| CC-Inj 9/3 19:15 | 11,300 | 19,400 | 74,900 |
| CC-Inj 9/4 02:00 | 11,300 | 19,900 | 23,300 |
| CC-Inj 9/4 09:52 | 11,400 | 19,200 | 66,300 |
| CC-Inj 9/4 14:00 | 11,900 | 23,800 | 96,400 |
| CC-Inj 9/4 18:00 | 12,400 | 23,800 | 90,300 |
| CC-Inj 9/5 00:00 | 12,200 | 19,800 | 68,300 |
| CC-Inj 9/5 06:20 | 12,000 | 33,700 | 80,800 |
| CC-Inj 9/5 11:05 | 12,100 | 17,800 | 80,900 |
| CC-Inj 9/5 13:05 | 12,300 | 25,600 | 78,300 |
| CC-Inj 9/5 15:05 | 12,200 | 24,800 | 79,800 |

set clearly responds to addition of the newly mixed injection solution at 18:00 on September 4 (Table 5). The fresh injection solution raises the lithium concentration by 750 mg $L^{-1}$ on average.

The chloride concentrations for the injection tank ranged from $2.33 \times 10^4$ to $9.64 \times 10^4$ mg $L^{-1}$. The average chloride concentration was $7.59 \times 10^4$ mg $L^{-1}$. For the planned 2 M lithium chloride tracer solution, the expected mass concentration was $7.10 \times 10^4$ mg $L^{-1}$, which agrees well with the average chloride concentration in the injection solution.

### *Stream and tributary tracer concentration*

The average lithium concentration at the upstream site, CC-(-0.051), was 3.53 µg $L^{-1}$. The lithium concentration measured at first sampling site downstream of the injection, CC-0.077, during the synoptic sampling was 6,060 µg $L^{-1}$. A 1,700-fold increase in total lithium concentration between CC-(-0.051) and CC-0.077 resulted from the injection of the LiCl tracer between these two sites (Figure 10). Tributary lithium concentration varied from 0.95 µg $L^{-1}$ at UT-1.580 to 128 µg $L^{-1}$ at UT-3.595. The lithium concentration at UT-3.595 is 36 times higher than the background lithium concentration measured at CC-(-0.051). The treatment plant effluent had a lithium concentration of 35.8 µg $L^{-1}$, which is ten times more than background. All other tributaries contain no more than three times the background lithium concentration.

The dissolved chloride concentration increased by a factor of 13.5 between CC-(-0.051) and CC-0.077 resulting from the injection of the LiCl tracer between these two sites (Figure 11). The average dissolved chloride concentration at CC-(-0.051) was 2.38 mg $L^{-1}$, and chloride concentration increased to 32.0 mg $L^{-1}$ at CC-0.077.

### *Flow rate calculations*

Several estimates and assumptions were made to calculate Coal Creek flow rate. To account for the effect of the three water diversions (the Town of Crested Butte drinking water intake, the Spann Nettick ditch, and the Halazon/Town Ranch ditch), we requested flow rate data from the Town of Crested Butte. The drinking water intake flow (at 5.296 km) was estimated as 79.3 L $s^{-1}$ (Larry Adams, personal communication, May 26, 2006). The flow estimates for the two irrigation diversions were 28.3 L $s^{-1}$ for the Spann Nettick ditch and 14.2 L $s^{-1}$ for the Halazon/Town Ranch ditch (Larry Adams, personal communication, May 26, 2006). Because diversion of water from Coal Creek does not affect the tracer concentration, the Coal Creek flows had to be manually decreased to account for these three diversions. These diversion flows were subtracted from the flows calculated for the sampling locations upstream of the diversions.

Overflow from Crested Butte's drinking water reservoir is returned to Coal Creek between CC-8.085 and CC-8.352 at a rate of 60.0 L $s^{-1}$. This rate was calculated by subtracting average daily drinking water usage for September ($1.67 \times 10^6$ L $d^{-1}$,

Larry Adams, personal communication, May 26, 2006) from the volume of flow diverted from Coal Creek to the drinking water reservoir (79.3 L $s^{-1}$, or $6.85 \times 10^6$ L $d^{-1}$).

The synoptic sites were assigned so that only one tributary was located between two in-stream synoptic sample sites. Tracer-dilution equations account only for one tributary between two samples sites. Tributaries UT-6.573, UT-6.692, and UT-6.668 were not detected during site assignment, but were found during synoptic sampling. Two unnamed tributaries, UT-6.573 and UT-6.692, entered Coal Creek between in-stream sampling sites CC-6.505 and CC-6.605. Also, both UT-6.668 and UT-6.782 entered Coal Creek between CC-6.605 and CC-6.872. For each of these tributaries, the flow rate was estimated as a percentage of the total inflow between the sites bracketing the tributaries. These estimates were based on visual assessments made by field personnel. Both UT-6.573 and UT-6.692 were assigned half of the total inflow between sites CC-6.505 and CC-6.605. UT-6.668 was estimated to contain 90% of the total inflow between CC-6.605 and CC-6.872, while UT-6.782 was estimated to comprise the remaining 10%.

The lithium concentration in unnamed tributary UT-3.595 was several times greater than background lithium concentration. Observed flow at UT-3.595 was described as only a "trickle" by field personnel. When the standard tracer-dilution equation (Equation 4) was applied at UT-3.595, the calculated flow for this tributary was 2,400 L $s^{-1}$. This extremely high flow rate resulted because the lithium concentration of UT-3.595 was only 8 µg $L^{-1}$ less than the lithium concentration at CC-3.811. The standard tracer-dilution equation breaks down when the in-stream tracer concentration is not at least twice as great as the tributary tracer concentration. To avoid assigning UT-3.595 an unrealistically high, flow for UT-3.595 was estimated as 1% of Coal Creek flow (Equation 6).

For the calculation of flow based on chloride dilution, an additional modification was used to account for flow from the Mt. Emmons Treatment Plant effluent channel at 5.340 km. The chloride concentration in this tributary was about 1.1 times greater than the upstream chloride concentration. The standard tracer-dilution equation (Equation 4) is not valid if tributary tracer concentration is greater than the in-stream tracer concentration. Equation 6 (Table 3) was used to account for flow from the treatment plant. Equation 6 depends on a field estimate of tributary flow as a fraction of Coal Creek flow. Field personnel estimated flow from the treatment plant channel as 5% of Coal Creek flow. The treatment plant was not discharging at the time of sampling, but a low flow was visible. This treatment plant flow was attributed to either natural drainage or residual treatment plant effluent flow.

The chloride concentration downstream of unnamed tributary UT-5.517 was greater than the upstream chloride concentration. When Equation 4 was applied, the flow rate decreased from upstream to downstream, and the resulting flow from UT-5.517 was calculated as negative. To correct for this anomaly, UT-5.517 was assigned a small positive flow of 1.00 L $s^{-1}$ to enable the calculation of a meaningful loading rate at UT-5.517.

*Flow rates based on lithium and chloride dilution*

Flow rates calculated based on lithium dilution increased from upstream to downstream sites in response to decreases in lithium concentration in Coal Creek (Figure 10). The flow rates were calculated with Equations 4, 5, and 6. The flow rate increased from 7.9 L $s^{-1}$ at first sampling site, CC-0.077, to 2,300 L $s^{-1}$ at the last sampling site, CC-9.387. The maximum calculated flow rate of 2,540 L $s^{-1}$ occurred just upstream of CC-9.387. The flow rate increased with distance downstream of the injection site at all locations except between CC-6.872 and CC-7.070 and between CC-8.974 and CC-9.387. These are the sites where lithium concentrations increased slightly. Tributary flows varied from a minimum of 2.15 L $s^{-1}$ at unnamed tributary UT-3.595 to a maximum of 406 L $s^{-1}$ at unnamed tributary UT-6.668.

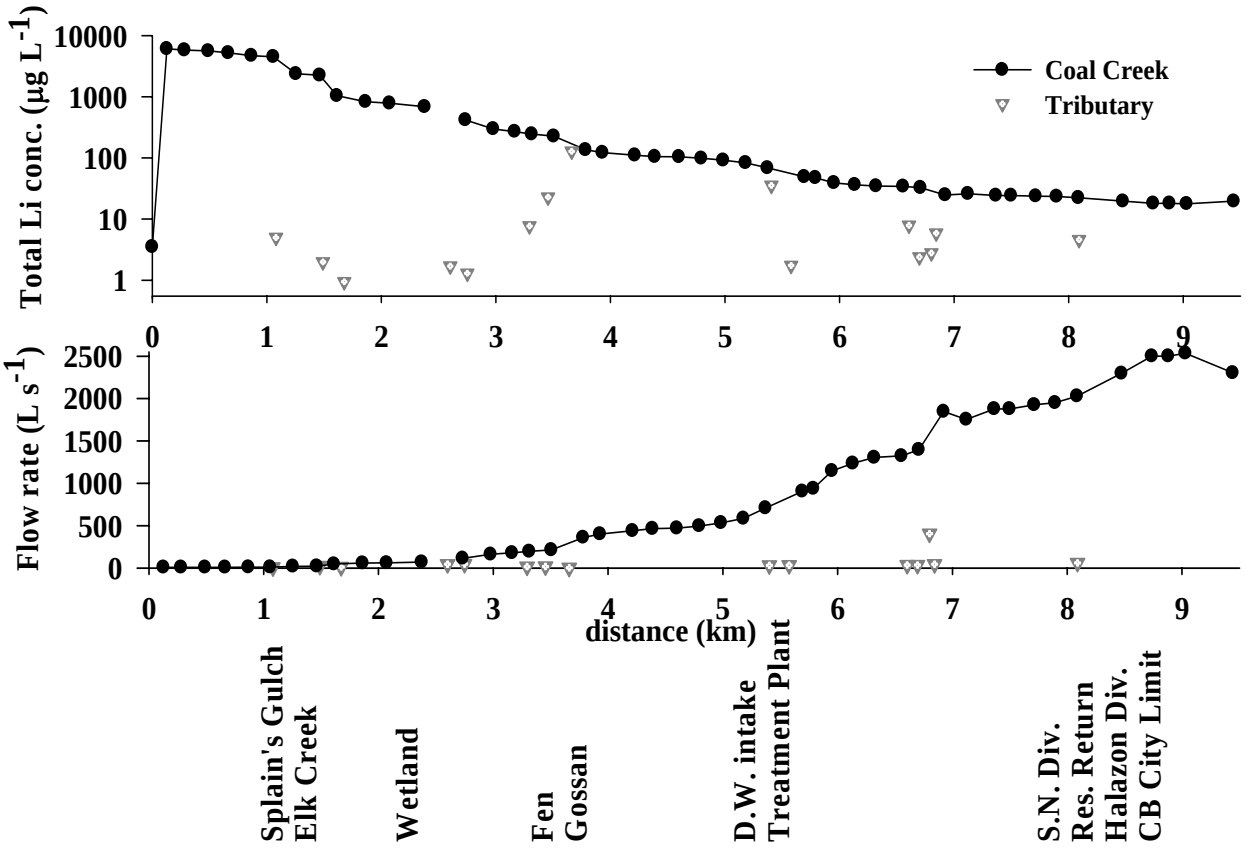


**Figure 10.** Coal Creek and tributary total lithium concentration and flow rate calculated using lithium concentration dilution. The flow rates determined by lithium dilution were deemed inaccurate. The flow rates used for the metal loading calculations were determined by chloride dilution (Figure 11).

Flow rates calculated based on chloride dilution steadily increased from 10.4 to 122 L $s^{-1}$ between CC-(-0.051) and CC-5.094 (Figure 11). Four flow rate decreases were observed between CC-3.811 and CC-5.312. Locations where flow rate slightly decreases

are locations where chloride concentration slightly increased with downstream distance. The maximum flow rate of 122 L $s^{-1}$ occurs at CC-5.094. The flow rate decreased from 111 to 45.0 L $s^{-1}$ between CC-5.312 and CC-5.642. Between CC-5.312 and CC-5.642, the Crested Butte drinking water intake diverts 79.3 L $s^{-1}$ and the Mt. Emmons Treatment Plant effluent channel contributed 1.60 L $s^{-1}$ (sample was taken after the plant discontinued effluent release for the day). Flow increased from 45.0 L $s^{-1}$ at CC-5.642 to 85.2 L $s^{-1}$ at CC-6.872. Slight flow fluctuations were measured between CC-6.872 and CC-7.844. The Halazon ditch diversion reduces flow in Coal Creek between CC-8.085 and CC-8.352 and flow from the drinking water reservoir is returned to Coal Creek at 8.097 km between these two sites. There is a 40.8 L $s^{-1}$ net flow rate increase between CC-8.085 and CC-8.352. Flow decreases slightly from CC-8.352 to CC-9.387 in response to slightly increasing chloride concentration. Site distances descriptions, and final flow rates as calculated using chloride-dilution are shown in Table 6.

The flow rates obtained using chloride dilution calculations appear to more accurately describe actual flows in Coal Creek. Just prior to the tracer study, the Coal Creek flow rate was estimated as a maximum of 142 L $s^{-1}$ (Larry Adams, personal communication, May 26, 2006). The maximum flow rate of 2,500 L $s^{-1}$ based on lithium dilution is unreasonable. The flow rates calculated using chloride dilution were much closer to estimated flows. Flow rates based on chloride dilution were used to calculate metal loading rates because they appear to more accurately reflect actual Coal Creek flow.

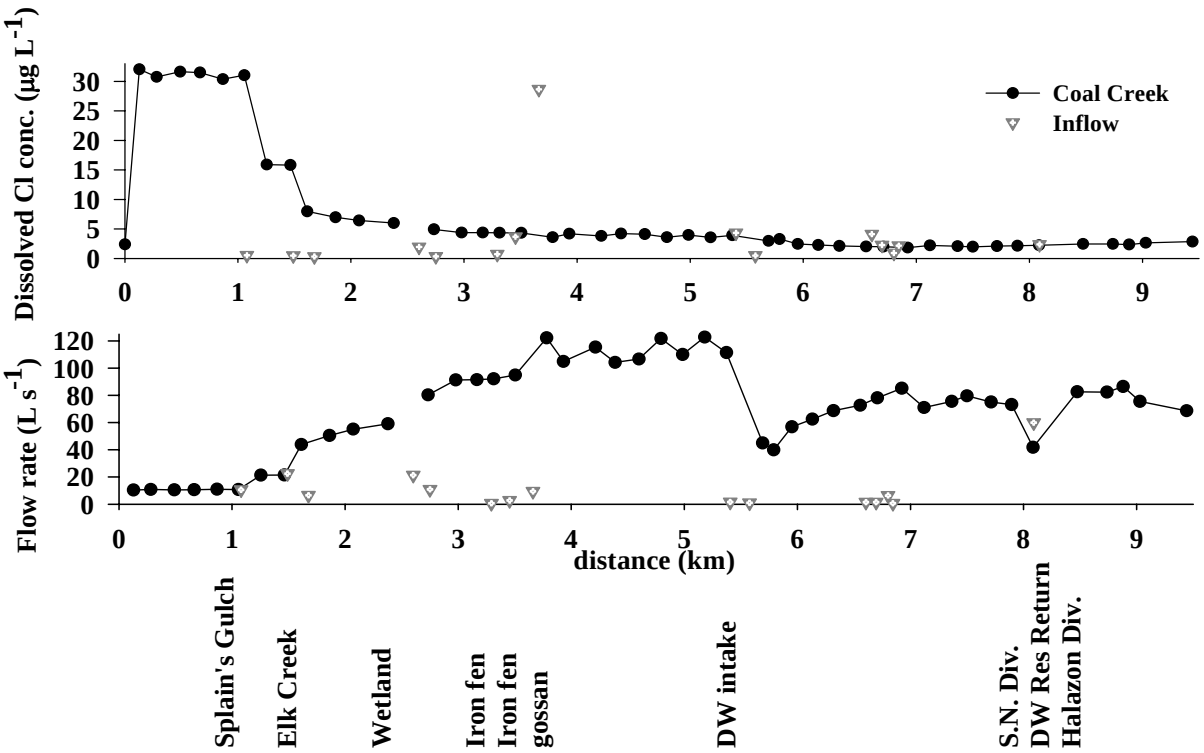


**Figure 11**. Coal Creek and tributary dissolved chloride concentration and flow rate calculated using chloride concentration dilution. These flow rates were used for the metal loading calculations.

**Table 6.** Flow rates of Coal Creek sample sites, tributaries, and diversions. Site name reflects distance (km) from the upstream sample site. Flow rates (L $s^{-1}$) are based on chloride dilution (Figure 11). "CC" is the abbreviation for Coal Creek and "UT" is the abbreviation for an unnamed tributary.

| Site Name | Site Description/Details | In-stream Flow Rate (L $s^{-1}$) | Tributary Flow Rate (L $s^{-1}$) |
|---|---|---|---|
| CC-(-0.051) | upstream site, background sampling | | |
| CC-0.000 | injection site | | |
| CC-0.077 | | 10.37 | |
| CC-0.231 | elevation 2967 m | 10.83 | |
| CC-0.438 | | 10.51 | |
| CC-0.613 | | 10.56 | |
| CC-0.816 | | 10.98 | |
| CC-1.006 | | 10.73 | |
| SPG-1.008 | Splain's Gulch | | 10.59 |
| CC-1.204 | | 21.32 | |
| CC-1.412 | elevation 2927 m | 21.40 | |
| EC-1.425 | Elk Creek (Standard Mine drainage) | | 22.46 |
| CC-1.562 | | 43.86 | |
| UT-1.580 | | | 6.60 |
| CC-1.811 | downstream of beaver dam | 50.47 | |
| CC-2.021 | wetland area | 55.07 | |
| CC-2.327 | wetland area | 59.05 | |
| CC-2.467 | wetland area, sampling error[1] | | |
| UT-2.511 | | | 21.32 |
| CC-2.580 | | 80.37 | |
| UT-2.670 | | | 10.91 |
| CC-2.978 | elevation 2895 m | 91.28 | |
| CC-3.165 | wetland area | 91.47 | |
| UT-3.212 | iron fen drainage, primary | | 0.68 |
| CC-3.314 | iron fen seeps | 92.15 | |
| UT-3.455 | iron fen seeps | | 2.75 |
| CC-3.558 | iron fen seeps | 94.89 | |
| UT-3.595 | iron gossan drainage, primary | | 9.49 |
| CC-3.811 | | 122.2 | |
| CC-3.895 | | 104.9 | |
| CC-4.186 | | 115.4 | |

**Table 6.** Flow rates of Coal Creek sample sites, tributaries, and diversions. Site name reflects distance (km) from the upstream sample site. Flow rates (L $s^{-1}$) are based on chloride dilution (Figure 11). "CC" is the abbreviation for Coal Creek and "UT" is the abbreviation for an unnamed tributary.

| Site Name | Site Description/Details | In-stream Flow Rate (L $s^{-1}$) | Tributary Flow Rate (L $s^{-1}$) |
|---|---|---|---|
| CC-4.284 | upstream of jeep trail across creek | 104.2 | |
| CC-4.562 | | 106.6 | |
| CC-4.780 | elevation 2851 m | 121.8 | |
| CC-4.978 | | 110.0 | |
| CC-5.094 | | 122.7 | |
| CC-3.72 | | 111.4 | |
| 5.296 | Crested Butte drinking water intake | 79.29 | |
| 5.340 | Mt. Emmons Treatment Plant discharge | | 1.61 |
| CC-5.642 | upstream of Wildcat Trail bridge | 44.96 | |
| UT-5.517 | | | 1.00 |
| CC-5.739 | | 39.91 | |
| CC-5.900 | | 56.83 | |
| CC-6.082 | elevation 2809 m | 62.42 | |
| CC-6.268 | | 68.76 | |
| CC-6.505 | | 72.64 | |
| UT-6.573 | | | 1.45 |
| UT-6.692 | | | 1.45 |
| CC-6.605 | | 78.14 | |
| UT-6.668 | | | 6.38 |
| UT-6.782 | | | 0.71 |
| CC-6.872 | | 85.23 | |
| CC-7.070 | elevation 2782 m | 71.06 | |
| CC-7.314 | | 75.60 | |
| CC-7.448 | | 79.56 | |
| CC-7.662 | | 75.03 | |
| CC-7.844 | elevation 2767 m | 73.15 | |
| 8.047 | Spann Nettick (Smith Ranch) diversion | | -28.32 |
| CC-8.085 | | 41.80 | |
| 8.097 | Crested Butte drinking water reservoir return | | 60.01 |
| 8.177 | Halazon (Town Ranch) diversion | | -14.16 |
| CC-8.352 | upstream of Crested Butte town line | 82.60 | |
| CC-8.670 | corner of First Street and Sopris Avenue | 82.38 | |
| CC-8.824 | corner of Second Street and Elk Avenue | 86.50 | |

**Table 6.** Flow rates of Coal Creek sample sites, tributaries, and diversions. Site name reflects distance (km) from the upstream sample site. Flow rates (L $s^{-1}$) are based on chloride dilution (Figure 11). "CC" is the abbreviation for Coal Creek and "UT" is the abbreviation for an unnamed tributary.

| Site Name | Site Description/Details | In-stream Flow Rate (L $s^{-1}$) | Tributary Flow Rate (L $s^{-1}$) |
|---|---|---|---|
| CC-8.974 | upstream of bridge, Maroon Street | 75.55 | |
| CC-9.387 | downstream of foot bridge on Butte Avenue | 68.66 | |

[1] sample taken from stagnant pool in wetlands; very low tracer concentration.

### *Metals in Coal Creek and tributaries*

Concentrations and loading rates for iron, manganese, aluminum, zinc, copper, cadmium, lead, nickel, chromium, arsenic, and barium will be presented in the following sections. Total and dissolved concentrations were measured for each of these metals and metalloids. All metal toxicity standards apply to dissolved metal concentrations unless otherwise stated.

Dissolved metal concentrations were greater than total metal concentrations for iron, copper, nickel, and chromium at several sites as reported by the EPA contract laboratory. Only total loading rates are graphed for these metals to exclude error associated with a possible positive interference. Obviously, the dissolved metal concentration should never be greater than the total metal concentration. An analytical error is suspected, but we have not confirmed the cause of this discrepancy. All metal concentrations were measured using both ICP-AES and ICP-MS and this error occurred using both analytical techniques. Inspection of the metals analyses for blanks (high-purity water) lended some insight. The EPA measured high concentrations of dissolved iron, nickel, and chromium in the blanks, but total concentrations were either not detected or considerably lower than dissolved concentrations (Table 7). These results suggest a positive interference with dissolved measurements. A positive (or negative) spectral, physical, or chemical interference can cause concentration measurements to be greater than or less than the true concentration. A positive spectral interference occurs when overlap from the spectral line of one element creates a false high concentration measurement for a different element. Physical interferences occur when nebulization and transport processes change the viscosity and surface tension of the sample matrix. Chemical interferences include compound formation, ionization effects, and solute vaporization (EPA, 2006). Another explanation for this discrepancy may be a "memory effect." This occurs when a sample with a high metal concentration is analyzed and the sample chamber is not rinsed adequately prior to running the following sample. The cause of the dissolved/total discrepancy was undetermined. All of the metal analyses were conducted at the EPA's contract laboratory, and establishing direct contact with laboratory personnel was not possible.

**Table 7.** Dissolved and total metal concentrations in blanks (mean ± one standard deviation). BDL is "below detection limit." ICP-AES is inductively coupled plasma-atomic emission spectrometry and ICP-MS is inductively coupled plasma-mass spectrometry.

| | ICP-AES | | ICP-MS | |
|---|---|---|---|---|
| Metal | Dissolved ($\mu g\ L^{-1}$) | Total ($\mu g\ L^{-1}$) | Dissolved ($\mu g\ L^{-1}$) | Total ($\mu g\ L^{-1}$) |
| iron | 361±202 | BDL | | |
| nickel | 56.1±32.9 | 3.85±3.37 | 52.0±30.6 | 3.07±2.97 |
| chromium | 41.3±35.3 | 5.5±4.9 | 70.5±41.0 | 4.5±4.5 |

*Iron concentrations and loading rates.* Coal Creek iron concentrations ranged from undetectable at several sites to a maximum of 483 $\mu g\ L^{-1}$ total iron at CC-3.165 (Figure 12). Coal Creek total iron concentration never exceeds the chronic toxicity standard for aquatic life of 1,000 $\mu g\ L^{-1}$ total recoverable iron. No acute aquatic life standard exists for iron. The 30-day dissolved iron standard for a drinking water supply is 300 $\mu g\ L^{-1}$ (CDPHE, 2005). Analytical results for dissolved iron show that this standard is exceeded at eight in-stream sites. In-stream dissolved iron concentrations are higher than in-stream total iron concentrations at several sites and unnamed tributaries. Total iron concentration was significantly higher than dissolved iron concentration in unnamed tributaries UT-2.670, UT-3.455, UT-3.595, UT-6.692, and the drinking water reservoir return, indicating a significant colloidal fraction. The greatest difference occurred at UT-6.692. UT-6.692 contained 1,960 $\mu g\ L^{-1}$ total iron and 608 $\mu g\ L^{-1}$ dissolved iron.

The total iron loading rate remained constant from CC-0.077 to CC-2.327 near an average of 0.25 kg $d^{-1}$. The maximum in-stream iron loading rate of 3.81 kg $d^{-1}$ occurred at CC-3.165, just upstream of iron fen drainage (Figure 12). From CC-6.082 to CC-7.070, iron was undetectable at all sites except CC-6.605, which had a very low iron concentration. The loading rate was zero over this reach due to the undetectable iron concentrations.

The drinking water reservoir return flow at 8.097 km contributed the highest tributary loading rate of 1.92 kg $d^{-1}$. It comprised 42% of the tributary total iron loading rate (Table 8). UT-2.511 contributed 1.04 kg $d^{-1}$ and 23% of the tributary iron loading rate. UT-3.595, the tributary which drains the gossan (Figure 3), contributed 0.61 kg $d^{-1}$ and 13% of the iron loading rate (Table 8).

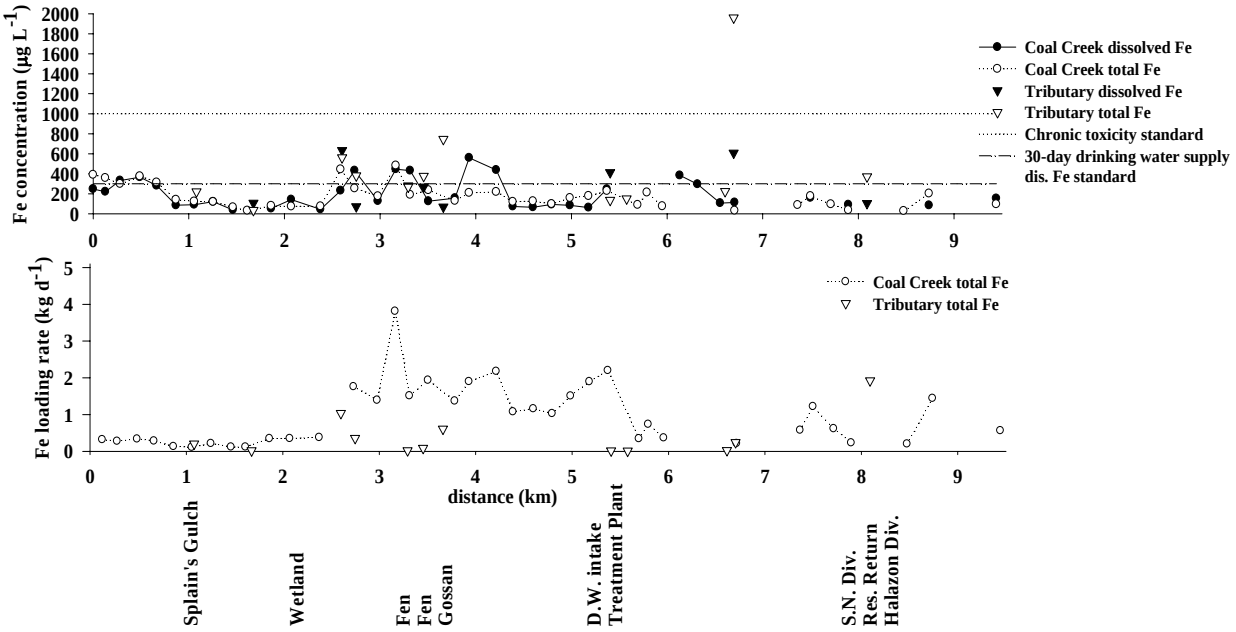


**Figure 12.** Coal Creek and tributary total and dissolved iron concentration, chronic toxicity standard, 30-day dissolved iron standard for a drinking water supply, and total iron loading rate. Missing data points reflect iron concentrations below the Environmental Protection Agency CRQL of 100 µg $L^{-1}$.

**Table 8**. Tributary loading rates expressed for total (above) and dissolved (below) metals as a percentage of the cumulative tributary loading rate (Equation 7) for each metal. "METP" is the Mt. Emmons Treatment Plant.

| Source/ Tributary | Tot Fe (%) | Tot Mn (%) | Tot Al (%) | Tot Zn (%) | Tot Cu (%) | Tot Cd (%) | Tot Pb (%) | Tot Ni (%) | Tot Cr (%) | Tot As (%) | Tot Ba (%) |
|---|---|---|---|---|---|---|---|---|---|---|---|
| Splain's Gulch-1.008 | 4.4 | 0.2 | 0.5 | < 0.1 | 5.7 | < 0.1 | 22 | 11 | 8.7 | 4.6 | 4.5 |
| Elk Creek-1.425 | < 0.1 | 0.2 | < 0.1 | 16 | 9.4 | 32 | 6.9 | 2.5 | 1.5 | 21 | 12 |
| UT-1.580 | 0.4 | 0.2 | < 0.1 | 0.8 | 2.9 | < 0.1 | < 0.1 | 0.8 | 0.6 | 4.0 | 2.1 |
| UT-2.511 | 23 | 2.4 | 0.9 | 1.8 | 20 | < 0.1 | < 0.1 | 45 | 48 | 10 | 7.6 |
| UT-2.670 | 7.9 | 0.5 | < 0.1 | 2.9 | 8.7 | < 0.1 | < 0.1 | 16 | 18 | 2.5 | 3.8 |
| UT-3.212; iron fen | 0.5 | 2.1 | 3.3 | 3.1 | 0.9 | 3.1 | 0.8 | 0.8 | 0.7 | 0.4 | 0.9 |
| UT-3.455; iron fen | 1.9 | 9.0 | 13 | 10 | 2.0 | 12 | 4.1 | 0.9 | 0.3 | 0.3 | 2.0 |
| UT-3.595; gossan | 13 | 62 | 76 | 49 | 13 | 39 | 10 | 18 | 19 | 2.7 | 12 |
| METP effluent | 0.4 | 1.5 | 2.3 | 1.3 | 2.5 | 2.6 | 0.7 | 0.2 | 0.2 | 0.7 | 0.4 |
| UT-5.517 | 0.3 | < 0.1 | 0.4 | 0.2 | 0.7 | < 0.1 | 0.7 | 0.1 | 0.1 | 0.3 | 0.3 |
| UT-6.573 | 0.6 | 0.1 | 0.5 | < 0.1 | 0.7 | < 0.1 | 1.8 | < 0.1 | < 0.1 | 0.3 | 2.8 |
| UT-6.692 | 5.4 | 4.4 | < 0.1 | 0.3 | 0.9 | 0.5 | 0.4 | 0.3 | 0.3 | 7.8 | 2.0 |
| UT-6.668 | < 0.1 | < 0.1 | < 0.1 | 0.8 | 2.4 | < 0.1 | 1.6 | < 0.1 | < 0.1 | 2.8 | 12 |
| UT-6.782 | < 0.1 | < 0.1 | < 0.1 | < 0.1 | 0.3 | < 0.1 | 0.8 | < 0.1 | < 0.1 | 0.3 | 0.8 |
| reservoir return | 42 | 17 | 3.1 | 14 | 30 | 11 | 50 | 3.4 | 2.7 | 42 | 37 |
| | | **Diss Mn (%)** | **Diss Al (%)** | **Diss Zn (%)** | **Diss Cu (%)** | **Diss Cd (%)** | **Diss Pb (%)** | | | **Diss As (%)** | **Diss Ba (%)** |
| Splain's Gulch-1.008 | | < 0.1 | < 0.1 | 0.1 | 4.0 | < 0.1 | < 0.1 | | | < 0.1 | 4.5 |
| Elk Creek-1.425 | | 0.3 | < 0.1 | 15 | 8.0 | 33 | 15 | | | 25 | 11 |
| UT-1.580 | | 0.3 | < 0.1 | 0.1 | 2.6 | < 0.1 | < 0.1 | | | 5.4 | 2.7 |
| UT-2.511 | | 2.9 | < 0.1 | 0.6 | 22 | < 0.1 | < 0.1 | | | 15 | 8.4 |
| UT-2.670 | | 0.3 | < 0.1 | 1.4 | 8.2 | < 0.1 | < 0.1 | | | 3.4 | 3.9 |
| UT-3.212; iron fen | | 2.7 | 3.6 | 3.5 | 0.9 | 3.7 | 3.3 | | | < 0.1 | 0.9 |
| UT-3.455; iron fen | | 10 | 14 | 12 | 2.1 | 15 | 14 | | | < 0.1 | 2.1 |
| UT-3.595; gossan | | 68 | 78 | 59 | 8.7 | 46 | 20 | | | 2.7 | 12 |
| METP effluent | | 2.0 | 2.1 | 1.4 | 2.3 | 3.1 | 2.0 | | | < 0.1 | 0.5 |
| UT-5.517 | | < 0.1 | < 0.1 | 0.2 | 0.6 | < 0.1 | < 0.1 | | | < 0.1 | 0.3 |
| UT-6.573 | | < 0.1 | < 0.1 | < 0.1 | 0.5 | < 0.1 | < 0.1 | | | 0.2 | 2.4 |
| UT-6.692 | | 5.1 | < 0.1 | 0.1 | 0.8 | 0.3 | < 0.1 | | | 6.1 | 2.2 |
| UT-6.668 | | < 0.1 | < 0.1 | 0.3 | 2.5 | < 0.1 | < 0.1 | | | < 0.1 | 13 |
| UT-6.782 | | < 0.1 | < 0.1 | < 0.1 | 0.3 | < 0.1 | < 0.1 | | | < 0.1 | 0.8 |
| reservoir return | | 8.6 | 3.0 | 6.2 | 36 | < 0.1 | 46 | | | 42 | 36 |

*Manganese concentration and loading rate*. The maximum total manganese concentration of 101 μg $L^{-1}$ was measured at CC-2.327, directly in the center of the wetland reach (Figure 13). CC-2.467 and CC-2.580, on the downstream end of the wetland reach, also had high total manganese concentrations of 88.9 and 79.9 μg $L^{-1}$, respectively. Tributaries upstream of CC-2.327 did not contain high manganese concentrations. Tributary inputs did not contribute to the high manganese concentrations from CC-2.327 to CC-2.580. The source of manganese was either groundwater or wetland input.

A small increase in manganese concentration occurred downstream of the Mt. Emmons Treatment Plant at 5.340 km. Concentration increased from 29.9 μg $L^{-1}$ total manganese at CC-5.312 to 43.9 μg $L^{-1}$ at CC-6.268. Concentrations decreased slightly with downstream distance. Manganese concentrations did not fully decrease to background concentrations along the study reach. Manganese concentrations in Coal Creek were well below the chronic and acute toxicity standards at all sites. For this reason, these standards were not included on the graph. The 30-day dissolved manganese standard for a drinking water supply is 50 μg $L^{-1}$. This standard was exceeded at CC-2.327 to CC-2.580, CC-3.165 to CC-3.558, CC-4.284, CC-6.082, and CC-6.268. A sharp decrease in manganese concentration occurred at CC-6.505, approximately 1.1 km downstream of the treatment plant. Most manganese was present in the dissolved form.

Of the tributaries, UT-3.595 contained the largest manganese concentration with 1,370 μg $L^{-1}$ dissolved manganese and 1,530 μg $L^{-1}$ total manganese. UT-6.692 also had high manganese concentrations with 669 μg $L^{-1}$ dissolved manganese and 712 μg $L^{-1}$ total manganese. Tributary total and dissolved manganese concentrations were similar for all tributaries except UT-3.595.

The Coal Creek manganese loading rates closely resembled Coal Creek manganese concentrations (Figure 13). The maximum loading rate of 0.62 kg $d^{-1}$ dissolved manganese occurred at CC-2.580. The loading rate remained elevated near an average of 0.46 kg $d^{-1}$ from CC-2.327 – CC-5.094. The loading rate decreased downstream of CC-5.312 in response to the drinking water flow diversion. A sharp loading rate decrease occurred at CC-6.505 in response to the low manganese concentration at that site.

The largest tributary dissolved manganese loading rate of 1.12 kg $d^{-1}$ came from UT-3.595 and comprised 67% of the manganese loading in Coal Creek. Though UT-3.212, UT-3.455, the treatment plant channel, and UT-6.692 had high manganese concentrations, flow from these tributaries was too low to produce a significant loading rate. The drinking water return channel was the only other tributary with a loading rate above the in-stream loading rate. It contributed 0.35 kg $d^{-1}$ total manganese and 17% of the cumulative tributary manganese loading rate (Table 8).

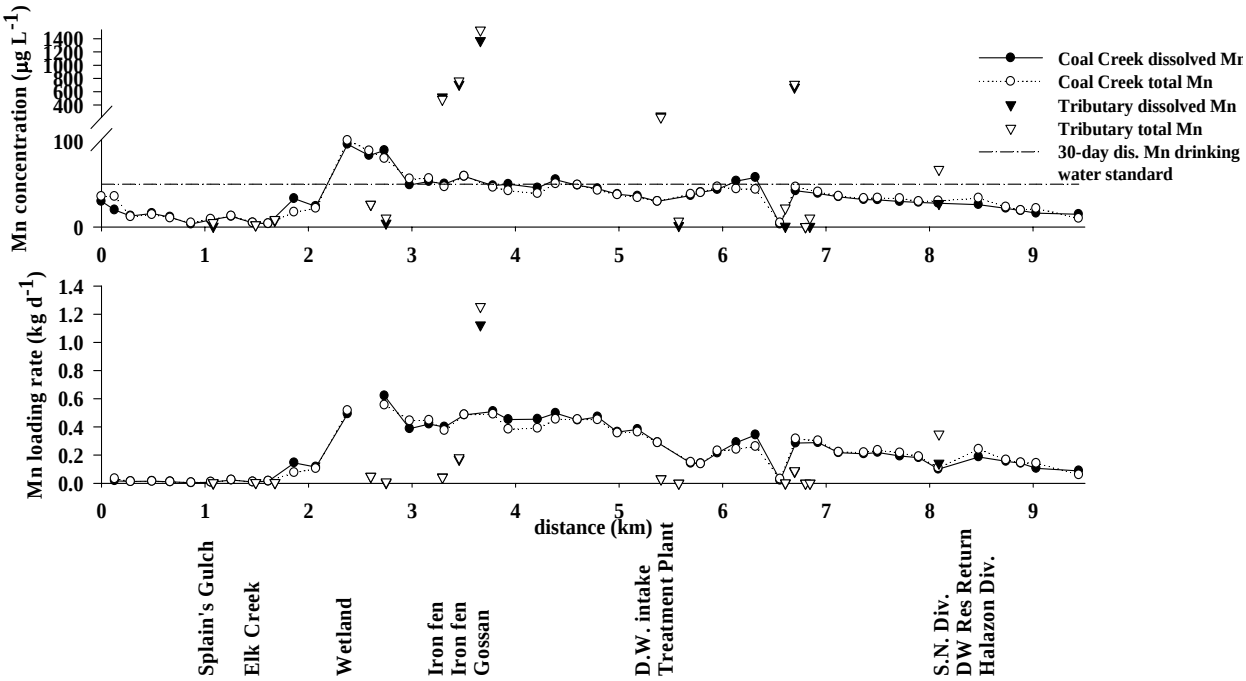


**Figure 13.** Coal Creek and tributary total and dissolved manganese concentration, 30-day drinking water supply dissolved manganese standard, and total and dissolved manganese loading rate.

*Aluminum concentrations and loading rates*. Aluminum concentrations were below the chronic toxicity standard of 87 µg $L^{-1}$ total recoverable aluminum for sites CC-(-0.051) to CC-5.312 (Figure 14). Sites CC-1.204 to CC-3.314 contained no measurable aluminum. A small rise in aluminum concentration was observed between CC-5.642 and CC-7.448. CC-6.268 had the highest dissolved aluminum concentration with 221 µg $L^{-1}$. CC-6.505 had the highest total aluminum concentration with 294 µg $L^{-1}$. The CDPHE specifies that the chronic total recoverable aluminum criterion will not apply when pH is greater than or equal to 7.0 and when hardness is greater than or equal to 50 mg $L^{-1}$ as $CaCO_3$. This was the case for all Coal Creek sites with aluminum concentrations above 87 µg $L^{-1}$. Aluminum concentrations above 87 µg $L^{-1}$ are not in violation of aquatic life standards in Coal Creek. In this instance, aluminum is regulated based on the 750 µg $L^{-1}$ total recoverable aluminum criterion (CDPHE, 2005). This acute aluminum toxicity standard was not exceeded at any in-stream site.

The unnamed tributaries UT-3.212 and UT-3.455, which drain the iron fen, and UT-3.595, which directly drains the gossan, had total and dissolved aluminum concentrations greater than 750 µg $L^{-1}$. UT-3.595 had the highest dissolved and total aluminum concentrations of 5,750 µg $L^{-1}$ and 6,610 µg $L^{-1}$, respectively. The Mt. Emmons treatment plant discharge also had total and dissolved aluminum concentrations greater than 750 µg $L^{-1}$. During synoptic sampling, the treatment plant discontinued the daily effluent release. A second sample was taken from the Mt. Emmons Treatment Plant effluent channel on September 6, 2005, at 10:49 when

effluent was being released. This sample was taken to detect any differences in constituents when effluent was being released and when it was not. This sample is not graphed in Figures 10 and 11 because it was not collected during the synoptic sampling. On September 6, this tributary contained 728 µg $L^{-1}$ dissolved aluminum and 1,020 µg $L^{-1}$ total aluminum.

The aluminum loading rate reached a maximum value at the same locations as the aluminum concentration (Figure 14). The dissolved loading rate reached a maximum of 1.31 kg $d^{-1}$ at CC-6.268. The total loading rate reached a maximum of 1.85 kg $d^{-1}$ at CC-6.505, approximately 1.1 km downstream of the treatment plant. A smaller spike of 1.30 kg $d^{-1}$ total aluminum occurred at CC-8.974, within the Crested Butte city limit upstream of the bridge on Maroon Street. UT-3.595 contributed the greatest aluminum loading rate of the tributaries with 5.01 kg $d^{-1}$ total aluminum. This was 76% of the tributary total aluminum loading rate. UT-3.455 contributed 0.86 kg $d^{-1}$ total aluminum, which is 13% of the total aluminum loading rate. Though UT-3.212 and the treatment plant channel contained high aluminum concentrations, the loading rate was not substantial because of the low flows at these sites. UT-3.212 contributed 3.3% of the total aluminum loading rate and the treatment plant effluent added only 2.3% (Table 8).

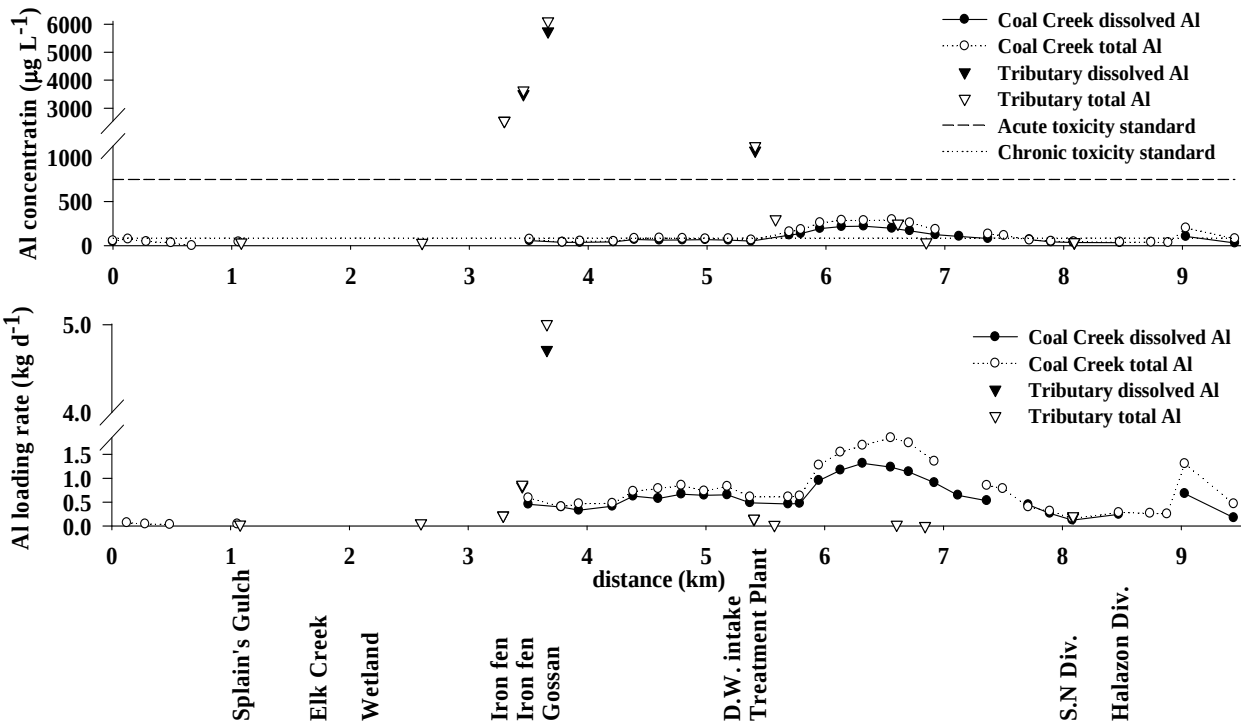


**Figure 14.** Coal Creek and tributary total and dissolved aluminum concentration, acute and chronic toxicity standards for aquatic life, and total and dissolved aluminum loading rate.

*Zinc concentrations and loading rates*. The maximum in-stream zinc concentration occurred at CC-6.268 (Figure 15). CC-6.268 total and dissolved zinc concentrations are 187 µg $L^{-1}$ and 199 µg $L^{-1}$, respectively. Acute toxicity standards were exceeded at CC-1.562 to CC-2.021, CC-3.558, and CC-4.284 to CC-5.312. Coal Creek zinc concentrations exceeded CDPHE chronic toxicity standards at sites CC-1.562 to CC-2.327 (just downstream of Elk Creek), CC-3.558 (downstream of iron fen drainage), and CC-4.284 to CC-5.312 (just downstream of the iron gossan drainage). Though there were high in-stream zinc concentrations from CC-5.642 to CC-8.085 (immediately downstream of the Mt. Emmons effluent channel at 5.340 km), toxicity standards were not exceeded during the sampling event. The Mt. Emmons Treatment Plant released effluent throughout the day, causing a large influx of calcium to Coal Creek. The increased calcium concentration produced an increase in hardness downstream of the effluent channel. Because zinc toxicity standards are hardness-based, values for the toxicity standards increased downstream of the treatment plant effluent channel.

Several tributaries exceeded the chronic and acute toxicity standards: Elk Creek, UT-3.212, UT-3.455, UT-3.595, and the treatment plant effluent channel. The concentration of zinc was highest in UT-3.595. UT-3.212, UT-3.455, and UT-3.595 contain drainage from the iron fen. These three tributaries contributed the highest zinc concentrations to Coal Creek.

Total and dissolved zinc concentrations had very similar values along the entire study reach. At ten in-stream sites and four tributaries, dissolved zinc concentrations were slightly greater than total zinc concentrations.

A spike in the total zinc loading rate from 0.0041 to 0.49 kg $d^{-1}$ was observed directly downstream of the Elk Creek confluence. Elk Creek contributed a zinc loading rate of 0.51 kg $d^{-1}$. This rate comprised 16% of zinc contributions to Coal Creek (Table 8). UT-3.595, which enters Coal Creek between CC-3.558 and CC-3.811, contributed the largest dissolved zinc loading rate of 1.99 kg $d^{-1}$ and 49% of zinc contributions. Zinc influx from UT-3.595 produced a spike in Coal Creek zinc loading rate from 0.77 kg $d^{-1}$ at CC-3.558 to 1.31 kg $d^{-1}$ at CC-4.284. The maximum in-stream zinc load in Coal Creek was 1.42 kg $d^{-1}$ at CC-4.780, which is located midway between the iron fen drainages and the drinking water intake. The zinc loading rate abruptly decreased between CC-5.312 and CC-5.642 in response to loss of flow to the drinking water diversion. The Spann Nettick diversion produced a similar, but less pronounced, zinc loading rate decrease between CC-7.844 and CC-8.085. A loading rate is not graphed at point CC-2.467 because a sampling error occurred and a flow rate at this site could not be determined. The zinc concentration at CC-2.467 was less than that of the surrounding sites, which supports our surmisal that the sample at CC-2.467 was taken from a stagnant pool in the wetlands.

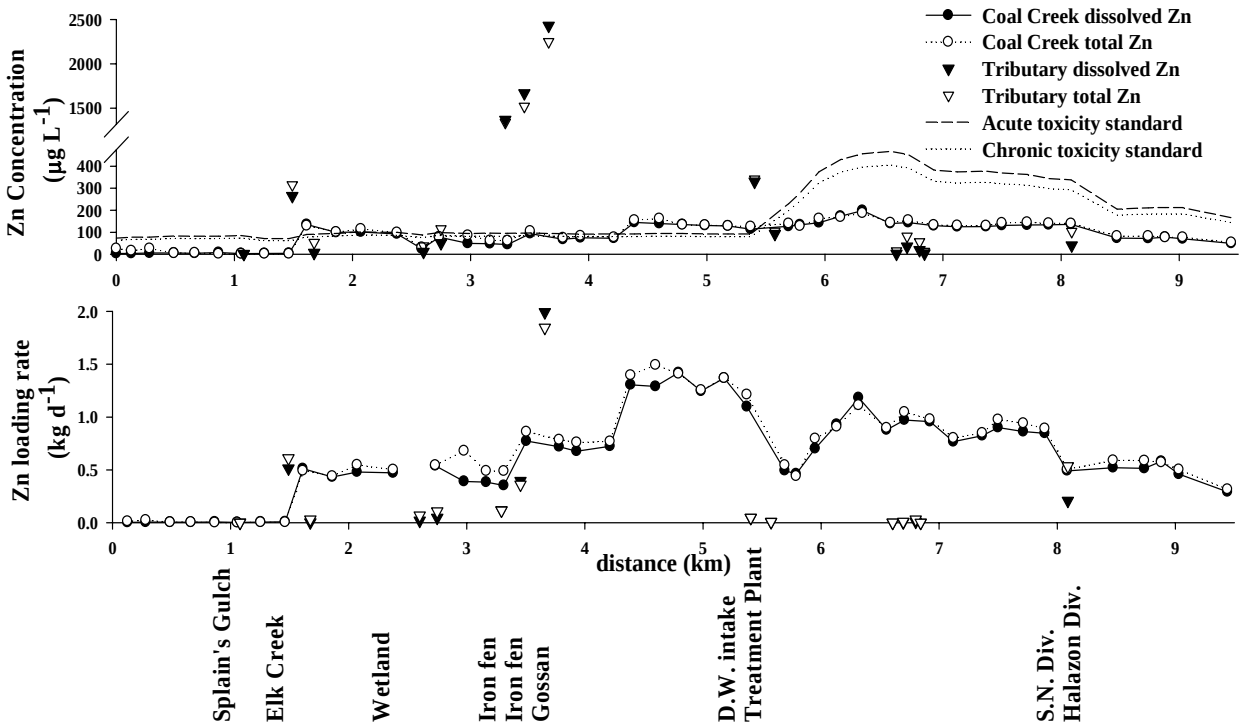


**Figure 15.** Coal Creek and tributary total and dissolved zinc concentration, chronic and acute toxicity standards, and total and dissolved zinc loading rate.

*Copper concentration and loading rate*. Copper concentration showed a small increasing trend from the upstream to the downstream end of the study reach (Figure 16). The maximum total copper concentration of 3.65 µg $L^{-1}$ was measured at CC-8.974, within the Crested Butte city limit just upstream of the bridge on Maroon Street. No in-stream sites exceeded the chronic toxicity standard for aquatic life. The acute toxicity standard is much greater than in-stream concentrations and is not shown in Figure 16. The highest tributary total copper concentrations were measured at UT-3.595 (gossan drainage) and the treatment plant effluent channel.

The copper loading rate also showed a small increasing trend from the upstream to the downstream end of the study reach (Figure 16). The maximum total copper loading rate of 0.024 kg $d^{-1}$ occurred at CC-8.974. The loading rate decreased as a result of the drinking water and Spann Nettick diversions. All tributary loading rates were less than adjacent in-stream loading rates except at UT-2.511 and the drinking water reservoir return channel. UT-2.511 contributed 20% of total tributary inputs and the drinking water reservoir return flow contributed 30% (Table 8).

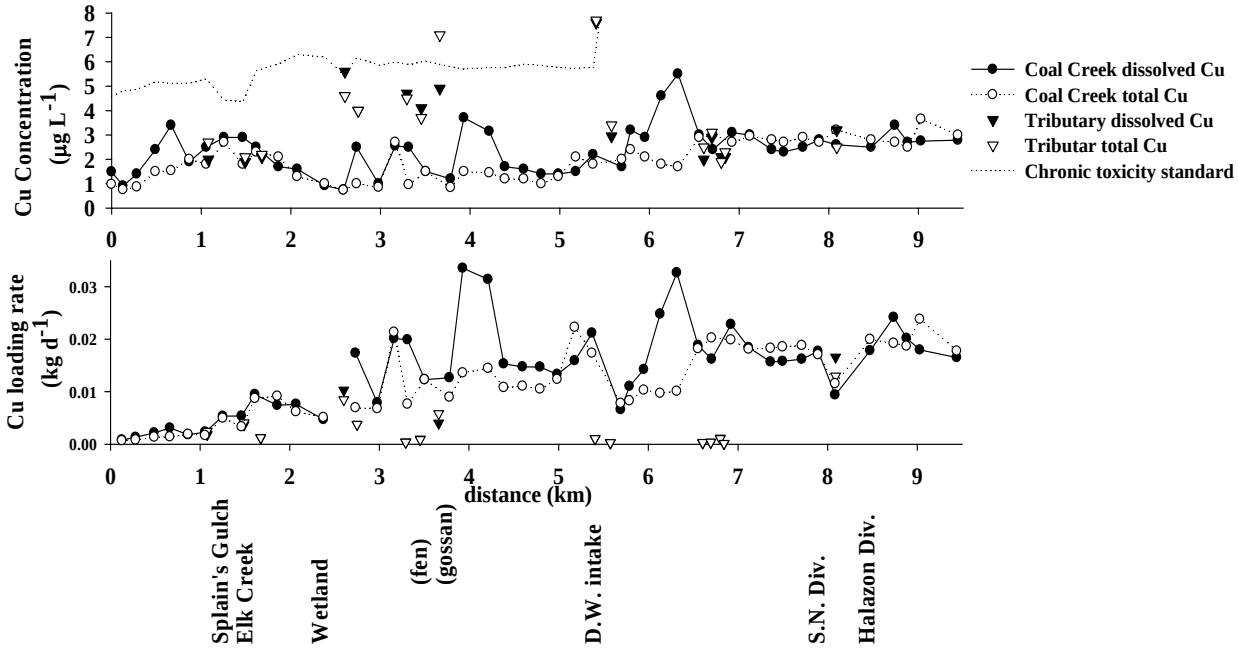


**Figure 16.** Coal Creek and tributary total and dissolved copper concentration, chronic aquatic life toxicity standard, and total and dissolved copper loading rate.

*Cadmium concentrations and loading rates*. Cadmium concentrations remained stable near an average of 0.46 µg $L^{-1}$ from CC-1.412 (0.4 km downstream of Splain's Gulch) to CC-5.312, immediately upstream of the Mt. Emmons Treatment Plant effluent (Figure 17). Cadmium was not detected in samples from CC-(-0.051) to CC-1.204 or in Splain's Gulch. CC-6.268 contained the maximum in-stream dissolved cadmium concentration of 1.6 µg $L^{-1}$. A small rise in cadmium concentration was observed between CC-5.642 and CC-8.085. The average concentration between these sites was 1.09 µg $L^{-1}$. Effluent from the Mt. Emmons Treatment Plant channel was the likely source of this slight rise in cadmium concentration. Downstream of the drinking water reservoir return at 8.097 km, cadmium was diluted to concentrations close to those of CC-1.412 to CC-5.312.

The chronic toxicity standard for aquatic life for cadmium was exceeded over numerous reaches of Coal Creek. The cadmium toxicity standards are hardness-based; therefore, these standards increased significantly downstream of the Mt. Emmons Treatment Plant due to the high calcium content of the effluent. If the chronic toxicity standard upstream of the treatment plant were extended to downstream sites to represent times when effluent is not released, it is possible that several more sites between CC-5.642 and CC-8.085 would have exceeded the chronic standard. The acute and trout acute standards were not exceeded at any in-stream sites. The 1-day total recoverable cadmium standard for a drinking water supply is 5 µg $L^{-1}$. This standard is not shown because all in-stream sites are well below this concentration.

The iron fen and gossan drainages (UT-3.212, UT-3.455, and UT-3.595), contributed the highest cadmium concentrations. In-stream concentration did not increase downstream of the iron fen drainages. Elk Creek and the Mt. Emmons Treatment Plant channel also contributed concentrations above in-stream levels.

The maximum dissolved cadmium loading rate of $9.50 \times 10^{-3}$ kg $d^{-1}$ occurred at CC-6.268. The loading rate increased from CC-1.412, upstream of Elk Creek, to CC-6.268. The drinking water supply diversion caused a drop in total loading rate, as did the Spann Nettick diversion.

UT-3.595 and Elk Creek contributed the greatest tributary cadmium loading rate (Figure 17). The total cadmium loading rate was $4.92 \times 10^{-3}$ kg $d^{-1}$ at UT-3.595 and $4.08 \times 10^{-3}$ kg $d^{-1}$ at Elk Creek. UT-3.595 contributed 39% of the total tributary cadmium loading rate while Elk Creek added 32%. UT-3.455 added 12% of the total cadmium loading rate and the drinking water return added 11%. Though the total cadmium loading rate from the treatment plant channel was only $3.26 \times 10^{-4}$ kg $d^{-1}$ and 2.6% of the cumulative tributary loading rate, the in-stream loading rate was greatest downstream of the treatment plant (Table 8).

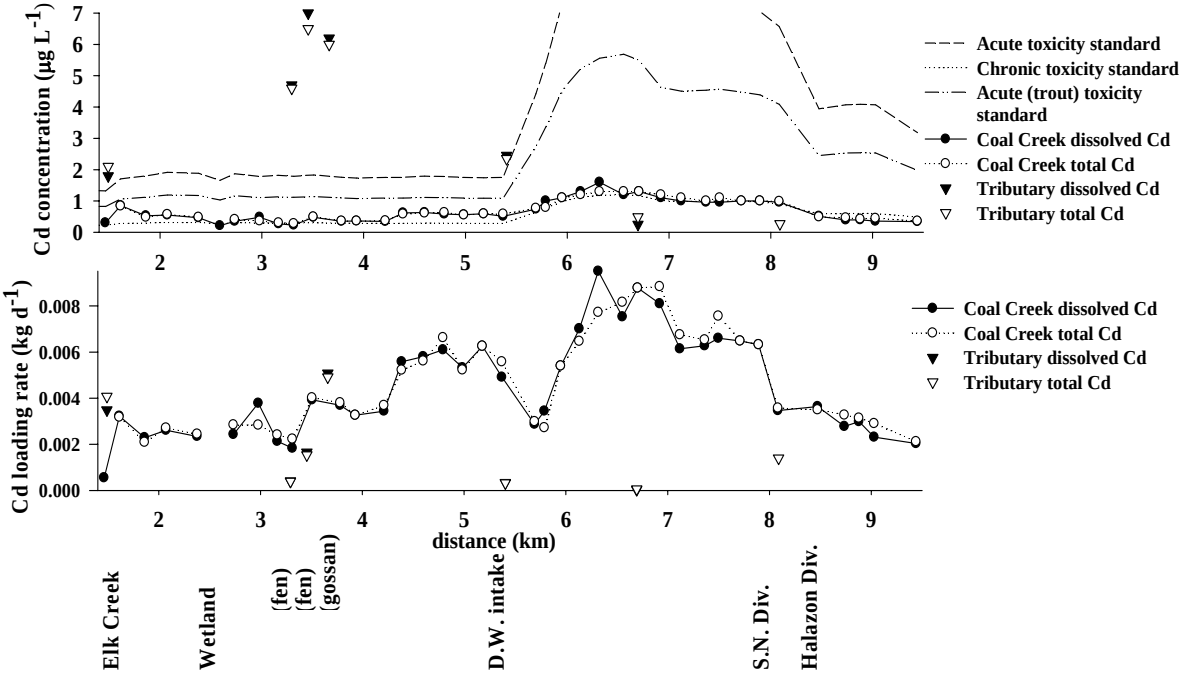


**Figure 17**. Coal Creek and tributary total and dissolved cadmium concentration, chronic, acute, and acute (trout) toxicity standards, and total and dissolved cadmium loading rate.

*Lead concentrations and loading rates*. Lead concentrations were low in Coal Creek. The average total lead concentration from the upstream background site to CC-3.558 was 0.23 µg $L^{-1}$, with the exception of site CC-1.811, which had a total lead concentration of 1.13 µg $L^{-1}$ (Figure 18). The maximum in-stream lead concentration occurred at CC-3.895 and was 1.50 µg $L^{-1}$ total lead. The chronic and acute toxicity standards for dissolved lead were not exceeded at any Coal Creek sites. The 1-day dissolved lead drinking water supply standard of 50 µg $L^{-1}$ was also not exceeded at any site. The acute toxicity and drinking water standards are much greater than in-stream concentrations and are not shown in Figure 18. Total and dissolved lead concentrations were not detected at all but six sites between CC-3.811 and CC-8.974. Total and dissolved lead concentrations were similar, indicating that most lead exists in the dissolved form and that the colloidal fraction is small.

Splain's Gulch was the tributary with the highest total lead concentration. UT-3.455, UT-3.595, UT-6.782, and UT-6.573 also contained significant total lead concentrations.

CC-3.895 has the greatest total lead loading rate of 0.014 kg $d^{-1}$. CC-6.782 and CC-6.605 also had total lead loading rates greater than the average loading rate of $1.1 \times 10^{-3}$ kg $d^{-1}$. The drinking water return at 8.097 km contains the largest tributary total lead loading rate, 50% of the cumulative tributary loading rate. Splain's Gulch adds 22% of the tributary total lead loading rate and UT-3.595 adds 10% (Table 8).

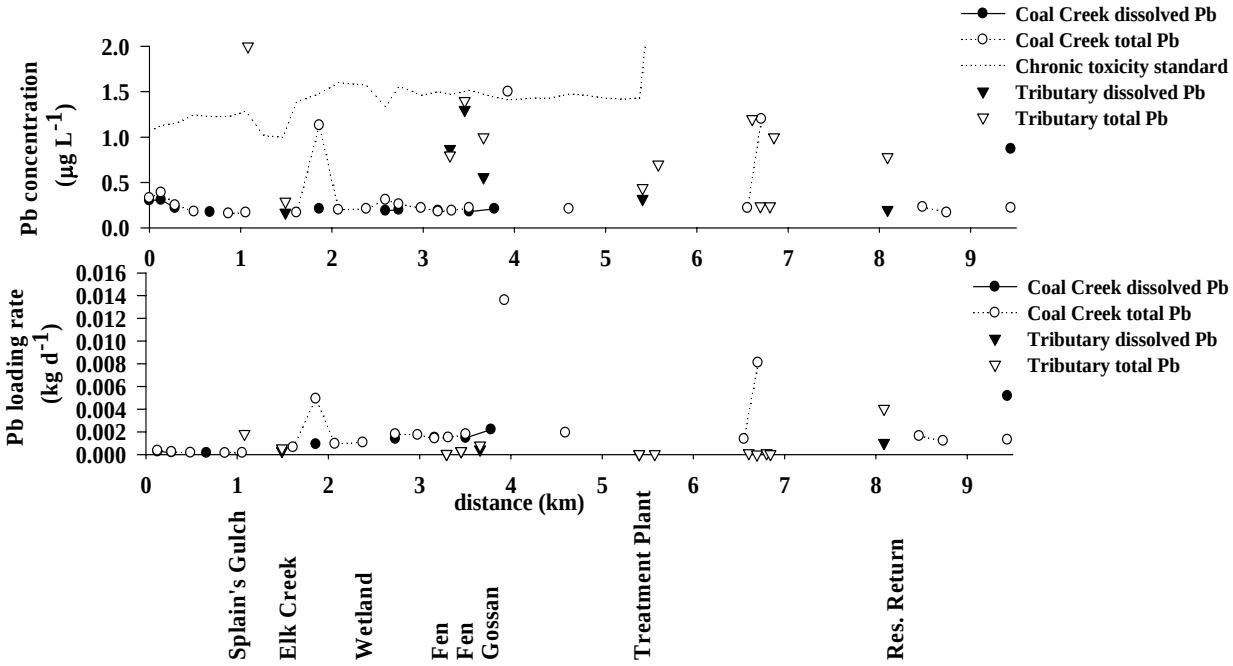


**Figure 18**. Coal Creek and tributary total and dissolved lead concentration, chronic toxicity standard for aquatic life, and total and dissolved lead loading rate. Missing data points are sites with lead concentrations less than the Contract Required Quantitation Limit.

*Nickel concentration and loading rate.* The total nickel concentration exceeded the chronic aquatic life toxicity standard for dissolved nickel only at CC-3.165 (Figure 19). The acute toxicity standard is not exceeded at any in-stream locations and is therefore not shown. The total nickel concentration fluctuated along the length of the study reach. Higher concentrations were measured at CC-1.204, CC-5.739, and CC-8.974.

The four tributaries with the greatest total nickel concentrations were Splain's Gulch, UT-2.511, UT-2.670, and UT-3.595 (gossan drainage). The elevated nickel concentrations at CC-1.204 and CC-3.165 may have resulted from high nickel input from Splain's Gulch, UT-2.511 and UT-2.670.

The maximum total nickel loading rate of 0.38 kg $d^{-1}$ occurred at CC-3.165 (Figure 19). Elevated loading rates were located from CC-3.895 to CC-4.186, CC-4.978 to CC-5.312, and CC-8.974. The highest tributary loading rate of 0.12 kg $d^{-1}$ came from UT-2.511 and was 45% of cumulative tributary loading rate. UT-3.595 contributed 18% of the tributary loading rate with 0.048 kg $d^{-1}$ (Table 8).

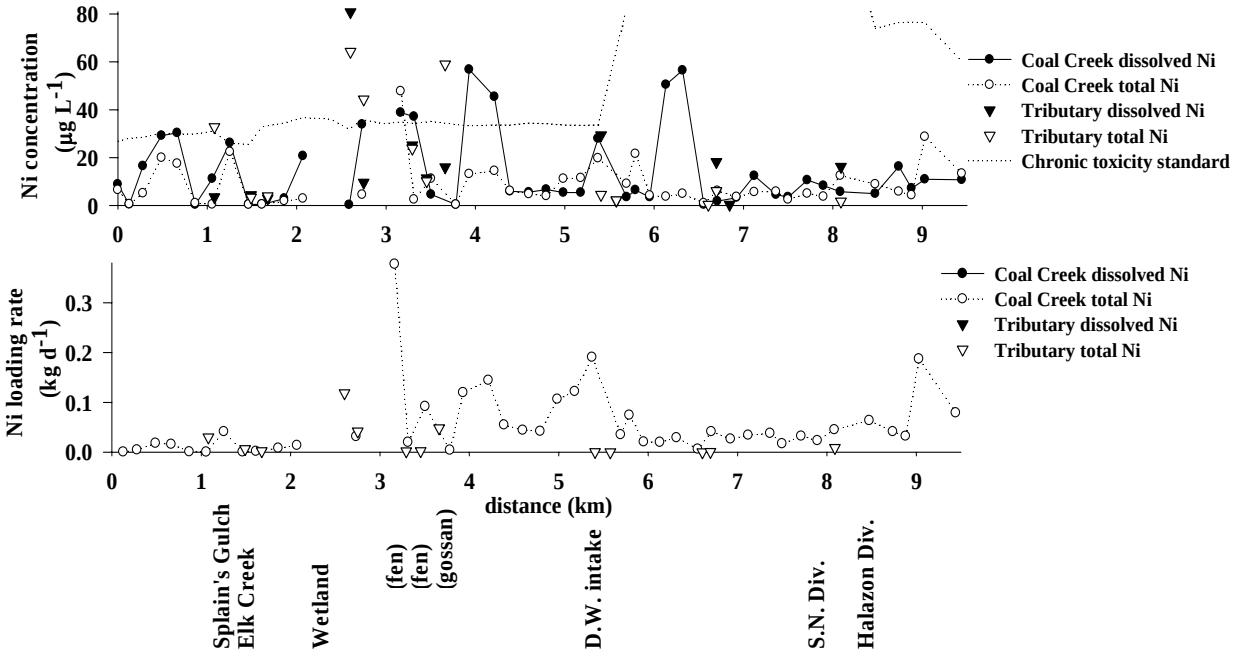


**Figure 19.** Coal Creek and tributary total and dissolved nickel concentration, chronic toxicity standard for aquatic life, and total nickel loading rate.

*Chromium concentration and loading rate*. Dissolved chromium concentrations in Coal Creek fluctuated substantially (Figure 20). The highest total chromium concentrations were measured at CC-0.613, CC-3.165, CC-5.739, and CC-8.974. If the majority of chromium was in the dissolved state and all of the chromium was in the +VI oxidation state, the total chromium concentrations exceeded the chronic and acute toxicity standards for dissolved chromium(VI) at numerous sampling sites. The 1-day drinking water supply standard for hexavalent total chromium was exceeded at CC-0.613 and CC-3.165, immediately upstream of the iron fen. The highest tributary total chromium concentration of 123 µg $L^{-1}$ was measured at UT-2.511. UT-2.670, UT-3.212, UT-3.595, and Splain's Gulch also contained relatively high total chromium concentrations.

The total chromium loading rate was less than 0.10 kg $d^{-1}$ over most of the tracer test reach, but spikes in loading rates were observed (Figure 20). The highest loading rates occurred at CC-3.165, CC-5.312, and CC-8.974. The maximum in-stream loading rate at CC-3.165 was just downstream of the larger tributary loads at UT-2.511 and UT-2.670, though these tributary loads are not as large as the load at CC-3.165. The other spikes in in-stream loading rate were unrelated to tributary input. These increases in chromium loading rate may have been a result of groundwater inputs.

UT-2.511 had the largest tributary total chromium loading rate, 48% of the total tributary chromium loading rate (Table 8). UT-3.595 contributed 19% and UT-2.670 contributed 18%.

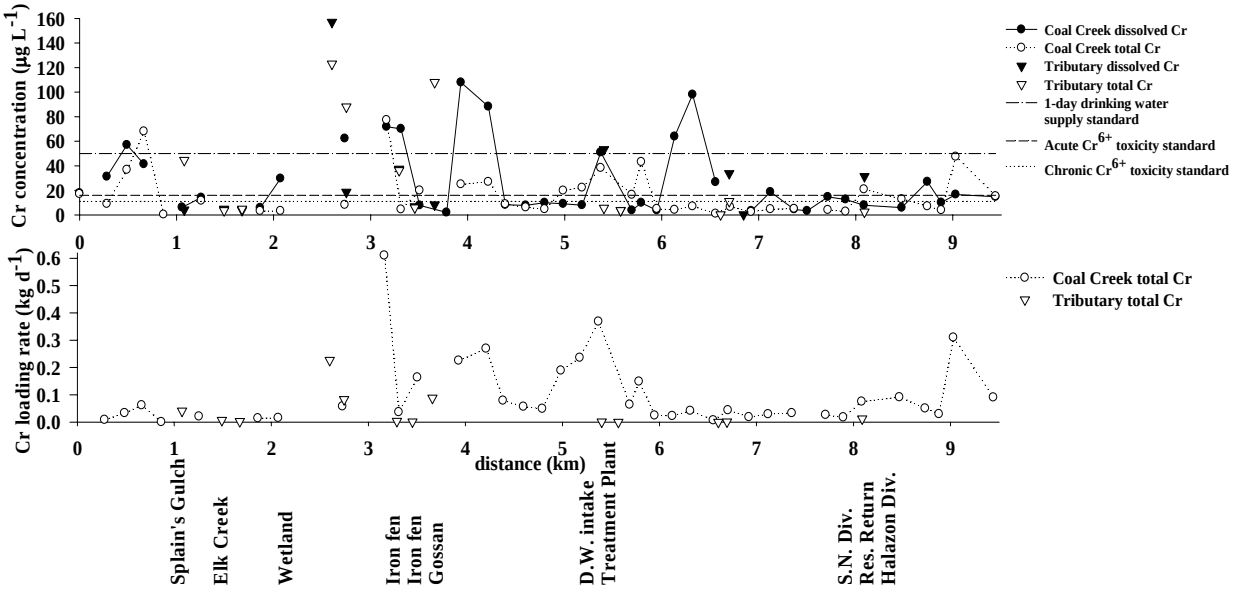


**Figure 20**. Coal Creek and tributary total and dissolved chromium, 1-day drinking water supply standard for chromium(III) and chromium(VI), acute and chronic chromium(VI) toxicity standard, and total chromium loading rate.

*Arsenic concentration and loading rate*. Arsenic concentrations decreased from upstream to downstream. The maximum arsenic concentrations of 15.9 μg $L^{-1}$ dissolved arsenic and 21.4 μg $L^{-1}$ total arsenic occurred at CC-0.077 (Figure 21). The colloidal fraction was greatest at CC-0.077 (5.9 μg $L^{-1}$).

The arsenic aquatic life standards are not hardness-dependent. The acute standard is 340 μg $L^{-1}$ and the chronic standard is 150 μg $L^{-1}$ (CDPHE, 2005). In-stream and tributary concentrations are well below the standards at all sample sites. The 30-day total recoverable arsenic standard for a drinking water supply is 10 μg $L^{-1}$. This standard is a maximum contaminant level established under the federal Safe Drinking Water Act (CDPHE, 2005). The maximum contaminant level was exceeded only over the first 1.1 km of the tracer test reach. The standard for fish ingestion is 7.5 μg $L^{-1}$. This standard was exceeded over the initial 1.2 km of the study reach. Tributary arsenic concentrations were below in-stream concentrations except for at UT-6.692 and the drinking water reservoir return.

The maximum arsenic loading rate of 0.035 kg $d^{-1}$ dissolved arsenic occurred at CC-5.094, 0.210 km upstream of the drinking water intake (Figure 21). Three distinct segments of the loading rate curve were apparent. The loading rate averaged 0.013 kg $d^{-1}$ dissolved arsenic over the first 2.327 km of the tracer test reach. The loading rate spiked in response to increased flow rates beginning at CC-2.580. The average arsenic loading rates from CC-2.580 to CC-5.312 were 0.028 kg $d^{-1}$ dissolved arsenic. Following CC-5.312, the loading rate decreased in response to the drinking water flow diversion and decreasing arsenic concentration. The average loading rate from CC-5.642 to CC-9.387 was 0.0058 kg $d^{-1}$ dissolved arsenic.

Tributary loading rates were lower than in-stream loading rates except at the drinking water reservoir return channel, which contributed 42% of the tributary total arsenic loading rate (Table 8). Elk Creek added 21% and UT-2.511 added 10%.

*Barium concentration and loading rate*. Coal Creek barium concentration averaged 35 μg $L^{-1}$ dissolved barium and 38 μg $L^{-1}$ total barium from over the first 1.412 km of the tracer test reach (Figure 22). A concentration drop occurred at CC-1.562 due to dilution from Elk Creek. The barium concentration averaged 25 μg $L^{-1}$ dissolved barium and 25 μg $L^{-1}$ total barium between CC-1.562 and CC-5.642. Barium concentration increased downstream of CC-5.739. No aquatic life standards for barium are in effect. The 1-day drinking water standard is 1000 μg $L^{-1}$ total recoverable barium while the 30-day drinking water standard is 490 μg $L^{-1}$ (CDPHE, 2005). In-stream and tributary concentrations were below these standards at all sites.

The four closely grouped tributaries from 6.573 to 6.782 km downstream of the injection, UT-6.573, UT-6.692, UT-6.668, and UT-6.782, had some of the highest barium concentrations. The maximum in-stream concentration occurred approximately 2.156 km downstream of these tributaries.

The barium loading rate generally showed an increasing trend, except where the loading rate dropped in response to the drinking water and Spann Nettick diversions (Figure 22). The maximum total barium loading rate of 0.42 kg $d^{-1}$ occurred at CC-8.824.

All tributary loading rates were less than in-stream loading rates. The drinking water return channel contributed 37% of the cumulative tributary barium loading rate (Table 8). UT-3.595 and UT-6.668 added 12% each.

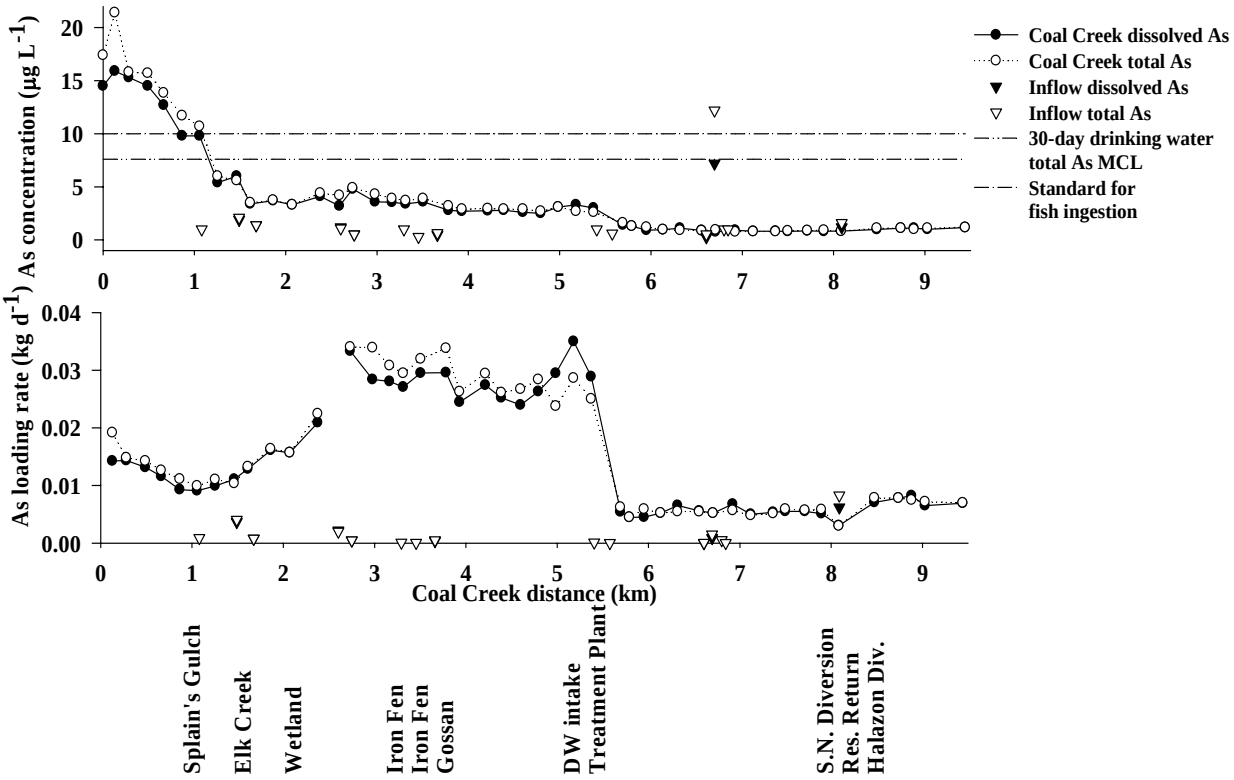


**Figure 21.** Coal Creek and tributary total and dissolved arsenic concentration, 30-day total recoverable arsenic maximum contaminant level (MCL) and health-based standards for a drinking water supply, and arsenic loading rate.

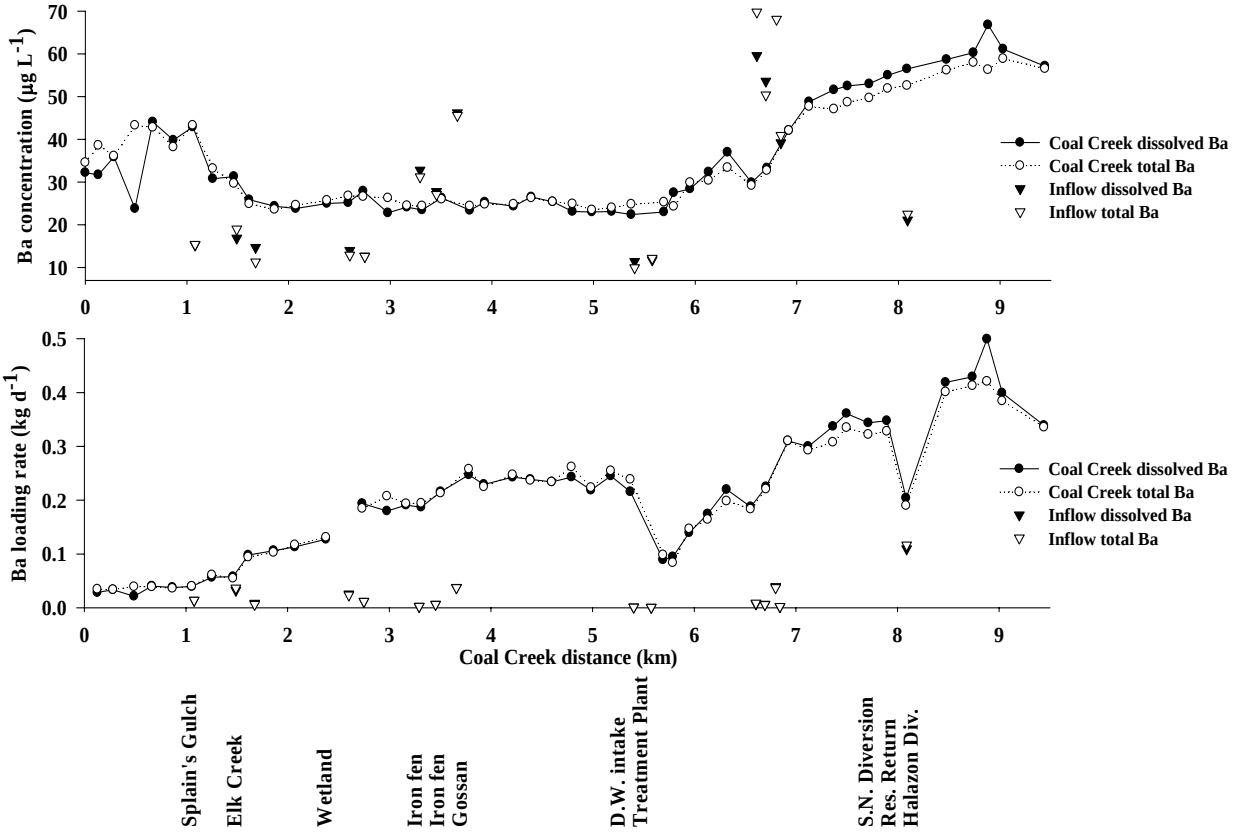


**Figure 22.** Coal Creek and tributary total and dissolved barium concentration and loading rate.

### *Electron microprobe images and elemental analysis*

Scanning electron microscopy (SEM) was used to assess morphology and elemental composition of colloidal material collected on the 0.45 µm filters at four in-stream and two tributary synoptic sample sites; CC-0.077, CC-0.231, CC-6.505, CC-9.387, UT-6.692, and the drinking water return. Though others are wary of using arbitrary filter mesh sizes to define dissolved constituents (Kennedy et al., 1974; Danielsson, 1982; Ryan and Gschwend, 1990; Pham and Garnier, 1998; Morrison and Benoit, 2001), historically, 0.45-µm filters have been used to separate dissolved constituents from particulates. Furthermore, the EPA required 0.45 µm filtration for the inductively-coupled plasma (ICP) analyses. With the morphology and elemental composition of the colloidal material, we can attempt to identify the mineralogy of the colloids (Mudroch et al., 1977).

Electron microprobe images for CC-0.077, CC-9.387, the drinking water reservoir return channel at 8.097 km, and UT-6.692 are presented in Figures 23-25. The figures show some of the minerals identified in these samples. An unidentified clay mineral, iron and manganese oxyhydroxides, and microcline were found at CC-0.077 (Figure 23).

The oxyhydroxides are filamentous. Albite, clay, iron oxyhydroxide, microcline, plagioclase, and quartz were some of the minerals present at CC-9.387 (Figure 23). Manganese oxyhydroxide was present in the drinking water reservoir return flow (Figure 24). The iron oxyhydroxide at UT-6.692 appeared to be bacterially controlled as indicated by the filamentous morphology (Figure 25). Particle sizes can be determined by comparing individual particles with the scale shown at the bottom of each micrograph.

The relative abundance of various elements was determined following the guidelines set forth by Mudroch et al. (1977) for several minerals using electron microprobe spectra. Elemental spectra for microcline (CC-0.077), illite (drinking water return channel), manganese oxyhydroxide (drinking water return channel), and iron oxyhydroxide (CC-9.387) minerals are shown in Figures 26 and 27. Oxygen and hydrogen do not appear in the oxyhydroxide spectra. This method has a poor sensitivity for light elements with atomic numbers less than 15 (Mudroch et al., 1997).

Table 9 presents a list of representative minerals found at each of the six samples sites that were investigated. The mineralogical composition was inferred based on electron microprobe images and elemental ratios apparent in the spectra (Mudroch et al., 1977). Though these minerals are considered representative of each respective sample, other minerals may also be present at these sites, but may not have shown up in these analyses. The relative predominance of these minerals as a fraction of the entire sample was not determined.

In-stream samples were not dominated by any one mineral. An array of minerals was present at each site. CC- 0.077 had no iron oxyhydroxide as expected for in-stream sites upstream of mining inputs. Conversely, iron oxyhydroxide was found at CC-0.231 although it is upstream of mine drainage. CC-6.692 did not contain the iron oxyhydroxides indicative of acid mine drainage impact, though this site is downstream of Elk Creek, the iron fen, the gossan, and the Keystone Mine. No pattern relating to the upstream versus the downstream mineralogical composition could be established. Both tributaries analyzed with the electron microprobe contained large amounts of either manganese or iron oxyhydroxides.

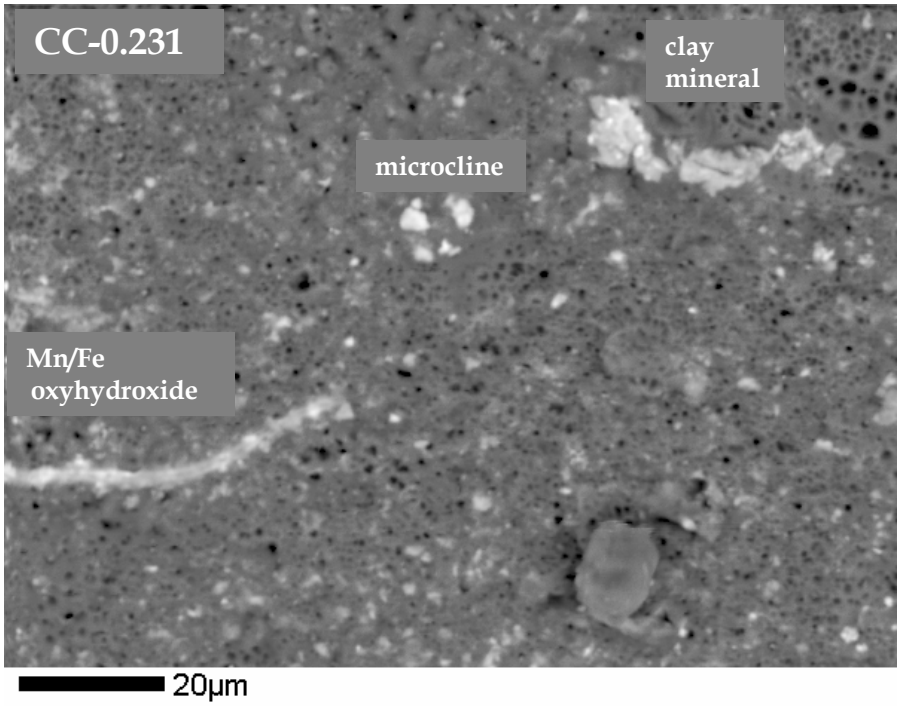


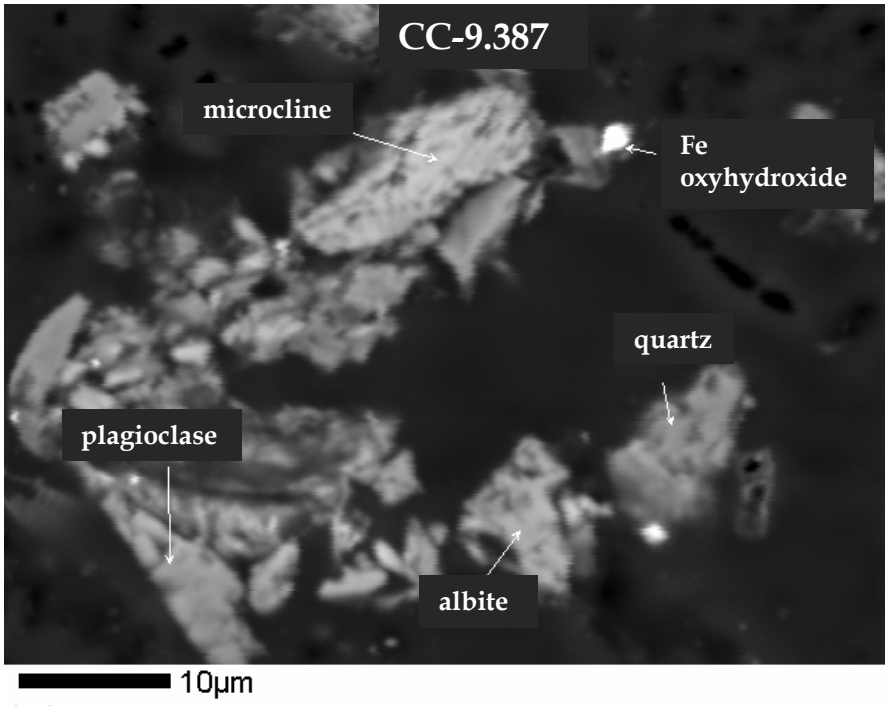


**Figure 23.** Electron microprobe images showing portions of colloids filtered from CC-0.231 (upper) and CC-9.387 (lower) water samples. The colloids were trapped on a 0.45 µm nylon membrane filter. Minerals were tentatively identified with the aid of elemental analysis. The magnification is 950× for the CC-0.231 micrograph and 2,000× for the CC-9.387 micrograph.

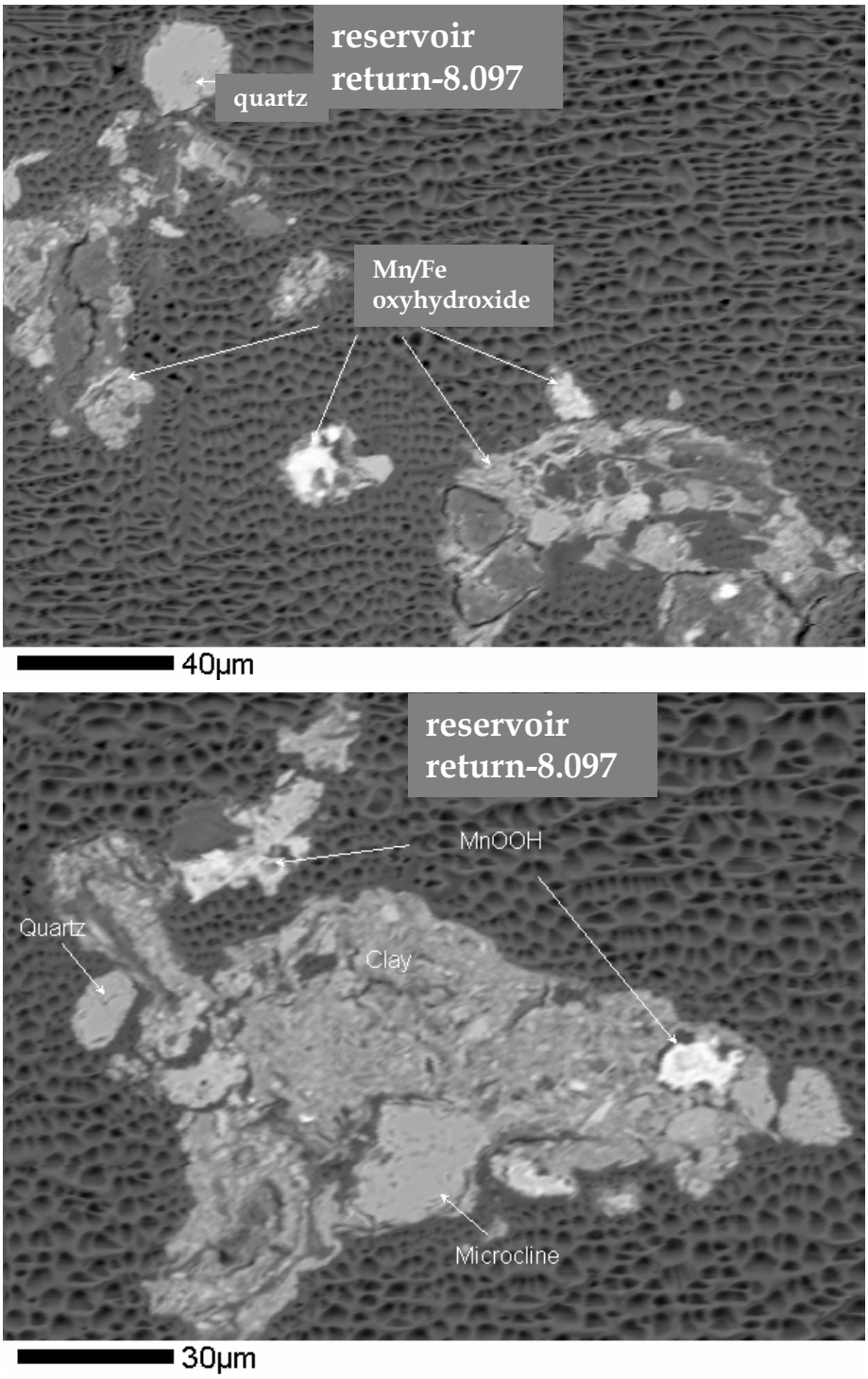


**Figure 24.** Electron microprobe images showing portions of colloids filtered from the drinking water reservoir return flow. Minerals were tentatively identified with the aid of elemental analysis. The magnification is 575.0× in the top micrograph and 733.3× in the bottom micrograph.

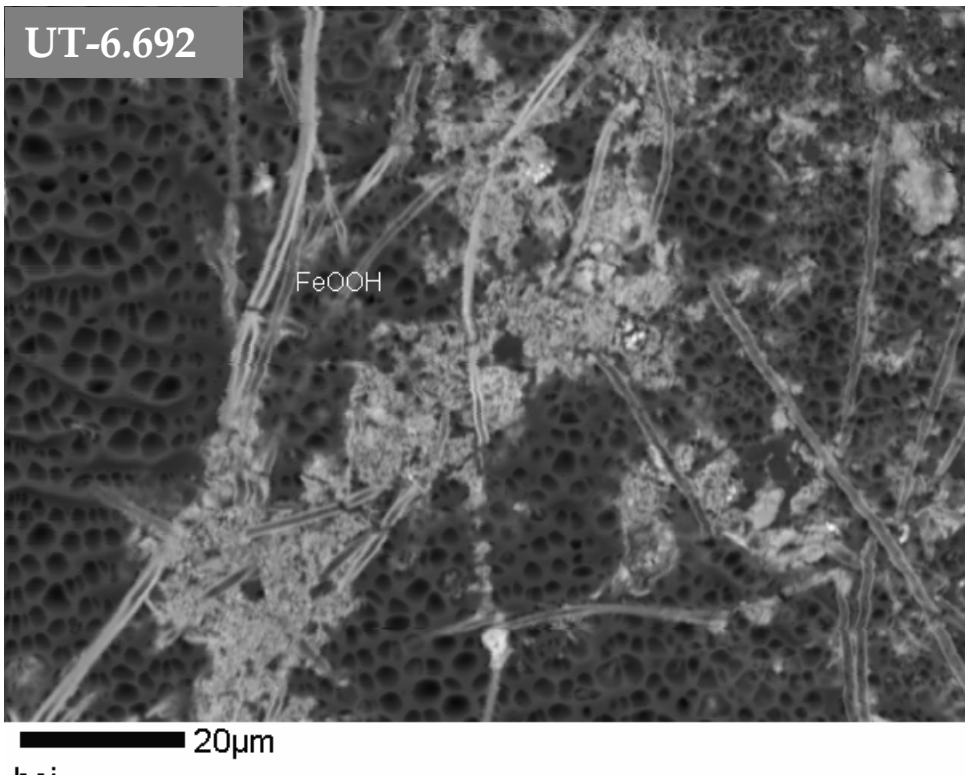


**Figure 25.** Electron microprobe images showing portions of colloids filtered from the UT-6.692 water sample. Minerals were tentatively identified with the aid of elemental analysis. The magnification is 1,100×.

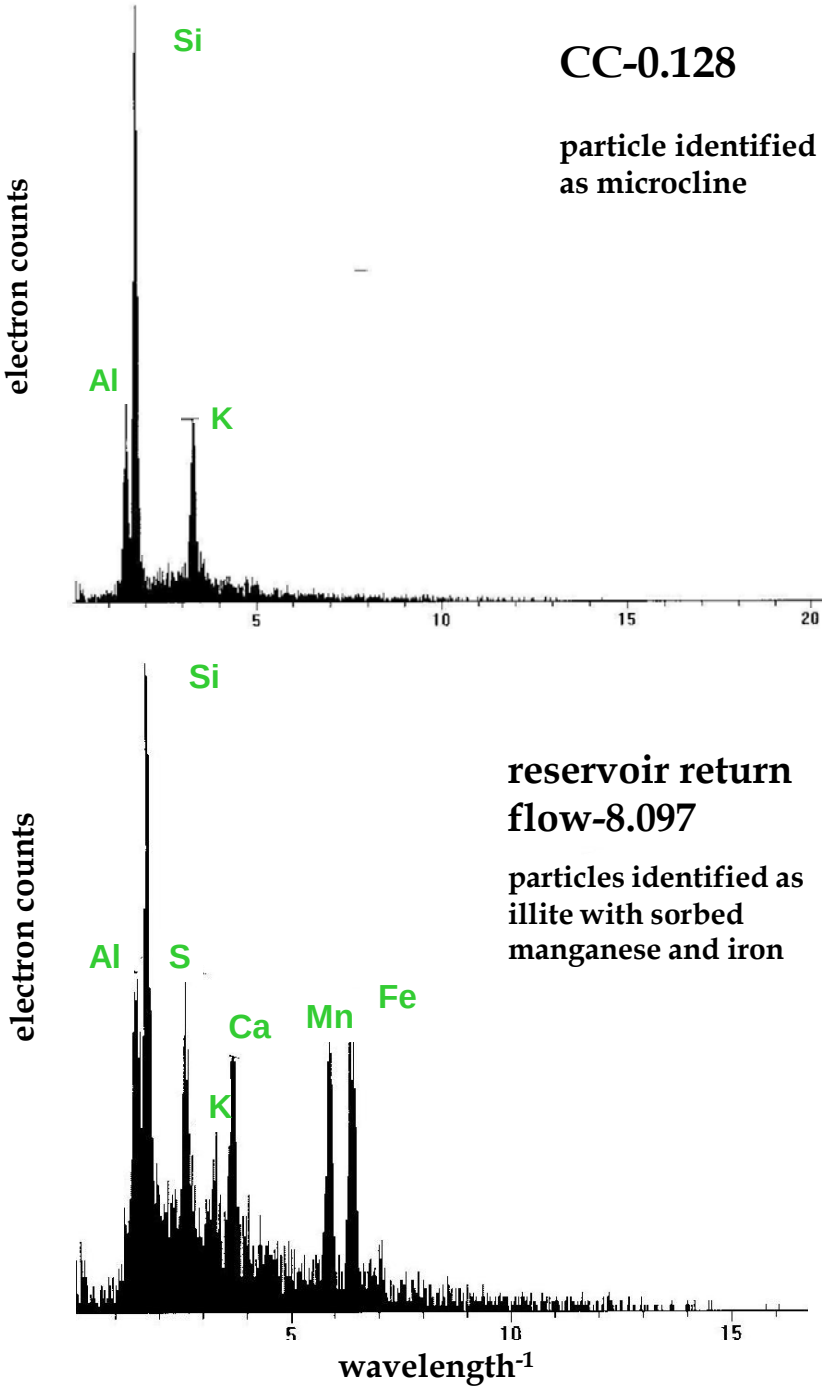


**Figure 26.** Elemental spectra for representative particles trapped on a 0.45 µm nylon filter at CC-0.077 (upper spectrum) and the drinking water reservoir return channel (lower spectrum). The upper spectrum was identified as microcline (potassium feldspar; $KAlSi_3O_8$) following the guidelines of Mudroch et al. (1977). The lower spectrum was identified as illite with adsorbed manganese and iron.

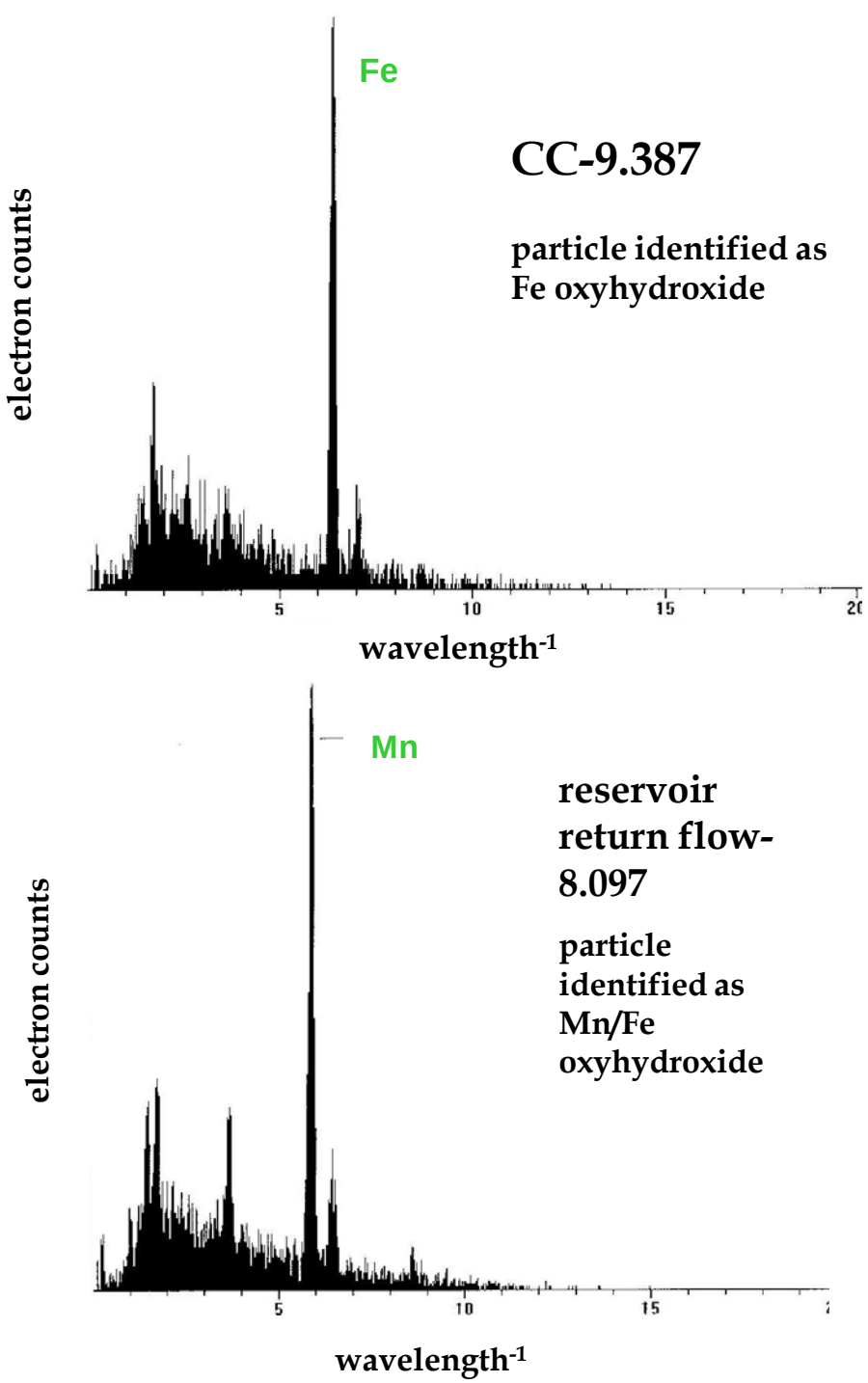


**Figure 27.** Elemental spectra for representative particles trapped on a 0.45 µm nylon filter at CC-9.387 (upper spectrum) and the drinking water reservoir return (lower spectrum). The upper spectrum is an iron oxyhydroxide. The lower spectrum is a manganese oxyhydroxide of unknown composition.

**Table 9.** Summary of scanning electron microprobe results for mineralogical composition of colloids collected on 0.45 μm filters. Mineralogy was inferred based on particle morphology and elemental analysis.

| Sample Site | Minerals Tentatively Identified |
|---|---|
| CC-0.077 | microcline, pyroxene |
| CC-0.231 | albite, calcite, iron oxyhydroxide, iron-manganese oxyhydroxide, microcline, plagioclase |
| CC-6.505 | albite, microcline, pyroxene, quartz |
| CC-9.387 | albite, calcite, iron oxyhydroxide, microcline, plagioclase, quartz |
| Drinking water reservoir return-8.097 | manganese oxyhydroxide, albite, clay minerals (illite?), iron oxyhydroxide, microcline, pyroxene, sphene, quartz |
| UT-6.692 | iron oxyhydroxide, calcite, pyroxene, quartz |

# DISCUSSION

### *Suitability of lithium and chloride as tracers*

An appropriate tracer must have several characteristics to qualify it for use in a tracer injection study. The tracer must be (1) conservative, or non-reactive and not prone to sorb to solid material, (2) insensitive to variations in pH and metal chemistry that occur naturally within the study reach, (3) at concentrations several times greater than background concentrations, (4) cost-effective, and (5) it must not pose a risk to human health or aquatic life (Bencala et al., 1986, Bencala et al., 1990).

Flow rates calculated using lithium dilution were gross overestimates with values as excessively high as 2,500 L $s^{-1}$ (Figure 10). This flow rate is approximately 80 times greater than the flow rate estimated by Coal Creek Watershed Coalition members (Tyler Martineau, personal communication, September 1, 2005) just prior to the tracer study and inconsistent with historical flow records as well as with the substantial volume of flow diverted from Coal Creek. We concluded that lithium did not behave conservatively in Coal Creek and that lithium dilution data was not useful in correctly estimating Coal Creek flows. Though lithium chloride was an effective tracer in Lefthand Creek (Wood et al., 2004), previous tracer studies in the Redwell Basin, a watershed adjacent to the Coal Creek watershed, show that lithium does not behave conservatively at pH greater than 6 (Briant Kimball, personal communication, November, 16, 2005). Even a tracer that sorbs moderately may not be suitable under low flow in a shallow stream frequently surrounded by wetlands like Coal Creek.

Shallow streams allow more contact between sorbing solutes in the water column and the streambed (Bencala, 1990). With an average pH of 7.38, moderate TOC concentrations, shallow depths, and surrounding wetlands, it is likely that lithium bonded to organic matter in the water column and the hyporheic zone. Based on lithium concentrations, the calculated flow doubles as Coal Creek passes a wetland (CC-2.021 to CC-2.580) (Figure 10), but it was clear in the field that flow did not actually double over this reach. Significant transient storage means a longer solute residence time through the wetland reaches. Longer residence times in zones with an abundance of sediment surfaces (wetlands) provide greater opportunity for reactions otherwise limited by availability of reactive surfaces or kinetic restraints (Broshears et al., 1993). The tracer-dilution equation breaks down when processes other than dilution affect the tracer concentration.

Lithium was originally thought to be a suitable tracer because background lithium concentrations were quite low in natural waters. A lithium salt tracer injection easily raises stream lithium concentration by at least an order of magnitude in streams with low background lithium concentrations. This fulfills the requirement that in-stream tracer concentration be substantially higher than inflow tracer concentration. The difference between in-stream and inflow tracer concentration must be greater than the analytical uncertainty associated with the concentration data (Bencala, 1987).

Lithium chloride is among the more expensive tracers; however, the cost was not inhibitory as only 67 kg was required to raise concentrations to adequate levels during low flow. Furthermore, aquatic ecosystems are not negatively impacted by the introduction of lithium chloride at the concentrations used for this study.

Previous studies show that chloride behaves conservatively as only physical processes such as dilution, dispersion, and transient storage influence the attenuation of chloride concentration. Biogeochemical reactions have minimal impact on chloride attenuation (Bencala, 1985; Bencala et al., 1986; Bencala et al., 1987; Bencala et al., 1990). Chloride is commonly referred to as the "universal tracer" because of its conservative behavior; however, it is also more likely to be present in moderate concentrations in natural waters (Bencala, 1990). Atmospheric deposition and weathering are sources of chloride in natural systems (Kimball et al., 2002).

***Steady-state conditions for tracer injection***

The tracer-dilution method is dependent upon a steady-state in-stream tracer concentration. Because the tracer injection flow rate fluctuated slightly and a tracer arrival curve at the most downstream site, CC-9.387, was not available, we cannot prove that the system was at steady-state. However, velocity estimates and available chloride concentration data for CC-9.387 support the arrival of the tracer at CC-9.387 and the establishment of steady-state in-stream conditions.

Based on the pulse sodium chloride injection, the average velocity along the first 1.3 km of the study reach was 0.22 km $h^{-1}$ (Table 4). If this velocity remained steady for the length of the study reach, then a LiCl injection period of 43 h would be required for the tracer to reach CC-9.387. This was a conservative estimate because the velocity was observed to increase as flow rate increased with downstream distance (with the exception of flow through the wetlands). The tracer was injected for 50.5 h, 7.5 h longer than required, to ensure that the tracer reached the CC-9.387 at the downstream end of the study reach.

Velocity estimates were also made based on the distance traveled by the calcium-laden effluent entering Coal Creek from the Mt. Emmons Treatment Plant. The treatment plant discontinued daily discharge at 16:00. Calcium concentrations are maximum at CC-6.268, CC-6.505, and CC-6.605, indicating the location of the trailing edge of the effluent "plug" in Coal Creek (Figure 9). These sites were sampled at 18:30, 17:50, and 18:12, respectively. Stream velocity between the treatment plant and these sites was calculated as the distance between the treatment plant and the site divided by the sample time minus 16:00. The average velocity along this reach was 0.528 km $h^{-1}$. This velocity is greater than that calculated for the first 1.3 km of the study reach, indicating that the observation that stream velocity increases with downstream distance was valid.

In Coal Creek, the background chloride concentration is 2.38 mg $L^{-1}$ (Figure 11). This background chloride concentration limited the analytical resolution of Coal Creek concentration data. The in-stream chloride concentration dropped to within 1.0 mg $L^{-1}$

of the background chloride concentration by CC-5.642 and to within 0.5 mg $L^{-1}$ of background concentrations at the most downstream site, CC-9.387 (Table 10). Several tributaries also contained chloride concentrations similar to in-stream chloride concentrations. The average chloride concentration at downstream end, CC-9.387, stabilized at 0.40 mg $L^{-1}$ greater than the background chloride concentration. This difference is greater than any differences caused by error in the chloride measurement and shows that the chloride tracer reached the downstream end of the study reach.

**Table 10.** Chloride concentrations at the upstream end, CC-(-0.051), and the downstream end, CC-9.387, of the injection reach.

| Sample Date and Time | CC-(-0.051) (mg $L^{-1}$) | CC-9.387 (mg $L^{-1}$) |
|---|---|---|
| 9/3/2005 12:10 | 2.36 | |
| 9/3/2005 14:12 | 2.11 | |
| 9/3/2005 14:12 | 2.45 | |
| 9/32005 16:08 | 2.57 | |
| 9/3/2005 18:07 | 2.26 | |
| 9/4/2005 02:00 | 2.59 | |
| 9/4/2005 10:05 | 3.14 | |
| 9/4/2005 14:02 | 1.95 | |
| 9/4/2005 18:00 | 2.24 | |
| 9/5/2005 11:06 | 2.50 | |
| 9/5/2005 13:02 | 2.34 | |
| 9/5/2005 11:10 | | 2.44 |
| 9/5/2005 12:00 | | 2.53 |
| 9/5/2005 12:45 | | 3.01 |
| 9/5/2005 13:30 | | 2.66 |
| 9/5/2005 14:15 | | 2.55 |
| 9/5/2005 14:15 | | 2.87 |
| 9/5/2005 15:00 | | 2.96 |
| 9/5/2005 15:45 | | 2.85 |
| 9/5/2005 16:30 | | 2.67 |
| 9/5/2005 16:30 | | 2.97 |
| 9/5/2005 17:15 | | 2.69 |
| 9/5/2005 18:00 | | 2.61 |
| 9/5/2005 18:45 | | 2.40 |
| 9/5/2005 18:45 | | 2.71 |
| 9/5/2005 19:30 | | 3.56 |
| 9/5/2005 19:50 | | 3.25 |
| **Average** | **2.40** | **2.80** |

### *Hardness and the treatment plant effluent*

The Mt. Emmons Treatment Plant adds lime during the treatment process to achieve a pH above 10 (John Perusek, personal communication, July 15, 2005). The pH is increased to precipitate and remove cadmium and manganese in the plant's flotation process. The calcium used during the treatment process enters Coal Creek when the effluent is released. The sharp spike in calcium concentration downstream of the Mt. Emmons Treatment Plant effluent produces a similar sharp spike in hardness.

The sites with high calcium and hardness concentrations graphically depict the downstream movement of the treatment plant effluent "plug" (Figure 9). The treatment plant discontinues effluent release by about 16:00 each day. The release is not steady; it varies from 0.00 to 78.9 L $s^{-1}$ over the day (John Perusek, personal communication, July 15, 2005). All synoptic samples from CC-5.642 to CC-9.387 were taken between 17:42 and 19:45 on September 5, 2005. Calcium and hardness concentrations reached maxima at CC-6.505, approximately 1.2 km downstream of the treatment plant (UT-5.340). This lag distance between the treatment plant and the peak represents the distance traveled by the effluent "plug" between 16:00, when the treatment plant discontinued discharge of the effluent, and 17:50, when CC-6.505 was

sampled. The resulting flow velocity is about 0.18 m $s^{-1}$, which is about three times faster than the velocity measured by the preliminary salt injection before the lithium chloride injection (0.061 m $s^{-1}$). The sharp drop in calcium concentration and hardness between CC-6.605 and CC-6.872 may represent a change in the treatment plant effluent discharge rate, but detailed records of the effluent discharge rate were not available. The decline in calcium concentration and hardness between CC-8.085 and CC-8.352 is a result of dilution from the drinking water reservoir return flow.

Large daily fluctuations in calcium concentration and hardness in Coal Creek are expected. When the treatment plant is discharging effluent, downstream calcium concentration will be approximately 12 times greater than upstream calcium concentration at low flow. Consequently, hardness and hardness-based aquatic life toxicity standards will also show daily fluctuations. Hardness-based acute and chronic toxicity standards are not to be exceeded more than once every three years on average and should be computed using the lowest daily calcium and magnesium concentrations (CDPHE, 2005). When hardness drops, toxic metal uptake by aquatic organisms increases because less calcium and magnesium is present to compete with the toxic metals for binding sites on gills and in the digestive tract. For comparison purposes, hardness-based standards upstream of Mt. Emmons discharge can be extrapolated to sites downstream to represent conditions when elevated calcium is not present in Coal Creek.

### *Aquatic life and drinking water supply standard exceedances*

Metal concentrations in Coal Creek exceeded CDPHE acute and chronic standards for aquatic life and drinking water supply standards at several sample sites along the study reach (Table 11). Cadmium, chromium, nickel, and zinc exceeded the chronic toxicity standard. Cadmium, chromium, and zinc exceeded the acute toxicity standard. Arsenic exceeded the drinking water supply and fish ingestion standard for along the initial 1.2 km of the study reach. Chromium, iron, and manganese also exceeded the drinking water standard at several sample sites.

The calcium input from the Mt. Emmons Treatment Plant produced in-stream increases in the hardness-based aquatic life standards when the plant was discharging. When the plant discontinues discharge, the calcium concentrations in Coal Creek are expected to decrease, producing subsequent decreases in the hardness-based aquatic life standards. Some metals with concentrations below aquatic life standards when the plant is discharging are likely to exceed standards when the plant is not discharging. To predict when this occurred, the hardness-based standards upstream of the treatment plant were assumed to extend downstream. The metal concentrations added to Coal Creek when the plant was discharging and when it was not were also considered. Bold sample sites in Table 11 designate that aquatic life standards were not exceeded during treatment plant discharge, but are predicted to be exceeded when the plant is not discharging.

**Table 11.** Coal Creek sample sites where the chronic and acute aquatic life toxicity standards and the drinking water supply standard were exceeded. **Bold** indicates sites where daily decreases in calcium concentrations corresponding to times when the treatment plant is not discharging could decrease aquatic life standards enough to cause exceedances.

| Metal | Chronic Standard Exceeded | Acute Standard Exceeded | Drinking Water Standard Exceeded |
|---|---|---|---|
| Aluminum | None | None | -- [1] |
| Arsenic | None | None | CC-(-0.051)-CC-1.006 |
| Barium | -- | -- | None |
| Cadmium | CC-1.562-2.327, CC-2.580-2.978, CC-3.314-5.642, CC-5.900-6.082, CC-6.605-7.070, CC-7.662-8.085, **CC-5.739, CC-6.268-6.505, CC-7.314-7.448, CC-8.352-9.387** | **CC-5.900 - CC-7.070** | None |
| Chromium | CC-(-0.051), CC-0.438-0.613, CC-1.204, CC-3.165, CC-3.558, CC-3.895-4.186, CC-4.978-5.739, CC-8.085-8.352, CC-8.974-9.387 | CC-(-0.051), CC-0.438-0.613, CC-1.204, CC-3.165, CC-3.558, CC-3.895-4.186, CC-4.978-5.739, CC-8.085, CC-8.974 | CC-0.613, CC-3.165 |
| Copper | None | None | None |
| Iron | -- | None | CC-0.231-0.438, CC-2.467, CC-3.165-3.314 CC-3.895-4.186, CC-6.082 |
| Lead | None | None | None |
| Manganese | None | None | CC-2.327-2.580, CC-3.165-3.558, CC-4.284, CC-6.082-6.268 |
| Nickel | CC-3.165 | None | None |
| Zinc | CC-1.562-2.327, CC-3.558, CC-4.284-5.312, **CC-5.642-8.085** | CC-1.562-2.021, CC-3.558, CC-4.284-5.312 **CC-5.642-8.085** | None |

[1] -- Standard does not exist

Because the treatment plant was not discharging at the time of synoptic sampling on September 5, the site was sampled a second time on the morning of September 6, 2005, when effluent was being released. Flow during the synoptic sampling was only 1.61 L $s^{-1}$. The exact flow rate on September 6 is unknown. Metals in the synoptic sample taken on September 5 are attributable to residual treatment plant flow. Relatively high concentrations of aluminum, cadmium, copper, iron, manganese, and zinc were present in the Mt. Emmons Treatment Plant effluent channel at 5.340 km on one or both of the sample days (Table 12). Aluminum, cadmium, copper, manganese, and zinc had lower concentrations on September 6, presumably as a result of dilution from the treatment plant effluent. Total aluminum concentration was 10% lower and dissolved aluminum was 33% lower on September 6. Total cadmium, copper, manganese, and zinc concentrations decreased by 62%, 21%, 63%, and 79%, respectively. The iron concentration increased from undetectable concentrations on September 5 to 136 µg $L^{-1}$ total iron on September 6. Aluminum, cadmium, copper, and zinc inputs raised Coal Creek loading rates for these metals downstream of the treatment plant (UT-5.340), despite a decrease in flow due to the drinking water intake diversion (Figure 28). The spatial distribution of the elevated in-stream calcium and aluminum, cadmium, copper, and zinc concentrations corresponds to the transport of treatment plant effluent along Coal Creek. For example, aluminum peaks approximately 1 km downstream of the treatment plant, with elevated aluminum concentrations 0.25 – 2.1 km downstream (Figure 15 and 29).

**Table 12.** Total and dissolved aluminum, copper, iron, manganese, and zinc concentrations in the Mt. Emmons Treatment Plant effluent channel at 5.340 km during synoptic sampling on September 5 (after discharge from the plant ceased) and during discharge on September 6. BDL is an abbreviation for "below detection limit".

| metal | treatment plant effluent after discharge | treatment plant effluent during discharge | decrease (%) |
|---|---|---|---|
| Al (µg $L^{-1}$) | | | |
| total | 1130 | 1020 | 10 |
| dissolved | 1080 | 728 | 33 |
| Cd (µg $L^{-1}$) | | | |
| total | 3.4 | 1.3 | 62 |
| dissolved | 3.4 | 1.5 | 56 |
| Cu (µg $L^{-1}$) | | | |
| total | 8.6 | 6.8 | 21 |
| dissolved | 8 | 7.2 | 10 |
| Fe (µg $L^{-1}$) | | | |
| total | BDL | 136 | -- |
| dissolved | BDL | -- [1] | -- |
| Mn (µg $L^{-1}$) | | | |
| total | 318 | 117 | 63 |
| dissolved | -- | 120 | -- |
| Zn (µg $L^{-1}$) | | | |
| total | 562 | 120 | 79 |
| dissolved | 567 | 93.2 | 84 |

[1] -- a valid concentration was not obtained

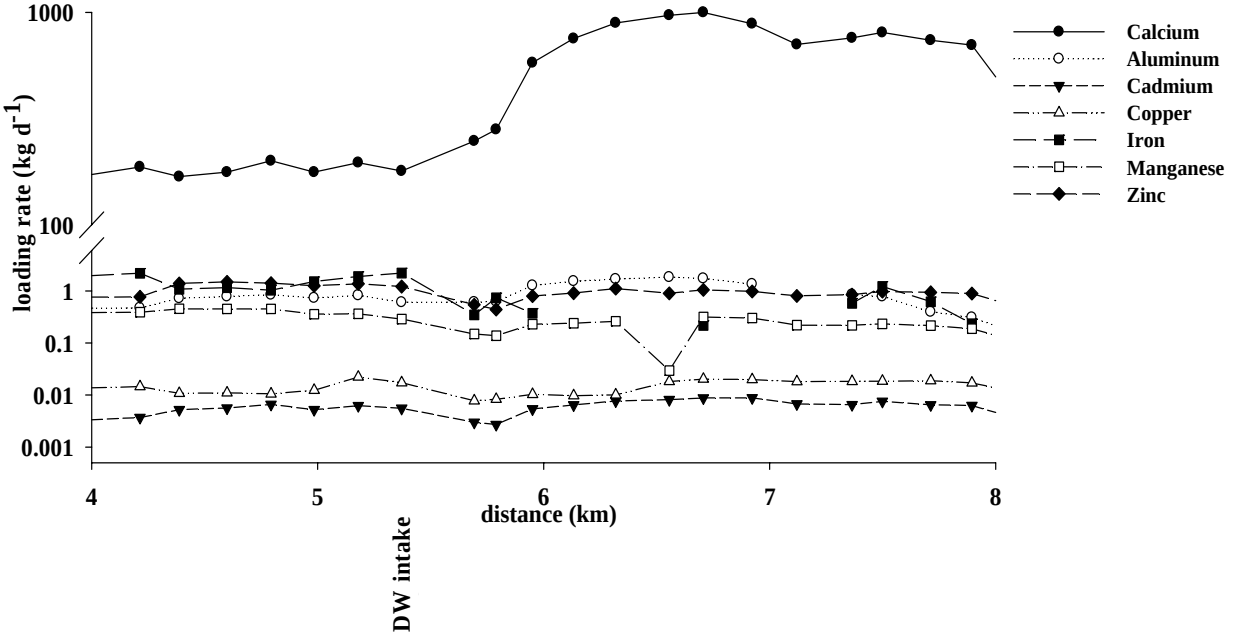


**Figure 28.** The loading rates for calcium along with aluminum, cadmium, copper, iron, manganese, and zinc for the 4-8 km section of Coal Creek to illustrate the effect of the Mt. Emmons Treatment Plant discharge (at 5.430 km, just downstream of the "DW intake") on Coal Creek metal loading rates.

### *Stream Flow*

From 1941 to 1946, the U.S. Geological Survey maintained a stream gauge on Coal Creek just downstream of the Elk Creek confluence. The location of the gauge was equivalent to the location of CC-1.811 used in this study. The USGS measured an average September flow rate of 58.2 L $s^{-1}$ and an average September 5 flow rate of 66.8 L $s^{-1}$ during those years. The flow rate at CC-1.811 calculated using the chloride dilution data was 50.5 L $s^{-1}$ on September 5, 2005. Possible climactic changes since the 1940s, the relatively short time span over which USGS measured flow rate, and the time gap between USGS data and the data pertaining to this study do not allow for a direct comparison. However, USGS flows are within 17 L $s^{-1}$ of the flow rates calculated using chloride dilution. This establishes confidence that tracer-dilution flow rates are reasonable and representative of true flow, at least for the upstream end of the study reach through CC-1.811.

Also, diversion flow rates were known, with the greatest flow of 79 L $s^{-1}$ removed by the Town of Crested Butte drinking water intake at 5.296 km. The Coal Creek flow rate was only 1.4 times greater than drinking water diversion flow rate as calculated using chloride dilution, but 8.9 times greater when calculated using lithium dilution (Figures 10 and 11). Visually estimated flows were much closer to the chloride-calculated flow rates.

Without stream gauge measurements for the day of the tracer study, exact hyporheic flow cannot be determined. Previous studies indicate that up to 40% of stream discharge may occur as underflow through the hyporheic zone in mountainous gravel-bed streams (Zellweger et al., 1989). A study of flow in Peru Creek in Summit County, Colorado, showed that the area of the hyporheic zone may increase by a factor of 2 through wetland reaches like those in Coal Creek (Jeffrey Wong, personal communication, July 12, 2006).

Three diversions of flow from Coal Creek and one flow return affected the flow rate during low flow. The Crested Butte drinking water intake is the most upstream flow diversion. The large flow reduction between CC-5.312 and CC-5.642 illustrates the significant impact the drinking water intake effects on Coal Creek (Figure 11). The intake removed 79 L $s^{-1}$, 71% of the Coal Creek flow rate just upstream of the intake. The Spann Nettick agricultural diversion removed 28 L $s^{-1}$ from Coal Creek between CC-7.844 and CC-8.085. The drinking water return flow re-enters Coal Creek at fluctuating rates between CC-8.085 and CC-8.352 and offset flow losses to the Halazon agricultural diversion during the tracer test. There was a net flow increase between CC-8.085 and CC-8.352. Tracer-dilution equations do not account for flow losses to diversions. Manual adjustments were required in order to account for these losses. The tracer-dilution equation (Equation 5) is a mass balance equation which assumes a decrease in in-stream tracer concentration resulting from surface or dispersed groundwater inflows. Because no decrease in tracer concentration results when flow is removed from a stream, this equation cannot be used in reverse to calculate diversion flow rates.

The accuracy of this estimated flow rate of the drinking water reservoir return was supported with a secondary flow rate calculation for the drinking water reservoir. Because the Mt. Emmons treatment plant created a spike in downstream calcium concentrations, it was found that calcium could be viewed as a tracer at the two sites bracketing the drinking water reservoir. When the standard tracer-dilution equation was applied using calcium as the tracer, a flow rate of 61.5 L $s^{-1}$ was obtained. This is only a 2.5% difference from the estimated flow rate, confirming that the flow rate used to calculate metal loading rates for the drinking water reservoir return was an accurate estimate.

### *Sources of metals and arsenic in the Coal Creek watershed*

*Overview*. All of the sampled tributaries as well as dispersed groundwater flow may serve as contributors of toxic metal concentrations and loading rates to Coal Creek. The following discussion will address the sources of each of the ten metals and arsenic analyzed for this study. The metal sources identified by this tracer test are only representative of the sources of metals under low flow. We expect that high flow conditions will effectively dilute metal concentrations. Dilution would result in fewer aquatic life and drinking water standard exceedances. However, we must also consider that higher flows will increase flow rates from mine adits as well as the iron fen and the

gossan. Such an increase may negate dilution effects as the effective metal concentration would remain the same as the metal inputs increased along with overall flow rates. In this instance, the metal loading rates would also greatly increase compared to loading rates at low flow.

*Tributaries passing through culverts*. Tributaries entering Coal Creek from culverts along County Highway 12 (the Kebler Pass Road) were sampled directly out of the pipes immediately south of the highway (Figure 6). A more appropriate sampling location would have been immediately upstream from the tributaries entry point into Coal Creek, but in most cases, the small flows coming from the culverts could not be traced down to Coal Creek – the flow typically disappeared into the subsurface. Some error may be associated with taking samples from the pipes under County Highway 12.

*Tributaries considered in this assessment*. Elk Creek was suspected of contributing elevated arsenic, barium, cadmium, chromium, copper, lead, and zinc loading rates to Coal Creek (EPA, 2005b). The iron fen was also suspected of contributing elevated metal concentrations to Coal Creek, particularly for aluminum, iron, manganese, and zinc (EPA, 2005b). Drainage from the iron fen enters Coal Creek from the north through the unnamed tributaries UT-3.212, UT-3.455, and UT-3.595. Though unnamed tributary UT-3.212 contains the majority of the iron fen drainage, it also received flow input from uncontaminated drainage from the north. UT-3.595 drains directly from the gossan area where barren limonite, or a natural aggregate of hydrous ferric oxide, is exposed at the ground surface.

Flow from the fen tributaries travels approximately 40 m downhill to Coal Creek. Field reconnaissance in June 2006, during high flow conditions, showed that the majority of the flow from these culverts is absorbed into the ground before entering Coal Creek. Approximately 50% of the flow from UT-3.212 and 100% of the flow from UT-3.455 and UT-3.595 re-entered the groundwater system before entering Coal Creek. During low flow, it is likely that even a larger percentage of the flow would be absorbed before entering Coal Creek. This may allow for removal of some contaminants through transport through the subsurface.

When assessing the impact of loading rates from the drinking water reservoir return flow, it was important to determine whether metal concentrations in this tributary were similar to Coal Creek metal concentrations just upstream of the drinking water intake at CC-5.312. The coefficient of variance between metal concentrations at these two sites was calculated and found to be significantly different in the drinking water return flow as compared to that of Coal Creek at CC-5.312 (Table 13). The average coefficient of variance of all eleven metals was 42.6%. This high degree of variation makes it necessary to treat the drinking water return flow as having its own chemical signature separate from that of Coal Creek at CC-5.312. This flow must be exposed to additional manganese and iron sources because the concentrations of these metals are higher in the drinking water return flow. The other metals are lower in concentration in the drinking water return flow. It is also important to note that the flow rate used in all metal

loading calculations for the drinking water reservoir return was estimated as the difference between the estimated rate of diversion at the drinking water intake and the average monthly drinking water usage rate (Larry Adams, personal communication, May 26, 2006). Error associated with these estimates may affect calculated loading rates from the drinking water reservoir return flow. Future monitoring of metal concentrations and flow rates at this site are recommended to confirm any metal sources arising from this tributary.

**Table 13**. The metal concentrations at CC-5.312, just upstream of the drinking water intake, and at the drinking water reservoir return flow tributary. BDL is an abbreviation for "below detection limit" and NA means a valid metal concentration was not available.

| metal | metal concentration upstream of drinking water intake ($\mu g\ L^{-1}$) | metal concentration in reservoir return flow ($\mu g\ L^{-1}$) | coefficient of variance (%) |
|---|---|---|---|
| Al Dissolved | 50.4 | 35.5 | 24.5 |
| Total | 63 | 40 | 31.6 |
| As Dissolved | 3 | 1.2 | 60.6 |
| Total | 2.6 | 1.6 | 33.7 |
| Ba Dissolved | 22.4 | 21.1 | 4.2 |
| Total | 24.8 | 22.5 | 6.9 |
| Cd Dissolved | 0.51 | BDL | -- [1] |
| Total | 0.58 | 0.27 | 51.6 |
| Cr Dissolved | NA | NA | -- |
| Total | 38.3 | 2.4 | 124.7 |
| Cu Dissolved | 1.8 | 3.2 | 39.6 |
| Total | 2.2 | 2.5 | 9.0 |
| Fe Dissolved | NA | NA | -- |
| Total | 229 | 371 | 33.5 |
| Pb Dissolved | BDL | 0.2 | -- |
| Total | BDL | 0.78 | -- |
| Mn Dissolved | 30 | 27.4 | 6.4 |
| Total | 29.9 | 67.3 | 54.4 |
| Ni Dissolved | NA | NA | -- |
| Total | 19.8 | 1.7 | 119.1 |
| Zn Dissolved | 114 | 40.1 | 67.8 |
| Total | 126 | 103 | 14.2 |
| | | **Average CV** | **42.6** |

[1] -- The coefficient of variance could not be calculated.

*Iron sources*. The iron loading rate increased by a factor of 4.6 at the downstream of end of UT-2.511. Unnamed tributary UT-2.511 contributed 23% of the cumulative iron loading rate. The majority of aquatic life concentration exceedances for iron occurred within 2.0 km downstream of UT-2.511 (Table 11). Clearly, UT-2.511 was a source of

increased downstream iron loading rate; however, the Coal Creek iron loading rate downstream of the tributary was greater than the loading rate input by the tributary.

Additional iron inputs may come from iron liberation downstream of the wetlands, a lack of surfaces for iron sorption, or groundwater iron input. The greatest iron loading rate of 42% of the cumulative tributary input occurred at the drinking water return tributary. However, the in-stream loading rate did not increase immediately downstream. It did spike 0.6 km downstream of the drinking water return flow, yet it is unclear whether this was related to inputs from the drinking water reservoir or from an unidentified source.

Though the dissolved iron data were inconclusive, daily variations of the dissolved iron concentrations may be occurring. Previous studies have found that dissolved iron concentrations are greatest at midday as a result of the photoreduction of dissolved ferric iron and iron oxyhydroxides (McKnight et al., 1992; Tate et al., 1995). Photoreduction of these species produces an increase in the dissolved ferrous iron concentrations with increasing solar radiation.

Despite possible daily fluctuations in dissolved iron concentration, it is hypothesized that almost all of the iron in Coal Creek is in the colloidal phase. In natural waters, iron precipitates to form amorphous and crystalline forms of iron oxyhydroxides around pH 6.5. The average pH of Coal Creek is 7.3; therefore, iron should be mostly in a colloidal form.

*Manganese sources.* Unnamed tributary UT-3.595, which drains the gossan, contributed 62% of the cumulative tributary manganese loading rate. The Coal Creek metal loading rate remains elevated and constant for more than 1.0 km downstream of this tributary despite increasing flows and no other significant manganese sources. This may signify the existence of dispersed groundwater manganese inputs in this reach. The two highest manganese loading rates occurred in the wetland reach, indicating that significant manganese inputs enter Coal Creek in this reach, perhaps through dispersed groundwater flow.

*Aluminum sources*. Unnamed tributary UT-3.595, which drains the gossan, also contributed the highest cumulative tributary aluminum loading rate of 76%. Because the iron fen tributary contributions do not substantially increase aluminum loading in Coal Creek, we surmise that the metals are attenuated in the soil and groundwater between the County Highway 12 and Coal Creek. Aluminum concentrations never exceeded aquatic life standards (Table 10). Recall that a large percentage of the drainage from the iron fen and gossan tributaries re-entered the groundwater system before entering Coal Creek. Flow rates increase downstream of the iron fen, indicating that iron fen drainage does enter Coal Creek as dispersed groundwater flow. However, tributary samples were taken from culverts immediately south of County Highway 12 and may not be representative water entering the stream. Transport through the soil allows opportunity for metal removal through sorption. Aluminum is readily adsorbed by oxides, clay minerals, and organic matter in the soils. Travel through the soil and

groundwater system provides adequate time and opportunity for these metals to sorb to soil material and be effectively removed from the water column before entering Coal Creek.

Though the aluminum loading rate of the treatment plant effluent is low (Table 8), the aluminum loading rate increases downstream of the site and mimics the shape of the treatment plant effluent "plug." The loading rate increases with downstream of the plant following the same pattern, though less pronounced, as the calcium concentration increases (Figure 26). This indicates that the treatment plant may qualify as a minor or trace aluminum source when discharging.

*Zinc sources*. Unnamed tributary UT-3.595, which drains the gossan, had the greatest zinc loading rates and 49% of the cumulative tributary loading rate (Table 8). The Coal Creek zinc loading rates showed only small increases downstream of the iron fen and gossan. Aquatic life standards were exceeded downstream of UT-3.595.

The Elk Creek zinc loading rate (0.61 kg $d^{-1}$) was 16% of the cumulative tributary zinc loading rate. Coal Creek zinc loading increased by a factor of 120 downstream of Elk Creek. Zinc concentrations exceeded the chronic toxicity standard downstream of Elk Creek.

*Copper sources*. Unnamed tributary UT-2.511 added 20% of the tributary cumulative total copper loading rate (Table 8) and produced downstream increases in the Coal Creek copper loading rate. UT-3.595, which drains the gossan, added 13% of the cumulative tributary copper loading rate and also affected downstream increases in the Coal Creek copper loading rate. The drinking water reservoir return flow at 8.097 km added 30% of the cumulative copper loading rate. The copper concentration of the return flow was about the same as that of Coal Creek (Table 12).

*Cadmium sources*. Both Elk Creek and unnamed tributary UT-3.595, which drains the gossan, contributed to the cadmium loading rates to Coal Creek. Elk Creek added 32% of the cumulative tributary total cadmium loading rate, while UT-3.595 added 39%. Aquatic life standards were exceeded downstream of both Elk Creek and UT-3.595 (Table 10). UT-3.455, one of the iron fen drainages, contributed 12% of the cumulative tributary loading rate.

*Lead sources*. The drinking water reservoir return flow contributed 50% of the cumulative lead loading rate. The lead concentration of the return flow was approximately 3 times greater than typical in-stream lead concentrations. Splain's Gulch contributed 22% of the cumulative tributary total lead loading rate. Splain's Gulch also had the highest lead concentration of any of the tributaries. Minor lead sources were UT-3.595, which drains the gossan, and Elk Creek.

*Nickel sources*. Unnamed tributary UT-2.511 contributed the highest cumulative tributary nickel loading rate of 45%. UT-2.670 and UT-3.595 (the gossan drainage)

contributed significant cumulative tributary loading rates of 16 and 18%, respectively. The in-stream loading rate spikes just downstream of UT-2.511 and UT-2.670 and concentrations exceed the chronic toxicity standard for aquatic life (Table 10). Splain's Gulch contributed 11% of the cumulative tributary loading rate (Table 8).

*Chromium sources*. The sources of chromium are very similar to the sources of nickel. Unnamed tributary UT-2.511 contributed the highest cumulative tributary chromium loading rate of 48%. UT-3.595, UT-2.670, and Splain's Gulch contributed loading rates of 19%, 18%, and 8.7%, respectively. Water quality standards are exceeded downstream of Splain's Gulch, UT-2.511 and UT-2.670, and the gossan drainage.

*Arsenic sources*. Arsenic concentrations and loading rates differ from the pattern of the other metals. The metals described above tend to show increasing concentrations and loading rates with downstream distance. Arsenic concentrations decreased from the upstream to downstream reaches of Coal Creek, but the loading rate increased up to the drinking water intake. This indicated that additional arsenic sources enter Coal Creek. The increasing arsenic loading rate was not a result of arsenic input from any of the sampled tributaries. It is possible that arsenic is released from wetlands or groundwater during low flow. Downstream of the drinking water intake, the loading rate decreases as a result of decreasing arsenic concentration and higher flow rates. Of the identified tributaries, Elk Creek contributed 21% of the cumulative tributary loading rate. Though concentrations were no higher than in-stream concentrations, the drinking water reservoir return flow contributed 42% of the cumulative tributary loading rate. UT-2.670 and UT-2.696 added 10% and 7.8% of the loading rate, respectively.

*Barium sources*. Barium input from UT-6.573, UT-6.692, UT-6.668, and UT-6.782 most likely increases barium concentrations downstream of these tributaries; however, the flow from these sites was so low that loading rates were not substantial. Of these four tributaries, UT-6.668 added the highest percentage of the cumulative tributary loading rate with 12%. Increases in barium concentration and loading rates upstream of the iron fen cannot be attributed to any of the sampled inflows. In-stream barium concentration is greater than the concentration of tributary input in this reach. Similarly to arsenic, barium must enter Coal Creek through dispersed groundwater flow or an unidentified tributary upstream of the study reach.

### *Implications of metal concentrations and loading rates for remediation*

The major metal sources for ten metals and arsenic under low flow have been identified (Table 14). The gossan drainage (UT-3.595) was a major source of aluminum, cadmium, iron, manganese, and zinc in Coal Creek. Unnamed tributary UT-2.511 was a major source of chromium, iron, and nickel. Elk Creek was a major source of cadmium and zinc as well as a trace source of arsenic, barium, copper, and lead.

The metals entering Coal Creek from Elk Creek and the Standard Mine drainage are expected to be eliminated by the EPA's remediation of the Standard Mine site. Remedial activities at the Standard Mine site include dewatering of the surface impoundment, channelization of surface flow, and removal of mining debris (EPA, 2005b). These activities began during the summer of 2006. Repository construction and removal of waste rock piles and tailings progressed during the summer of 2007. If the remediation is a success, Coal Creek cadmium and zinc concentrations and loading rates downstream of the Elk Creek confluence should significantly decrease and water quality standards should not be exceeded. The clean-up should also remove any trace amounts of arsenic, barium, copper, or lead entering Coal Creek through Elk Creek. The sediments of Elk Creek may release metals after the Standard Mine cleanup.

The Coal Creek wetland immediately downstream of the Elk Creek confluence may be effectively removing metals from solution. The methods employed in this study may underestimate the actual metal loading rates entering Coal Creek if metals are quickly attenuated by plant, sediments, or microbes in the wetland (Hernandez, 1995). It is likely that wetland sediments contain toxic metal concentrations.

Drainage from the iron fen and gossan creates the greatest number of water quality criteria exceedances and concentration and metal loading rate increases. Coal Creek is impaired more severely by drainage from the fen and gossan than by drainage from Elk Creek and the Standard Mine. Because the fen and gossan are natural deposits (Figure 3) that support a diverse array of vegetation and wildlife including the endangered *Drosera rotundifolia,* clean-up efforts may prove controversial.

Unnamed tributary UT-2.511 was not identified as a major metal source prior to this study. This tributary drains a portion of Evans Basin, which is located on the north side of Coal Creek between Elk Creek and the Keystone Mine (Figure 2). Flow at UT-2.511 was only 21.3 L $s^{-1}$ during the tracer test. The high metal loading rates at this site are predominantly a result of high metal concentrations. The source of these metals is unclear and future reconnaissance and research of this site is recommended.

Return flow to Coal Creek from the drinking water reservoir contained unexpectedly high percentages of the cumulative tributary loading rate for arsenic, barium, copper, iron, lead, manganese, and zinc. Metal concentrations at this site were generally not the highest tributary concentration; however, the flow rate calculated as the difference between the average drinking water intake rate and the drinking water usage rate (60.01 L $s^{-1}$) was the greatest of all the tributaries (Larry Adams, personal communication, May 26, 2006). The process resulting in the addition of these metals to the flow between the drinking water intake and the reservoir return is not known. Iron and manganese inputs enter the water somewhere between the drinking water intake and the reservoir return, while the other metals were diluted along this route (Table 13). We recommend that the source of the additional iron and manganese be located.

**Table 14.** Major, minor, and trace metal sources in the Coal Creek watershed. The major sources were defined as any source that caused water quality standards to be exceeded and/or contributed a cumulative tributary metal loading rate greater than or equal to 33%. Minor sources were those that added 12-32% of the cumulative tributary metal loading rate. Trace sources were those that added 5-11%. For arsenic and barium, input from an unidentified upstream tributary or dispersed groundwater flow overshadowed contributions from any of the other tributaries. The tributaries with the highest cumulative loading rates were considered trace sources.

| Metal | Major sources | Minor sources | Trace sources |
|---|---|---|---|
| Aluminum | UT-3.595 (gossan) | | |
| Arsenic | Unidentified upstream tributary and groundwater | | Elk Creek reservoir return UT-2.670 UT-6.692 |
| Barium | Unidentified upstream tributary and groundwater | | Elk Creek reservoir return UT-2.670 UT-6.668 |
| Cadmium | UT-3.595 (gossan) Elk Creek | UT-3.455 (fen) | reservoir return |
| Chromium | UT-2.511 | UT-3.595 (gossan) UT-3.212 | Splain's Gulch |
| Copper | | UT-2.511 DW Res Return wetlands? groundwater? | Elk Creek UT-2.670 Splain's Gulch |
| Iron | UT-2.511 UT-3.595 (gossan) reservoir return | wetlands? groundwater? | UT-2.670 UT-6.692 |
| Lead | reservoir return | Splain's Gulch | UT-3.595 (gossan) Elk Creek |
| Manganese | wetlands? groundwater? UT-3.595 (gossan) | reservoir return | UT-3.455 (fen) |
| Nickel | UT-2.511 | UT-3.595 (gossan) UT-3.212 | Splain's Gulch |
| Zinc | UT-3.595 (gossan) Elk Creek | reservoir return | UT-3.378 (fen) |

*Colloids and metal association*

Colloids are critical components in streams affected by acid mine drainage (AMD) because their extensive surface areas strongly influence metal partitioning. Colloids dictate the mobility and bioavailability of metals in the environment. The fate of metals in acid mine drainage-affected streams is dependent upon interactions with colloid surfaces through adsorption, complexation, nucleation or dissolution, and surface-controlled redox chemistry as well as stream chemistry (Macalady et al., 1990; Macalady et al., 1991; McKnight et al., 1992; Schemel et al., 2000; Sullivan and Drever, 2001; Zanker et al., 2002; Zanker et al., 2003). Iron oxyhydroxides are the dominant mineral in mine drainage, while aluminosilicates and aluminosilicates with iron oxyhydroxysulfates may also be present in smaller quantities. These colloids dominate because of the oxidation of iron(II) and the subsequent hydrolysis of $Fe^{3+}$ and $Al^{3+}$ in acid mine drainage solutions. As mine drainage is diluted by stream waters, a greater quantity of aluminosilicates with associated iron and sulfur, manganese oxyhydroxides, and quartz minerals comprise the colloidal fraction.

In Coal Creek, a diverse array of colloidal minerals was tentatively identified (Figures 23-27; Table 9). No pattern related to the presence of iron oxyhydroxides upstream and downstream of mine drainage could be established. Both tributaries analyzed with the electron microprobe, though not mine drainage sites, were predominantly composed of iron oxyhydroxides or manganese oxyhydroxides. Colloidal analyses showed that while one or two minerals may be dominant in tributaries, the mineralogy becomes more diverse upon entry to Coal Creek.

The large surface area of iron oxyhydroxide colloids promotes sorption of toxic metals like lead, copper, zinc, and cadmium. The sedimentation of iron oxyhydroxide colloids is detrimental to aquatic life by filling permeable openings in the streambed that are normally habitat for benthic invertebrates (Clements, 1994). Upon entry to waters of near-neutral pH downstream of mines, such as Coal Creek, trace metals that were adsorbed to the colloids in more acidic reaches may be immobilized due to colloid coagulation and sedimentation (McKnight et al., 1992;Kimball et al., 1995; Schemel et al., 2000; Sullivan and Drever, 2001; Galan et al., 2003; Zanker et al., 2003). For example, the solubility of aluminum hydroxide ($Al(OH_3)(s)$) is strongly pH-dependent. Aluminum is predicted to precipitate above a pH of 5, and precipitation often results in the coating of the streambed with aluminum hydroxide, a white precipitate. Such white precipitate was observed in drainage from the gossan tributary to Coal Creek.

Colloids have a net negative charge in most natural waters as a result of organic matter coatings. However, in streams affected by acid mine drainage, a plethora of fresh iron oxyhydroxide surfaces are likely to be present. Dissolved organic carbon (DOC) concentrations are also expected to be low, resulting in the possibility of positively-charged colloidal surfaces. The capacity of a colloid to sorb metals may be enhanced by modification of iron oxyhydroxide surfaces through sorption or co-precipitation of anions. For example, cadmium sorption has been enhanced by incorporation of silica on iron oxyhydroxide surfaces. Also, the sorption of DOC may

increase copper and aluminum oxide sorption onto iron oxyhydroxides (Macalady et al. 1991; McKnight et al., 1992).

For this study, water samples were filtered through 0.45 μm membranes because the EPA was providing the metal analysis and because the metal concentrations must be compared with historical data. This filtration method offers several distinct advantages: (1) removal of suspended sediment and "particulate" organic matter that would settle during transport and storage, (2) removal of bacteria and microorganisms that could cause biological transformations within the sample matrix, and (3) easy comparison of results from different studies. However, filtration by 0.45 μm membranes has also been widely criticized (Danielsson, 1982; Morrison and Benoit, 2001). The filter size cuts across the size range for suspended colloids and provides a poor definition of dissolved constituents. Also, filtration artifacts such as contamination, colloid and solute adsorption onto the membrane, and coagulation and clogging on the membrane filter can produce significant errors in trace metal measurements. Where iron is normally associated with the large-size colloidal fraction (>0.45 μm), cadmium, manganese, and zinc are generally found in several different colloidal size classes (Kennedy et al., 1974; Pham and Garnier, 1998). With respect to trace metals found in various size classes, filtration through an arbitrarily chosen mesh size such as 0.45 μm would allow some colloids to pass while others are retained. This can significantly skew measurements of the particulate and colloidal fraction.

The distribution of metals between the dissolved and colloidal phases can be described by a distriubution coefficient ($K_d^{obs}$, L kg$^{-1}$). $K_d^{obs}$ is an empirical metric that is dependent upon a diverse array of parameters which influence chemical and physical attenuation (EPA, 1999). $K_d^{obs}$ is described by the equation

$$K_d^{obs} = \frac{C_s}{C_w} \tag{10}$$

where $C_s$ (mg kg$^{-1}$) is the colloidal metal concentration and $C_w$ (mg L$^{-1}$) is the dissolved metal concentration. Colloidal mass was not measured, so the concentration of metals associated with the colloids could not be calculated, and an alternative computation was used to describe partitioning. The colloidal fraction ($f_{colloid}$) was calculated as

$$f_{colloid} = \frac{C_{total} - C_{dissolved}}{C_{total}} \tag{11}$$

where $C_{total}$ is the total (unfiltered) metal concentration and $C_{dissolved}$ is the dissolved (filtered) metal concentration. The difference between $C_{total}$ and $C_{dissolved}$ is the concentration of metal in the colloidal (0.45 μm-filtered) phase (mg L$^{-1}$). The colloidal fraction was calculated as an average over the length of the study reach for the eleven metals included in the study (Figure 29). The standard error is significant because the colloidal fraction varied significantly from site to site. Only aluminum, arsenic, lead, and zinc had positive $f_{colloid}$ values because dissolved concentrations exceeded total concentrations on average for the other seven metals.

It is expected that some fraction of the colloids passed through the 0.45 μm filters. This expectation was supported by the electron microprobe images (Figures 23-25) that

show pore sizes in excess of 0.45 μm. This artifact would contribute to dissolved concentrations very close to total concentrations. Analytical error associated with the closeness of total and dissolved concentrations resulted in negative values (physically impossible) for the colloidal fraction for the remaining seven metals. Other possible reasons for the discrepancy between total and dissolved colloidal concentrations have been previously discussed.

Lead dominates the colloidal fraction with a mean $f_{colloid}$ value of 0.83 (Figure 29). Aluminum has a mean $f_{colloid}$ value of 0.36, demonstrating the second highest capacity to bind with minerals that make up the colloidal phase, although some of the aluminum measured as colloidal is likely part of the colloidal minerals rather than adsorbed on the colloids. Arsenic and zinc are also present in the colloidal phase to a lesser degree than both lead and aluminum. Though dissolved iron concentrations were unavailable, it is expected that iron is predominantly available in the colloidal phase and that its $f_{colloid}$ value is higher than that of lead.

The speciation behavior of these metals is dependent on pH. The neutral pH of Coal Creek supports metal sorption to colloidal material (Smith et al., 1990). Substantial colloidal fractions were anticipated. The $f_{colloid}$ value for zinc and arsenic were low at approximately 0.1. Recent studies show that zinc is sorbed more strongly to organic matter (Kimball et al., 2002). This means that a significant portion of sorbed zinc may be contained in organic biofilms coating the stream bottom or in iron hydroxides or oxyhydroxides that settle from the water column. These zinc removal pathways may explain the low occurrence of zinc in the colloidal phase.

Although arsenic has been known to partition to iron oxyhydroxides more readily than lead and zinc, only a small fraction of arsenic existed in the colloidal phase in Coal Creek. Galan et al. (2003) found that trace metals accumulated in iron oxyhydroxides in the order

Fe > As > Pb > Cr > Ni > Cu > Mn > Cd > Zn

Though the lead colloidal fraction was much greater than the zinc colloidal fraction in Coal Creek, the arsenic colloidal fraction was much smaller than that of lead and did not follow suit with previous experimental findings (Figure 29). Arsenic may preferentially associate with larger iron oxyhydroxides that settle from solution.

A previous study on the Lefthand Creek watershed in Boulder County, Colorado, reported colloid aluminum fractions as high as 0.9 in streams affected by acid mine drainage (Wood et al., 2004). Thermodynamic predictions indicate that colloidal aluminum concentrations should be high at neutral pH in any system where aluminum exists in equilibrium with gibbsite or any other aluminosilicate. The smaller than expected colloidal aluminum fraction in Coal Creek may be a result of aluminosilicate colloids passing through the 0.45 μm membrane filter. Other environmental factors such as complexation by dissolved phase natural organic ligands may be responsible for the significant dissolved aluminum concentrations (Kimball et al., 1995).

The high colloidal lead fraction correlates well with expected partitioning behavior for this metal. Lead is expected to dominate the colloidal phase because it

readily adsorbs to colloids (Abd-Elfattah and Wada, 1981; Brown and Hem, 1984; EPA, 1999; Macalady et al., 1990; Dzombak and Morel, 1990; Wood et al., 2004; Bautts, 2006). One study found that lead absorbs to minerals in the following order (Abd-Elfattah and Wada, 1981):

iron oxide < halloysite < imogolite, allophane < humus, kaolinite < montmorillonite

Iron oxyhydroxides were one of the major chemical components found in the selected samples analyzed for colloidal elemental composition (Figures 23, 25-27). The presence of iron oxide minerals in Coal Creek would support lead adsorption into the colloidal phase, particularly at neutral pH.

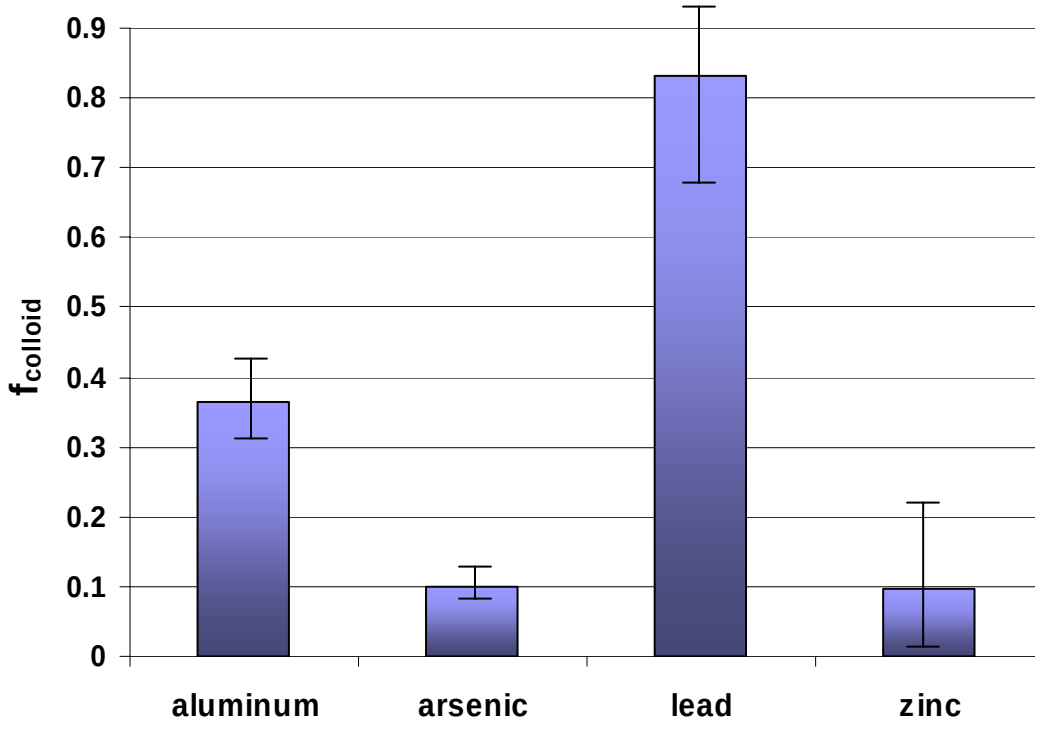


**Figure 29.** The colloidal fraction ($f_{colloid}$) of aluminum, arsenic, lead, and zinc in Coal Creek.

The partitioning behavior of lead and zinc was compared to published surface complexation constants, $K_{int}$, for these metals (Table 15; Dzombak and Morel, 1990). No comparable $K_{int}$ values were available for aluminum or arsenic. A higher surface complexation constant signifies a greater affinity for the metal to bind to a hydrous ferric oxide. The intrinsic surface complexation constant for aluminum and arsenic is expected to be between those for zinc and lead. The low colloidal zinc fraction is consistent with the surface complexation constant and observed zinc partitioning at other acid mine drainage sites during low flow (Kimball et al., 1995). A larger colloidal zinc fraction is expected under high-flow conditions due to the resuspension of colloids that aggregate and settle when flow is low. This hypothesis was not tested in Coal Creek.

Iron and manganese oxyhydroxides, silica, and aluminum were the major chemical components found in the tributary samples selected for elemental analysis (Figures 23-27). Manganese oxyhydroxide was the dominant mineral at the drinking water return tributary (Figures 24 and 26). Colloidal manganese concentrations were higher at this tributary than at any other tributary and much higher than in-stream colloidal manganese. The presence of manganese oxyhydroxide in the colloidal fraction coupled with the large colloidal fraction concentrations indicate that significant removal of manganese from the water column to colloidal particulates is occurring in the drinking water reservoir return flow.

**Table 15.** Intrinsic surface complexation constants for lead and zinc adsorption on hydrous ferric oxide (Dzombak and Morel, 1990).

| Metal | Intrinsic surface complexation constant ($K_{int}$) |
|---|---|
| lead | $10^{4.65}$ |
| zinc | $10^{0.99}$ |

This same phenomenon occurred with respect to iron at UT-6.692. The colloidal iron concentration at UT-6.692 is greater than at any other in-stream or tributary site. The total iron concentration at UT-6.692 is approximately 6 times higher than in-stream average. However, UT-6.692 only contributes 5.4% of the total tributary iron load. Flow at UT-6.692 was small and partially accounts for the small iron load despite the high iron concentration. Iron precipitation from the dissolved phase to ferric oxyhydroxide complexes most certainly accounts for further removal of iron from solution.

### *Hardness and metal partitioning*

Downstream of treatment plant effluent channel, Coal Creek hardness peaks at a concentration seven times greater than upstream hardness as a result of calcium input (Figure 8). Hardness, measured as the sum of calcium and magnesium concentration (Equation 2), competes with other divalent cations (metals) for binding sites on iron hydroxide complexes and organic matter (Macalady et al., 1990; Nelson et al., 1986; Allen et al., 1993). Metal concentrations in the colloidal phase are expected to decrease in response to increased competition with calcium downstream of the treatment plant. Weaker-binding metals such as zinc and cadmium are expected to be more affected than stronger-binding metals like lead. For instance, adsorption of cadmium to iron oxyhydroxides may be greatly reduced may the presence of zinc and calcium, resulting in enhanced mobility and bioavailability of cadmium. Both zinc and calcium have greater affinities than cadmium for binding with iron oxyhydroxides. This hypothesis could not be tested with the data available for this study due to large standard deviation associated with the colloidal fraction upstream and downstream of the treatment plant.

## CONCLUSIONS

The purpose of this research was to use tracer-dilution and synoptic sampling to identify sources of metals in Coal Creek. The impact of acid mine drainage from the Standard Mine (Elk Creek) and the iron fen and gossan on the Coal Creek watershed was investigated. Concentrations and metal loading rates for ten metals and arsenic were reported for a 9.4 km stretch of Coal Creek (Figures 12-22) and the major, minor, and trace sources of each of these metals were identified. Metal concentrations, loading rates, and metal sources are characteristic of low flow. Low flow is typically the most toxic to aquatic life because less water is available for dilution. Colloidal material was analyzed at select sites to provide a general assessment of the mineralogical composition of Coal Creek and its tributaries. Relationships between the dissolved and colloidal phase metal fractions were compared to established partitioning behavior for aluminum, arsenic, lead, and zinc.

Cadmium, chromium, and zinc exceed chronic and acute aquatic life toxicity standards at several locations along the study reach (Table 11). Drinking water supply standards were exceeded by arsenic, iron, and manganese (Table 11), though these exceedances were not at the location of the drinking water intake.

The Mt. Emmons Treatment Plant contributed large calcium concentrations to Coal Creek when discharging. The influx of calcium caused hardness-based aquatic life toxicity standards to increase downstream of the plant during the time of synoptic sampling. Large daily fluctuation in the calcium concentrations and hardness-based aquatic life toxicity standards downstream of the treatment plant are expected. Cadmium and zinc are expected to exceed aquatic life standards at additional locations downstream of the treatment plant when it is not discharging (Table 10).

The gossan was found to be the major threat to Coal Creek water quality (Table 13). The gossan contributed elevated aluminum, cadmium, iron, manganese, and zinc concentrations and loading rates. UT-2.511 was the second greatest threat to water quality. This tributary was not previously suspected of adding metals to Coal Creek, however, it contributed elevated levels of chromium, iron, and nickel to the stream. It is recommended that potential metal sources emanating from this tributary be further investigated. Elk Creek was found to be a major contributor of cadmium and zinc to Coal Creek, producing aquatic life standard exceedances and elevated loading rates for these two metals. An unidentified upstream surface tributary or dispersed groundwater flow added arsenic and barium to Coal Creek.

The colloidal fraction was examined for aluminum, arsenic, lead, and zinc (Figure 29). Lead dominated the colloidal phase followed by aluminum. Arsenic and zinc had significantly smaller colloidal fractions. A diverse array of colloidal minerals were present in Coal Creek, including the iron oxyhydroxides and aluminosilicates characteristic of acid rock drainage solutions. However, these minerals did not dominate the colloidal fraction and their presence or absence in colloid samples could not be related to their location upstream or downstream of acid rock drainage sources.

Increases in hardness were produced downstream of the Mt. Emmons treatment plant as a result of high calcium concentrations in the treatment plant effluent. The source of this calcium is lime used during the treatment process to raise pH and precipitate metals. This increase in calcium concentration caused hardness-based aquatic life standards to increase. Colloidal metal fractions are expected to decrease downstream of the plant as a result of increased competition with calcium cations. A higher fraction of these metals would consequently be available in the dissolved phase, where they pose a threat to aquatic life and ecosystem health. However, no correlations between the colloidal fraction and the increase in hardness could be established with available data to investigate this hypothesis.

# REFERENCES


Abd-Elfattah, A. and Wada, K., 1981. Adsorption of lead, copper, zinc, cobalt, and cadmium by soils that differ in cation exchange material. *Journal of Soil Science* **32**: 71-283.

Allen, H.E., Perdue, E.M., and Brown, D.S., 1993. *Metals in Groundwater: Adsorption to Heterogeneous Surfaces*. Lewis Publishers, Boca Raton, Florida. pp. 1-36.

Bautts, S.M., 2006. An investigation of metal concentrations in waste rock piles, stream water, benthic macroinvertebrates, and stream bed sediments to assess long-term impacts of intermittent precipitation events in the Lefthand Creek watershed, northwestern Boulder County, CO. M.S. Thesis, University of Colorado, Boulder, Colorado. 150 pp.

Bencala, K.E., 1985. Performance of sodium as a transport tracer - experimental and simulation analysis. Selected Papers in the Hydrologic Sciences, U.S. Geological Survey Water Supply Paper 2270, 83-89.

Bencala, K.E., McKnight, D.M., Zellweger, G.W., and Goad, J., 1986. The stability of rhodamine WT dye in trial studies of solute transport in an acidic and metal-rich stream. Selected Papers in the Hydrologic Sciences, U.S. Geological Survey Water Supply Paper 2310, 87-95.

Bencala, K.E., McKnight, D.M., and Zellweger, G. W., 1987. Evaluation of natural tracers in an acidic and metal-rich stream. *Water Resources Research* **23**(**5**): 827-836.

Bencala, K.E, McKnight, D.M., and Zellweger, G.W., 1990. Characterization of transport in an acidic and metal-rich mountain stream based on a lithium tracer injection and simulations of transient storage. *Water Resources Research* **26**(**5**): 989-1000.

Broshears, R.E., Bencala, K.E., Kimball, B.A., and McKnight, D.M., 1993. Tracer-dilution experiments and solute transport simulations for a mountains stream, St. Kevin Gulch, Colorado. U.S. Geological Survey, Water-Resources Investigations Report 92-4081, 18 pp.

Brown, D.W., and Hem, J.D., 1984. Development of a model to predict the adsorption of lead from solution on a natural streambed sediment. U.S. Geological Survey Water-Supply Paper 2187, 35 pp.

CCCOSC, 2006. The Geneva Creek iron fen, Clear Creek Open Space Commission. Retrieved June 1, 2006 from http://www.co.clearcreek.co.us/OSWebsite/GenevaCreek.htm.

CCWC, 2006. Crested Butte, A National Historic District, Coal Creek Watershed Coalition. Retrieved May 26, 2006, from http://www.crestedbutte.govoffice2.com/index.asp?cType =B_B ASIC&SEC=%7BE820970E-625C-4CAA-ADF1-F95CB758956C%7D.

CDPHE, 2005. Regulation No. 31: The Basic Standards and Methodologies for Surface Water, 5 CCR 1002-31. Colorado Department of Public Health and Environment Water Quality Control Commission, Denver, Colorado.

CDPHE, 2006. List of Superfund sites in Colorado: Standard Mine. 2006, Colorado Department of Public Health and Environment, Hazardous Materials and Waste Management Division. Retrieved April 9, 2006 from http://www.cdphe.state.co.us/hm/rpstandard.htm.

Clements, W.H., 1994. Benthic invertebrate community responses to heavy metals in the Upper Arkansas River Basin, Colorado. *Journal of the North American Benthological Society* **13**: 30-44.

Danielsson, L.G., 1982. On the use of filters for distinguishing between dissolved and particulate fractions in natural waters. *Water Research* **16**:179-182.

Dzombak, D.A., and Morel, F.M.M., 1990. *Surface Complexation Modeling: Hydrous Ferric Oxide*. John Wiley & Sons, New York, New York. pp. 392.

EPA, 1999. Understanding variation in partition coefficient, $K_d$, values. U.S. Environmental Protection Agency Report No. 402-R-99-004A, 609 pp.

EPA, 2005a. Hazard ranking system documentation record: Standard Mine, CO0002378230, U.S. Environmental Protection Agency. Retrieved April 16, 2006 from http://www.epa.gov/region8/superfund/co/standard/.

EPA, 2005b. National Priorities List: Standard Mine, Gunnison National Forest, Colorado. Retrieved April 16, 2006 from http://www.epa.gov/superfund/sites/npl/nar1740.htm.

EPA, 2006. Multi-media, multi-concentration inorganic analyses ILM05.3. Retrieved May 18, 2006 from http://epa.gov/superfund/programs/clp/ilm5.htm.

Galan, E., Gomez-Ariza, J.L., Gonzalex, J.C., Fernandez-Caliani, Morales, E., and Giraldez, I., 2003. Heavy metal partitioning in river sediments severely polluted by acid mine drainage in the Iberian Pyrite Belt. *Applied Geochemistry* **18**: 409-421.

Hernandez, K.S., 1995. Acid mine drainage in the Rockford Tunnel wetland, Idaho Springs, Colorado: metal speciation and distribution. M.S. Thesis, University of Colorado, Boulder. pp. 153.

Hornbaker, A. L., 1984. Metal mining activity map of Colorado and directory, 1984. Map Series 24, Colorado Geological Survey, Department of Natural Resources, Denver, Colorado.

Kelly, W.C., 1958. Topical study of lead-zinc gossans. Bulletin 46, New Mexico Bureau of Mines and Mineral Resources, Socorro, New Mexico. 80 pp.

Kennedy, V.C., Zellweger, G.W., and Jones, B.F., 1974. Filter pore size effects on the analysis of Al, Fe, Mn, and Ti water. *Water Resources Research* **10**:785-790.

Kimball, B.A., 1997. Use of tracer injections and synoptic sampling to measure metal loading from acid mine drainage. U.S. Geological Survey Fact Sheet-245-96, U.S. Department of the Interior, West Valley City, Utah.

Kimball, B.A., Callender, E., and Axtmann, E.V., 1995. Effects of colloids on metal transport in a river receiving acid mine drainage, upper Arkansas River, Colorado, U.S.A. *Applied Geochemistry* **10**: 285-306.

Kimball, B.A., Runkel, R.L., and Gerner, L.J., 2001. Quantification of mine-drainage inflows to Little Cottonwood Creek, Utah, using a tracer-injection and synoptic-sampling study. *Environmental Geology* **40**: 1390-1404.

Kimball, B.A., Runkel, R.L., Walton-Day, K., and Bencala, K.E., 2002. Assessment of metal loads in watersheds affected by acid mine drainage by using tracer injection and synoptic sampling: Cement Creek, Colorado, USA. *Applied Geochemistry* **17**: 1183 – 1207.

Macalady, D.L, Smith, K.S., and Ranville, J.F., 1990. Acid mine drainage: Streambed sorption of copper, cadmium, and zinc. Colorado Water Resources Research Institute Completion Report No. 154, 16 pp.

Macalady, D.L., Ranville, J.F., Smith, K.S., and Daniel, S.R., 1991. Adsorption of copper, cadmium, and zinc on suspended sediments in a stream contaminated by acid mine drainage: The effect of seasonal changes in dissolved organic carbon. Colorado Water Resources Research Institute Completion Report No. 159, Colorado State University, Fort Collins, Colorado. 14 pp.

McKnight, D.M., Bencala, K.E., Zellweger, G.W., Aiken, G.R., Feder, G.L., and Thorn, K.A., 1992. Sorption of dissolved organic carbon by hydrous aluminum and iron oxides occurring at the confluence of Deer Creek with the Snake River, Summit County, Colorado. *Environmental Science & Technology* **26**: 1338-1396.

Morrison, M.A., and Benoit, G., 2001. Filtration artifacts caused by overloading membrane filters. *Environmental Science & Technology* **35**(**18**): 3774-3779.

Mudroch, A., Zeman, A.J., and Sandilands, R., 1977. Identification of mineral particles in fine grained lacustrine sediments with transmission electron microscope and x-ray energy dispersive spectroscopy. *Journal of Sedimentary Petrology* **47**: 244-250.

Mudroch, A., Azcue, J.M., and Mudroch, P., 1997. *Physico-Chemical Analysis of Aquatic Sediments*. Lewis Publishers, Boca Raton, Florida.

Paschke, S., Kimball, B., and Runkel, R., 2005. Quantification and simulation of metal loading to the upper Animas River, Eureka to Silverton, San Juan County, Colorado, September 1997 and August 1998. Scientific Investigations Report 2005-5054, U.S. Geological Survey, Reston, Virginia, 4-8.

Pham, M.K., and Garnier, J.M., 1998. Distribution of trace elements associated with dissolved compounds (0.45 μm – 1 nm) in freshwater using coupled (frontal cascade) ultrafiltrations and chromatographic separations. *Environmental Science & Technology* **32**(**4**): 440-449.

Schemel, L.E., Kimball, B.A., and Bencala, K.E., 2000. Colloid formation and metal transport through two mixing zones affected by acid mine drainage near Silverton, Colorado. *Applied Geochemistry* **15**:1003-1018.

Smith, K.S., Macalady, D.L., and Briggs, P.H., 1990. Partitioning of metals between water and flocculated bed material in a stream contaminated by acid mine drainage near Leadville, Colorado. Colorado Water Resources Research Institute Completion Report No. 154, 101-109.

Soule, J.M., 1976. Geologic hazards in the Crested Butte-Gunnison area, Gunnison County, Colorado. Publication No. GS-VDSD 34-45, Colorado Geological Survey, Department of Natural Resources, Denver, Colorado, 4-6.

Streufert, R.K., 1999. Geology and mineral resources of Gunnison County, Colorado. Resource Series 37, Colorado Geological Survey, Department of Natural Resources, Denver, Colorado. 76.

Sullivan, A.B., and Drever, J.I., 2001. Geochemistry of suspended particles in a mine-affected mountain stream. *Applied Geochemistry* **16**: 1663-1676.

Tate, C.M., Broshears, R.E., and McKnight, D.M., 1995. Phosphate dynamics in an acidic mountain stream: interactions involving algal uptake, sorption by iron oxide, and photoreduction. *Limnology and Oceanography* **40**(**5**): 938-946.

U.S. Energy, 2006. History of Mt. Emmons molybdenum project known as the "Luck Jack Project," U.S. Energy Corporation. Retrieved May 17, 2006 from http://www.usnrg.com/MolybdenumProjects.php.

USFS, 1981. Mount Emmons mining project environmental impact statement, Gunnison County, Colorado. U.S. Forest Service, Department of Agriculture, Report 02-04-81-03, Gunnison Colorado.

USGS, 2006. USGS 09111000 Coal Creek near Crested Butte, Colorado, U.S. Geological Survey. Retrieved May 31, 2006 from http://waterdata.usgs.gov/co/nwis/inventory/?site_no=09111000.

Wentz, D.A., 1974. Effect of mine drainage on the quality of streams in Colorado, Colorado Water Resources Research Institute, Circular No. 21.

Wood, A.R, Cholas, R., Harrington, L., Isenhart, L., Turner, N., and Ryan, J.N., 2004. Characterization and prioritization of mining-related metal sources in the streams and streambed sediments of the Lefthand Creek watershed, northwestern Boulder County, Colorado, 2002-2003, Report No. 04-01, Department of Civil, Environmental, and Architectural Engineering, University of Colorado, Boulder, Colorado.

WRCC, 2006. Crested Butte, Colorado, Monthly Climate Summary, Period of Record 6/1/1909 – 12/31/2005. Western Regional Climate Center. Retrieved May 29, 2006 from http://www.wrcc.dri.edu/cgi-bin/climMAIN.pl?cocres.

Zanker, H., Moll, H., Wolfgang, R., Brendler, V., Hennig, C., Reich, T., Kluge, A., and Huttig, G., 2002. The colloid chemistry of acid rock drainage solution from an abandoned Zn-Pb-Ag mine. *Applied Geochemistry* **17**: 633-648.

Zanker, H., Richter, W., and Huttig, G., 2003. Scavenging and immobilization of trace contaminants by colloids in the waters of abandoned ore mines. *Colloids and Surfaces A: Physicochemical and Engineering Aspects* **217**: 21-31.

Zellweger, G. W., Avanzino, R.J., and Bencala, K.E., 1989. Comparison of tracer-dilution and current-meter discharge measurements in a small gravel-bed stream, Little Lost Man Creek, California. U.S. Geological Survey Water-Resources Investigations Report 89-4150.